LUT UNIVERSITY
School of Engineering Science
Chemical Engineering and Water Treatment

Leo Airaksinen

Methods for improving tensile properties of sustainable cellulose fibers

Examiners: Prof. Tuomas Koiranen
D.Sc. Harri Kosonen

TIIVISTELMÄ

Lappeenrannan-Lahden teknillinen yliopisto LUT
LUT School of Engineering Science
Degree Programme in Chemical Engineering and Water Treatment

Keinot ympäristöä säästävien selluloosakuitujen lujuusominaisuuksien parantamiseksi

Diplomityö

2021

99 sivua, 47 kuvaa, 6 taulukkoa ja 1 liite

Tarkastajat: Professori Tuomas Koiranen, Tohtori Harri Kosonen

Hakusanat: Selluloosa, märkäkehräys, lujuusominaisuudet, kiteisyysaste, orientaatio, röntgensironta

Selluloosa on luonnollinen orgaaninen polymeeri, jota pystytään erottamaan puusta keittämällä esimerkiksi kraft- eli sulfaattiprosessilla. Sitä käytetään yleisesti raaka-aineena muun muassa paperiteollisuudessa, lääketeollisuudessa ja tekstiilien valmistuksessa.
Tässä työssä keskitytään pääasiassa sellun käyttöön tekstiilikuiduissa, etenkin regeneroituihin kuitutyyppeihin, joihin voidaan lukea mukaan mm. viskoosi- ja lyocell-kuidut. Regeneroiduilla kuiduilla tarkoitetaan kuituja, jotka on valmistettu muuttamalla selluloosa ensin liukoiseen muotoon esimerkiksi natriumhydroksidin ja rikkihiilen avulla, jonka jälkeen selluloosa regeneroidaan kiinteään muotoon esimerkiksi kehräysprosessilla, jossa liukoisessa muodossa oleva selluloosa pumpataan pienten reikien läpi vastaliuottimeen, jossa regeneroituminen takaisin kiinteään muotoon tapahtuu. Regeneroitujen kuitujen mekaanisia ominaisuuksia pystytään muokkaamaan venyttämällä polymeeriä kehräyksen yhteydessä, tai erilaisia lisäaineita käyttämällä.

Viskoosiprosessissa, joka on yleisin menetelmä valmistaa regeneroituja tekstiilikuituja, käytetty rikkihiili on ihmisille ja ympäristölle myrkyllinen aine. Lisäksi kyseinen prosessi vaatii suuria kemikaalimääriä. Kiinnostus uusien ekologisempien kehräysprosessien ja

liuotinsysteemien kehittämiseen onkin herännyt viime vuosina. Esimerkkejä tällaisista uusista prosesseista ovat selluloosan liuotus natriumhydroksidi/ureaseoksella ja ionisiin liuottimiin perustuva Ioncell-F -ilmarakokehräys.

Mekaaniset ominaisuudet kuten vetolujuus ja venymä ovat tärkeitä parametrejä, jotka määrittävät pääosin tekstiilikuitujen laadun. Tässä diplomityössä selvitettiin kirjallisuuden avulla regeneroitujen selluloosakuitujen lujuusominaisuuksiin etenkin kehräysprosessissa, vaikuttavia tekijöitä ja testattiin näitä laboratoriotason koejärjestelyillä. Prosessin parametrien tutkimiseen käytettiin hyväksi Taguchi-monimuuttujakoejärjestelyä, jolla pystytään tutkimaan useampaa parametriä samanaikaisesti. Kehrättyjen kuitujen tärkeitä lujuuteen vaikuttavia kemiallisia ominaisuuksia kuten kiteisyysastetta, kidekokoa ja orientaatiota tutkittiin käyttäen hyväksi infrapunaspektroskopiaa ja röntgensirontamenetelmää.

Kokeellisessa osuudessa saavutettiin kuitulujuus 20.6 cN/tex ja 14.1 % venymä, kun kuitujen regeneroimiseen käytettiin heikkoa happoa, joka mahdollisti riittävän hitaan regeneraation, jotta kuidun venytyssuhdetta pystyttiin kasvattamaan. Erikoistetulla kuidun jälkikäsittely menetelmällä saatiin sellukuidun lujuus korkeammalle tasolle kuin kaupallisilla viskoosikuiduilla (27.2 cN/tex), lähelle Modaalikuitujen lujuutta. Taguchi monimuuttuja kokeet paljastivat, että suurimmat lujuuteen vaikuttavat parametrit ovat kuidun venytyssuhde, sekä regenerointi altaan lämpötila. Venytyssuhteen kasvattaminen parantaa kuidun orientaatiota, joka taas parantaa lujuutta. Tämä havaittiin myös röntgensironta datan avulla, jonka perusteella pystyttiin todentamaan riippuvuus lujuuden ja kiteisyysindeksin sekä orientaation neliön välillä.

ABSTRACT

Lappeenrannan-Lahden teknillinen yliopisto LUT
LUT School of Engineering Science
Degree Programme in Chemical Engineering and Water Treatment

Methods for improving tensile properties of sustainable cellulose fibers

Master's thesis

2021

99 pages, 47 figures, 6 tables and 1 Appendix

Examiners: Professor Tuomas Koiranen, D.Sc. Harri Kosonen

Keywords: Cellulose, wet-spinning, tensile properties, crystallinity index, orientation, X-ray scattering

Cellulose is natural organic polymer that can be separated from wood with pulping processes like the kraft pulping. It is used as a raw material *e.g.*, in paper industry, pharmaceuticals and in textile manufacturing.

This thesis focuses mainly on the usage of cellulose in the textile fibers, especially in the regenerated fibers, like the viscose and lyocell. Regenerated fiber refers to fibers that are made by first dissolving cellulose with solvents like sodium hydroxide/ carbon disulphide followed by the regeneration of the cellulose to solid state for example in the spinning process, in which the dissolved cellulose is extruded through small holes into a bath containing anti-solvent solution that causes solidification of the fibers. The tensile properties of the regenerated fibers can be altered by stretching the polymer during the spinning or by different additives.

The most common method to produce regenerated textile fibers is known as the viscose process. This method utilizes carbon disulphide that is toxic for the environment and humans, in the dissolution stage of the process. There is also high chemical demand in the viscose process. For these reasons, the demand for novel methods to produce more

sustainable textile fibers has risen in the recent years. Few examples of these novel methods in-development include the Ioncell-F and cold-alkali based processes.

Tensile properties like tenacity and elongation at break are important in determining the quality of textile fibers. In this thesis, different parameters that affect the tensile properties of regenerated cellulose fibers were investigated using information found from the literature and tested in the experimental part of the thesis. A multivariable trial method known as the Taguchi design was utilized in simultaneously examining multiple process parameters. Fiber chemical properties that affect the tensile properties, like crystallinity index, crystallite size and orientation were measured using infrared spectroscopy and x-ray scattering methods.

In the experimental section, fiber tenacity of 20.6 cN/tex and elongation at break of 14.1 % were achieved, when weak acid was used in the regeneration of the fibers. This allowed the fibers to regenerate slowly, so the stretching ratio could be increased, which lead to good fiber tenacities. With the help of specialized post-treatment method, the tenacity of the filaments reached higher levels (27.2 cN/tex) than the commercialized viscose fibers, even close to level that of Modal fibers. The Taguchi multivariable trials revealed that the biggest factors affecting the fiber tenacity are the stretching ratio and the regeneration bath temperature. Increasing the stretching ratio, increases the orientation which leads to improved tenacity. This was also noted from the x-ray scattering data, from which a correlation between fiber tenacity and crystallinity index times the orientation squared was confirmed.

ACKNOWLEDGEMENTS

During the completion of my thesis, I have received great amount of help from my co-workers. First, I would like to thank my official supervisors Dr. Harri Kosonen and Prof. Tuomas Koiranen as well as my spiritual supervisor Pasi Virtanen for providing interesting topic and ideas on improving the thesis.

The spinning experiments were done in collaboration with lab technicians of great expertise. Without their help this thesis would have been left as a mere draft. So, I would like to point out my gratitude to Elina Mustonen, Maiju Paakkonen, Maria Meuronen, Juuso Drews, Minna Tiainen and Salla Räikkönen for their excellent work. Also, thanks to Dr. Guillermo Reyes Torres and Antti Koistinen of Aalto University for making the WAXS measurements possible.

I would also like to thank my other co- workers that provided support and valuable information throughout this process, especially my roommates Veera Ollikainen, Krista Grönlund, Mikko Nikunen and Anika Khan. Special thanks to Krista (Taguchi specialist) for analyzing the Taguchi results.

Last, I would like to thank my family and friends for helping me through these five years of studying

Lappeenranta, September 10, 2021

Leo Airaksinen

Table of Contents

Symbols 9

Abbreviations 10

1 Introduction 11

1.1 Goal of the thesis 12

2 Cellulose 13

2.1 Structure 13

2.2 Pulping processes 17

2.3 Applications 18

3 Regenerated cellulose 20

3.1 Cellulose dissolution 20

3.2 Coagulation 23

3.3 Spinning 25

3.3.1 Viscose processes 28

3.3.2 Lyocell 29

3.4 Fiber structures 31

4 Novel sustainable fiber processes 33

4.1 Sodium hydroxide- based processes 33

4.2 Ioncell-F 34

4.3 Spinnova 35

5 Improvement of fiber tensile properties 37

5.1 Spinning parameters 38

5.2 Spinning dope additives 40

5.3 Post-treatment 44

6 Experimental 48

6.1 Materials & methods 48

6.1.1. Pulp preparation and dissolution....48
6.1.2 Brookfield viscosity....48
6.1.3. Dope quality microscopy....48
6.1.4. Wet spinning of the fibers....49
6.1.5. Tensile testing....49
6.1.6 FTIR....49
6.1.7. WAXS....49
6.2 Results....50
6.2.1 Spinning parameters....50
6.2.1.1 Regeneration bath temperature....51
6.2.1.2 Spinning dope temperature....54
6.2.1.3 Hot stretching....56
6.2.1.4 Multistage stretching....58
6.2.1.5 Regeneration bath composition....60
6.2.1.6 Plasticization....64
6.2.1.7 Taguchi method trials....66
6.2.2 Filament post-treatment....74
6.2.3. Fiber chemical properties....80
7 Conclusions....84
References....86
Appendix I....93

Symbols

A	Cross-sectional area (m^2)
A_{am}	Area of the amorphous peak (-)
A_{Cr}	Total area of crystalline peaks (-)
C_{RI}	Crystallinity index (-)
C	Concentration of the solvent (mol/m^3)
c	Cellulose weight- % of the dope (-)
DP_N	Degree of polymerization (-)
d	Dope density (g/cm^3),
F	Force at break (cN)
F_{TU}	Tensile strength (Pa)
f	Experimental correction coefficient (-)
f_t	Total orientation factor (-)
G	Gibbs energy (kJ/mol)
H	Enthalpy (kJ/mol)
k	Scherrer constant (-)
L	Crystallite size (Å)
R_D	draw ratio (-)
R_S	Stretching ratio (-)
R_T	Total stretching ratio (-)
r	Radius of spinneret holes (m)
r_f	Radius of filament (m)
S	Entropy (J/K)
SN	Signal to noise ratio (-)
T	Linear density (dtex)
T_S	Temperature (K)
TCl	Total crystallinity index (-)
V_0	Extrusion velocity (m/min)
V_1	Velocity of the first godet (m/min).
V_2	Velocity of the final godet (m/min)
$\bar{Y}$	Data mean value (-)
β	Full width at half maximum (-)
$\boldsymbol{\theta}$	Bragg's angle (-)
σ	Fiber tenacity (cN/dtex)
σ_s	The standard deviation (-)
τ	Shear force (Pa)
η	Dope viscosity (Pas)
λ	X-ray wavelength (Å)

Abbreviations

CMC	Carboxymethyl cellulose
CNC	Cellulose nanocrystal
CNF	Cellulose nanofiber
DP	Degree of polymerization
EMIMAc	1-ethyl-3methyl-1H-imidazol-3-ium acetate
KZC	Potassium zirconium carbonate
MFC	Microfibrillated cellulose
NFC	Nanofibrillated cellulose
NMMO	N-methyl morpholine oxide
PEG	Polyethylene glycol
ZnO	Zinc oxide

1 Introduction

Cellulose is used in the production of many different end-products like paper, cardboard, and textiles. It is used in the most common regenerated textile fibers, also known as viscose. Viscose is a process that utilizes the dissolution of cellulose by derivatization with sodium hydroxide and carbon disulphide to form the so-called cellulose xanthate. The dissolved cellulose is extruded through small holes into a bath containing anti-solvent like sulphuric acid, after which the dissolved cellulose undergoes regeneration to the solid state. The regenerated fibers can then be used in yarn production and further in woven fabrics. (Lundahl, *et al.*, 2017)

The main disadvantage of the viscose process is the use of toxic carbon disulphide as a derivatizing agent. In recent years this has cultivated the development of novel cellulose solvent systems that utilize non-toxic and greener alternatives for the conventional processes. These kinds of solvents mostly consist of direct dissolution agents like sodium hydroxide (NaOH) with the additions of chemicals like urea, zinc oxide (ZnO) and polyethylene glycol (PEG). The mechanical properties of the regenerated cellulose fibers spun from these greener alternative solvent systems are usually reported to be lower than those of the regular viscose fibers. (Bialik *et al.,* 2020)

The focus of the literature part of the thesis is to study different parameters and methods that can affect the tensile properties of the fibers. These can include *e.g.,* spinning parameters, dope additives and post-treatment like cross-linking of the regenerated fibers, of which the post treatment methods and process parameters are examined in the experimental section of the thesis. A multi variable experimental Taguchi design method is also utilized in the examination of the spinning process parameters. Fiber chemical properties like the crystallinity index, crystallite size and orientation are measured for selected fibers using Fourier Transform Infrared Spectroscopy (FTIR) and Wide Angle Xray Scattering (WAXS).

1.1 Goal of the thesis

The goal of this thesis is to find and test industrially applicable methods that can improve the tensile properties; tenacity and elongation at break of man-made cellulose fibers; wet spun from a greener cold alkali dissolved cellulose dope that replaces the toxic carbon disulphide utilized in the viscose process. As elongation of a fiber is dependent on tenacity (increase in tenacity typically decreases the elongation at break), the best possible combination of both parameters is tried to be achieved in the experimental section of the thesis. The desirable combination would be 19 cN/tex tenacity and 19 % elongation at break, because this is the minimum requirement of Chinese national standard for the viscose staple fibers.

The experimental section focuses on observing the different process parameters that have or may have effects on these tensile properties. In the trials, both single- and multivariable experiment setups are used to study these effects. The multivariable trials are conducted using a Taguchi design method that observes the parameter effects on the mean output values as well as the variation in the process. Also, variety of fiber post-treatment methods and their effects on the properties of the filaments are experimented on.

Also, the thesis scratches the surface in the measurement of the underlying chemical properties of the fibers. These properties include crystallinity index, orientation degree and crystallite size, which are main properties responsible for the achieved tensile properties. The crystallinity indexes for selected samples are calculated based on the data produced by Fourier Transform Infrared Spectroscopy and Wide Angle X-ray Scattering. The orientation and crystallite size are also determined from the WAXS data, and an automated .LUA script is constructed to help in the batch processing of the data.

2 Cellulose

Cellulose is naturally occurring organic polymer that can be utilized as raw material in various areas of industry. It is mostly found from cell walls of plant fibers. It usually appears with other polymers like hemicelluloses and lignin, as well as some extractives. (Heinze, 2015)

Cellulose can be separated for example from wood material with the pulping process, in which the removal of lignin and hemicelluloses occur while keeping the cellulose fibers as intact as possible. Some of its common applications are in the paper industry, textiles, and pharmaceuticals. (Iglesias *et al.*, 2020)

2.1 Structure

Cellulose is a polysaccharide that is formed by the polycondensation of D-glucopyranose units, which are the cyclic isomer forms of the open-chain glucose molecules. The oxygen -based linkages of the adjacent pyranose units occurs between the first and fourth carbon atom known as the β-1,4 glycosidic bond, which causes the rotation of the chain axis by 180 ˚. The repeating unit formed by these anhydroglucose units is called the cellobiose. (Heinze, 2015)

Every anhydroglucose unit of cellulose has three hydroxyl groups, which can be found at C2, C3 and C6 carbon positions. Cellulose molecules have two chemically different chain ends, of which the other holds an anomeric carbon bound by the glycosidic bond (nonreducing end) and the other end holds an equilibrium of D-glucopyranose ring and aldehyde function (reducing end). The degree of polymerization (DP), which indicates the number of monomers in polymers, is typically from 1 000 to 30 000 for native cellulose. (Heinze, 2015) The molecular structure of the repeating unit of cellulose is presented in Figure 1.

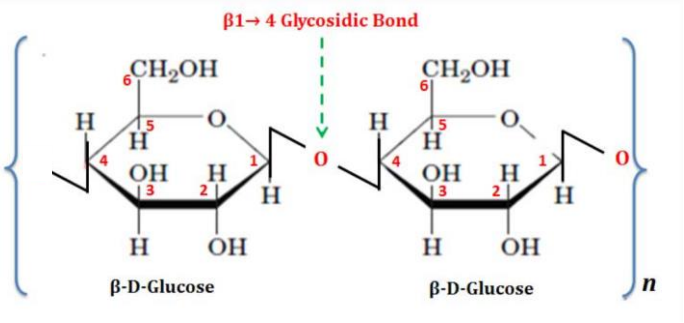

Figure 1. Molecular structure of the cellobiose repeating unit (Easy Biology Class)

The hydroxyl groups in the anhydroglucose units are responsible for the formation of inter- and intramolecular hydrogen bond networks. These bonding networks cause various known characteristics of cellulose like poor solubility in water and good stability. (Iglesias *et al.*, 2020) An example of the inter- and intramolecular hydrogen bonds found in cellulose chains are presented in Figure 2.

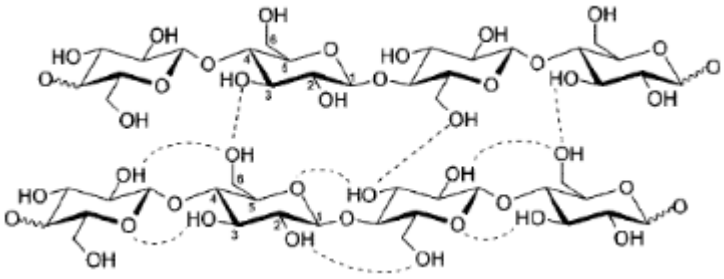

Figure 2. The inter- and intramolecular hydrogen bonds at various positions in cellulose (Pinkert et al., 2009)

Cellulose can exist in either crystalline or amorphous state, of which the amorphous part is more easily accessible to chemicals, micro-organisms, and water. The different known allomorphs of the crystalline cellulose include cellulose I_{α}, I_{β}, II, III_I, III_{II}, IV_I and IV_{II}. These allomorphs have different hydrogen bonding patterns and 3-dimensional structures which causes different reactivities of the allomorphs. (Heinze, 2015)

The cellulose II and III forms can be converted from cellulose I (native cellulose), by varying methods like mercerization (II) and ammonia treatment (III), while the IV-form can be generated by treating cellulose III with glycerol at high temperatures. (Kontturi, 2015) Commercially the most important crystalline forms of cellulose are the native I-form and the

II-form that is for example found in the regenerated cellulose fibers. (Heinze, 2015) Different transformation routes for cellulose allomorphs are displayed in the Figure 3. (Ciolacu & Popa, 2010)

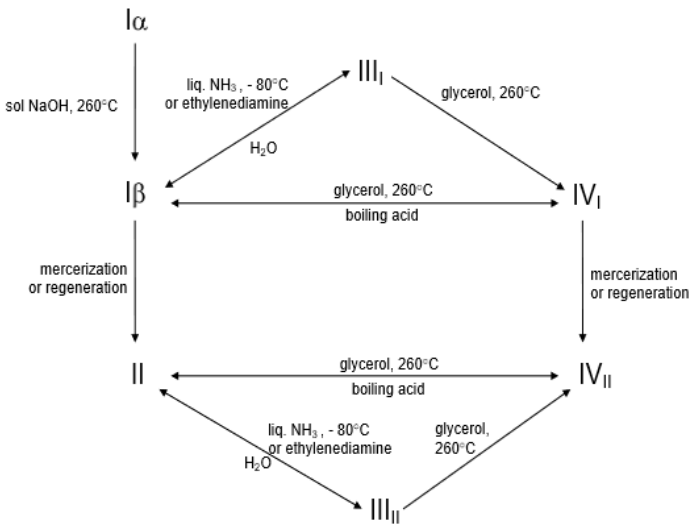

Figure 3. Transformation routes for different cellulose allomorphs (Ciolacu & Popa, 2010)

When about 40 cellulose polymer chains form linkages through hydrogen bonding and hydrophobic interactions, cellulose microfibrils of 0.015-0.025 µm in diameter and tens of µm in length are formed. The microfibril structure alters between highly ordered crystalline region (cellulose nanocrystals with diameters lower than 0.01 µm and lengths of 0.1-1 µm) and disordered amorphous region. Bundles of these microfibrils can further assemble into macrofibers with 10-50 µm in diameter and 1 000-3 000 µm in length due to crosslinking with pectin and hemicellulose. These form the structural basis for example in the cell walls of plants. Lignin and extractives like resins, fats and minerals are other common structural elements found in the cell walls. (Meng *et al.*, 2016), (Parry, 2016). The assembly of cellulose chains into fibers is presented in the Figure 4.

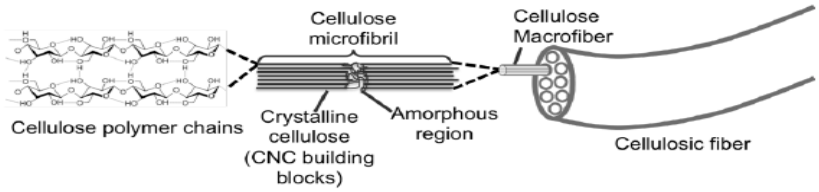

Figure 4. Assembly of cellulose chains into fibers (Parry, 2016)

As discussed, the cell wall of the plants mainly consists of cellulose and other polysaccharides. It contains of three layers called the middle lamella, primary- and secondary cell wall. The thin middle lamella layer operates in the adhesion and expansion of cells and is mostly made of pectins. On each side of the middle lamella are the hydrated gel structures called the primary walls, which are mainly composed of cellulose, hemicellulose, pectins, proteins and phenolic acids. The cellulose in the primary walls is as low oriented fibrillous layers. The primary walls are robust so that they can endure stresses exhibited by internal and external sources, while still being flexible enough to allow the extension of the cell wall that takes place during the growth of the cells. Finally, inside the primary walls is the structure made from cellulose, hemicellulose, and lignin, called the secondary cell wall that is responsible for decreasing the internal diameter size of the cell, known as lumen. The secondary wall can be divided into three layers called S1, S2 and S3. The S1 is the outermost and S3 is the innermost layer. The S2 layer makes up around 80 % of the cell wall mass. The high orientation and cellulose content of the S2 layer is important factor in developing stiffness in the structure of the wood. The S1 and S3 layers provide the elastic properties to the cell wall structure. In the Figure 5 is presented cell wall structures and the comprehensive picture of how individual cellulose chains act as structural units in the plant cells. (Sorieul *et al.*, 2016)

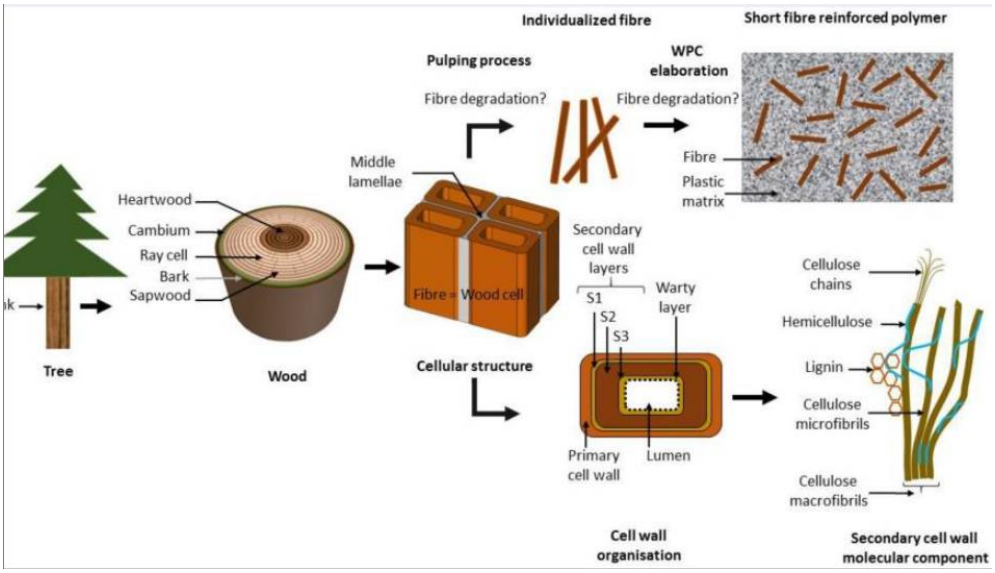

Figure 5. The comprehensive picture of wood structure (Sorieul et al., 2016)

2.2 Pulping processes

Wood is a major source from which cellulose can be separated from. It resides in the cell walls of the wood fibers as discussed earlier. Other important structural constituents include hemicellulose, lignin, and extractives. 65 to 70 percent of the wood dry weight can be accounted to cellulose and hemicellulose. Wood sources can be categorized into two main groups: hardwood and softwood. Hardwoods include species like birch and eucalyptus, while softwoods include spruce and pine. Properties of the wood vary between different categories, growing site and species. Such attributes can be for example carbohydrate or lignin content, fiber length and extractive types. (Iglesias *et al.*, 2020)

Pulping is a process, in which the lignin constituent is mainly removed from wood or other lignocellulosic biomass, while maintaining cellulose and the fiber structure of the source material efficiently. The pulping processes can be divided into mechanical, chemical, and semi chemical types. In paper and pulp industry the chemical process is the most used pulping type, of which sulfate (kraft) is the most widespread. Pulping is an important step in producing regenerated cellulose fibers, as in the fiber making commonly used pulp type; dissolving grade pulp is usually manufactured from sulfite or kraft pulp coupled with an acidic pre-hydrolysis step. (Iglesias *et al.*, 2020)

In the kraft process chipped wood material is digested at high temperatures and pressures

with the help of white liquor mixture, that is nowadays a combination of sodium hydroxide and sodium sulphide. The purpose of this is to dissolve the lignin fraction and separate wood fibers. The resulted pulp (brown stock) is then washed to separate it from the cooking chemicals (black liquor), after which the washed pulp is bleached to produce the final bleached product of high cellulose content, that can then be used for further applications like the papermaking. Bleached pulps can exhibit different properties like the presence of additional carbonyl and carboxyl groups in the cellulose chain due to oxidation reactions that can take place in the process. (Ciolacu & Popa, 2010) The cooking chemicals can be reused by utilizing a black liquor recovery cycle, which consists of various unit operations like evaporators, recovery boiler and causticizing. (Iglesias *et al.*, 2020) Flow chart of typical kraft process configuration is presented in Figure 6

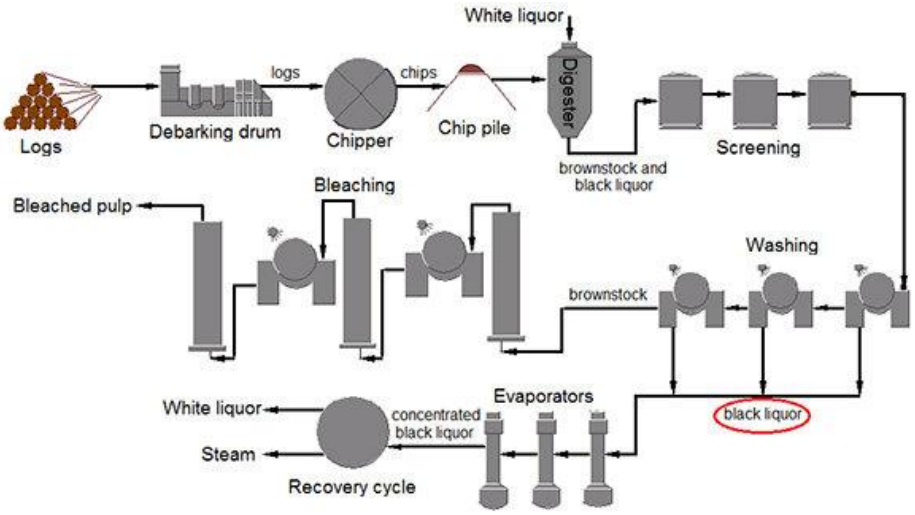

Figure 6. Flow chart of kraft process (Mathews et al., 2013).

2.3 Applications

Cellulose is widely used in different areas of industry. Few of the most common applications include the production of pulp, paper, and cardboard. (Gupta *et al.*, 2019) Dissolving pulp that has high cellulose content, is used in the production of regenerated cellulose materials like the viscose staple fibers, cellophane film, and cellulosic derivatives like the cellulose acetate. The viscose fibers are generated through wet-spinning process, after which the fibers can be *e.g.*, woven into fabrics, that in turn can be used in manufacturing of textiles. (Kumar

& Christopher, 2017)

Biofuel industry has growing interest in the usage of cellulose as a source material to produce fuel with lower carbon footprint compared to conventional fuels like diesel and petrol. Cellulose can be converted into ethanol by degrading the polymer chain first into sugars, by the help of acid hydrolysis or with the action of enzymes for example. The sugars can then be fermented to produce ethanol, that can be further used as biofuel substrate. Some bacteria can also degrade cellulose into methane and carbon dioxide to produce biogas. (Gupta *et al.*, 2019) Other uses for cellulose or its derivatives include the food industry, pharmaceutical applications and composite materials. (Gupta *et al.*, 2019) Examples of different cellulose applications are displayed in Figure 7.

Figure 7. Cellulose based products (European Pulp Industry Sector, -)

3 Regenerated cellulose

Regenerated cellulose is material, which is produced by dissolving cellulose or its derivative in a suitable solvent, followed by a solid-liquid phase separation, also known as, regeneration in a spinning process to produce cellulose II fibers. These fibers can further be used for example in the textile industry. The most common processes to produce regenerated cellulose fibers include viscose and lyocell. (Niaounakis, 2017)

The cellulosic fibers produced by regeneration processes can be categorized as man-made fibers. The man-made fibers are usually produced with the spinning processes and can be of organic or inorganic origin. The most important non-cellulose based man-made fibers include polyester, polyacrylonitrile, polyamide and polyurethane. (Tobler-Rohr, 2011) The man-made fibers are categorized in the Figure 8.

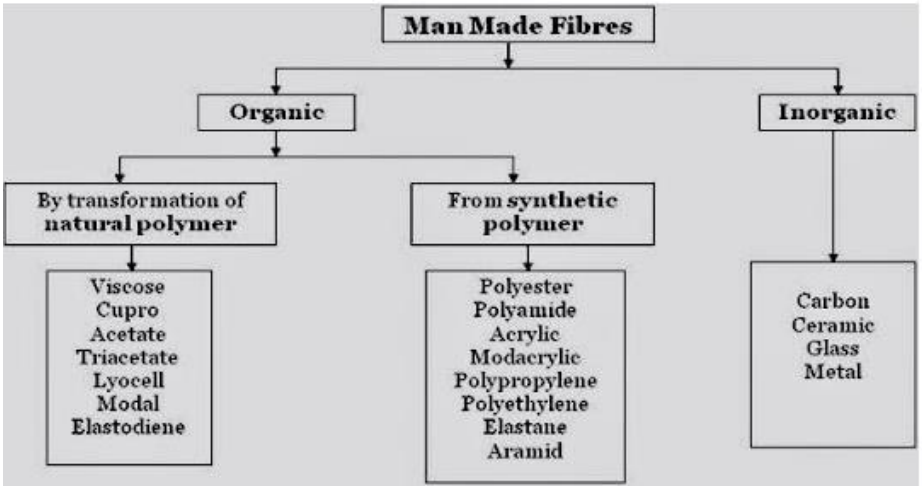

Figure 8. Man-Made fibers (Tekstil Sayfasi, 2014)

3.1 Cellulose dissolution

Dissolution is an important process step in producing cellulose based man-made fibers, which controls the efficiency as well as the final properties of the product. As known, cellulose has poor solubility in water and many common organic solvents, due to strong hydrogen bonding network. Over time, different solvents have been developed to overcome these limitations. Cellulose solvents can be categorized as derivatizing and non-derivatizing (direct) dissolution processes. The derivatizing solvents include the formation of unstable cellulose intermediates like cellulose xanthate or cellulose carbamate. Cellulose xanthate

derivative, which is the most widely used derivatizing solvent, is used for example in the manufacturing of viscose fibers. The direct dissolving solvents include ethylenediamines, N-methylmorpholine-N-oxide (NMMO), dimetylsulfoxide (DMSO), N,N,-dimethylacetamide (DMAc), ionic liquids and sodium hydroxide with additives like urea, thiourea and PEG. (Singh *et al.*, 2015) In Figure 9 is categorized the different cellulose dissolution processes according to the dissolution type.

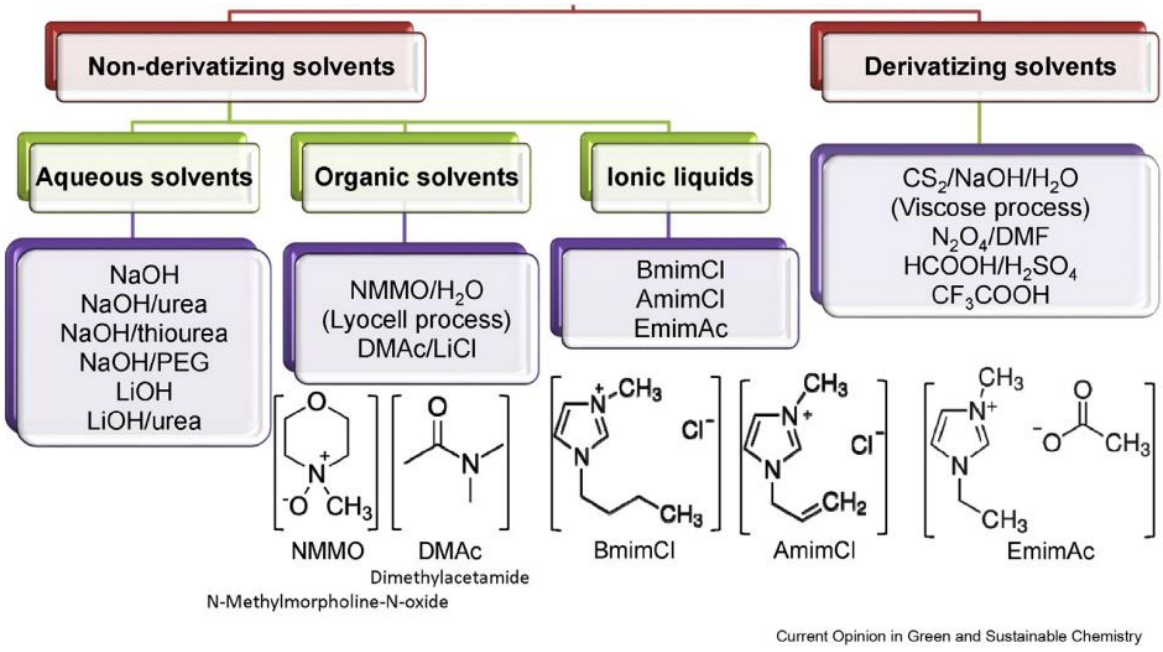

Figure 9. Cellulose dissolution processes categorized into derivatizing and non-derivatizing (direct) dissolution processes (Alexandridis et al., 2018)

The solubility of cellulose depends on the degree of polymerization (DP), crystallinity, content of the cellulose in the solvents system and different pre-treatment methods. Dissolution conditions like temperature, solvent concentration and the use of additives affect the process also. (Medronho *et al.*, 2012) The dissolution of cellulose can occur when the Gibbs energy change of the cellulose-solvent system reaches negative value, indicating spontaneous occurrence of the dissolution. (Vehviläinen, 2015) To achieve this condition for cellulose/alkali-system, the temperature of the solution needs to be low; usually below 0 °C and the NaOH concentration needs to be in specific range usually 1.5M- 2.5M. (Hagman *et al.*, 2017). The Gibbs energy change can be calculated with Equation 3.1 (Vehviläinen, 2015).

$$dG = \text{dH- } T_S \text{ dS} \quad (3.1)$$

where G is the Gibbs energy (kJ/mol), H is the enthalpy (kJ/mol), T_S is the temperature (K) and S is the system entropy (J/K).

When observing the dissolution mechanism from macroscopic perspective, the cellulose fibers undergo swelling, while in contact with the solvent, which is thought to result from the breakages of the inter- and intramolecular hydrogen bonds in the fibers. Ballooning effect occurs, when the secondary wall of the fibers swell, causing the bursting of the primary wall followed by its rollup. The rolled primary wall then prevents swelling of fiber in uniform way, which in turn results in balloon-like fibers. (Cuissinat & Navard, 2006)

As more solvent penetrates the balloon structure, the pressure inside the balloon rises. When the pressure exceeds the strength of the fiber surface layer, the bursting of the balloon followed by the dissolution of the whole fiber will occur. When the solvent is better, a faster dissolution can occur. This involves the diffusion of solvent into the amorphous or porous regions of the fiber leading to longitudinal fragmentation of the fibers, that will shortly lead to complete dissolution. The dissolved cellulose solution, also known as dope, is typically viscous gel like fluid. The fibers can also stay in swollen or partly dissolved state depending on the characteristics of the dissolution process. (Zhang *et al.*, 2012)

The dissolution can occur at molecular level, like is demonstrated to be in the case of ionic liquid solvents, or by forming colloidal suspensions with aggregates of few hundred cellulose chains. The latter type of dissolution is believed to occur with most solvent systems. (Singh *et al.*, 2015) The Figure 10 is representation of the ballooning effect of the fiber, when exposed to the solvent.

Figure 10. Ballooning effect in the fiber dissolution (Singh et al., 2015)

3.2 Coagulation

When the cellulose in the dissolved state is introduced to a coagulation bath, a phase separation of the dissolved cellulose into solid fiber and liquid solvent occurs due to breakage of the cellulose/solvent interactions. The phase-separation can be caused by regeneration from the derivatized solution, ion exchange, dehydration, neutralization, or de-solvation, depending on the nature of the applied solvent and the coagulation bath chemicals. The terms coagulation and regeneration are often used in the literature interchangeably, even though coagulation refers to more unspecific phase-separation, and regeneration to the recovery of cellulose polymer from its derivatized state. After immersion, the surface of the cellulose dope instantly solidifies forming a semipermeable membrane structure that controls the rate of diffusion of the coagulation chemicals into forming filament and the solvent chemicals out of the fiber. During the solidification cellulose II is formed instead the native cellulose I that is found prior the dissolution. (Vehviläinen, 2015)

In Figure 11 is displayed one coagulation mechanism example, which is caused by the regeneration from the cellulose xanthate derivative by using acid as coagulant. This type of coagulation is used in the viscose process.

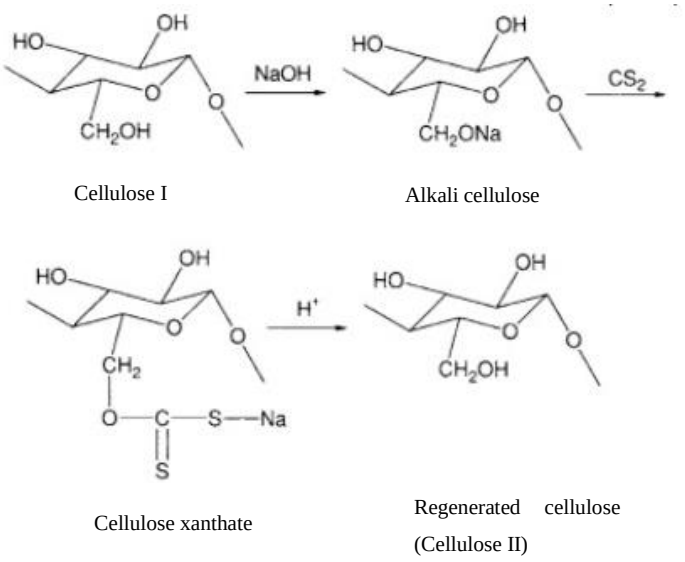

Figure 11. Derivatizing dissolution of cellulose and regeneration with acid (Rodgers & Waddell, 2013)

The kinetics of the cellulose coagulation process is primarily dominated by the counter diffusion process, meaning the inward diffusion of the coagulation chemicals into the dope solution and the outward diffusion of the solvent and other chemicals like salts from the dope. The rate of coagulation is an important parameter, that greatly affects the properties of the regenerated fibers. The diffusion rate of the solvent in the wet-spinning process can be depicted with Fick's second law as seen from Equation 3.2. The mass diffusion in the axial direction is generally considered to be negligible as the process can be thought of as infinite length cylinder. (Liu & Hu, 2006)

$$\frac{dC}{dt} = D\frac{1}{r_f} * \frac{d}{dr_f}\left(r\frac{dC}{dr_f}\right) \tag{3.2}$$

in which C is the concentration (mol/m^3), r_f is the filament radius (m) and D is the diffusion coefficient (m^2/s).

As can be seen from Equation 3.2 the diffusion rate can be controlled by altering the process conditions like the chemical concentrations, filament radius and by altering parameters that have influence on the diffusion coefficient like additives, and temperature. For example. in the viscose process, where sulphuric acid (H_2SO_4) is used as a coagulant to recover cellulose from its derivatized state, the concentration of hydrogen ions (H^+) plays important role in

determining the regeneration kinetics. Addition of electrolytes such as sodium sulphate (Na_2SO_4) and zinc sulphate ($ZnSO_4$) into the coagulation bath can lower the amount of available H^+ in the solution and thus slow down the counter diffusion and consequently the rate of regeneration. The salts in the coagulation bath can also dehydrate the formed filament due to osmotic pressure, which could lead to formation of more tenacious fibers. However, the effect of the salt concentration has been noted to be minimal when using regular salt concentrations in the spinning process.

Coagulation rate which is mostly determined by the diffusion process (Equation 3.2) determines the solidity of spun fiber in the following process step. This is important in spinning process as it is desired that regenerated fibers stay in softer gel-like state before stretching is applied to allow the filaments to be stretched more, thus increasing the fiber orientation and consequently tenacity. (Medronho, & Lindman, 2015, Eriksson, 2015)

3.3 Spinning

Spinning process can be conducted by extruding the spinning dope through an apparatus, called the spinneret, containing hundreds to thousands of small holes, into a coagulation bath. When the spinning dope enters the spinneret holes, shear forces are induced. This aligns the fibers parallel to the axis improving the mechanical properties of the fiber. (Lundahl, *et al.,* 2017) In Figure 12 is presented filaments exiting the spinneret holes.

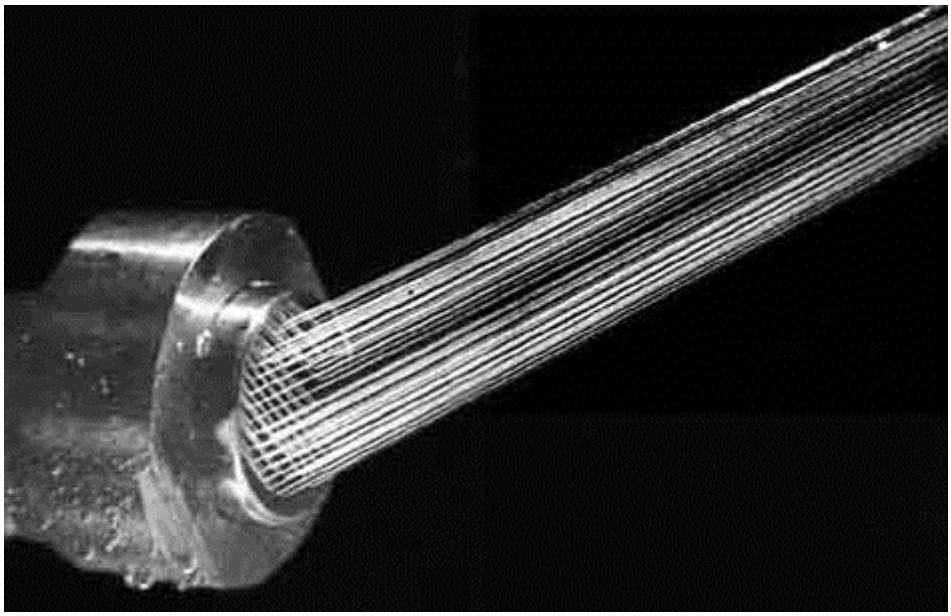

Figure 12. Filaments extruded through spinneret holes

Upon entering the coagulation bath, the dope solidifies, and thus the formed filament can be taken up by rollers of varying speed, also known as godets. The fibers can be stretched to align the cellulose polymer chains with the axis of the fiber causing increased orientation and thus enhancement of the filament's mechanical properties. Orientation is the angle between the cellulose chains and the axis of the fiber. If the stretching is conducted when the fiber has not yet formed strong permanent bonds and is in a soft gel-like state, higher alignment of the fibers can be achieved and thus better orientation. (Vehviläinen, 2015) The theoretical maximum tenacity induced only by the stretching of the fiber, should be achieved at the maximum stretching level, meaning just before the point at which the filament starts to break during the spinning process. (Eriksson, 2015)

The stretching of the fibers can for example be conducted in the coagulation bath by the speed difference of the first godet and the outward flow velocity of the dope through the spinneret. The ratio of these velocities is known as draw ratio and can be calculated with Equation 3.3. (Vehviläinen, 2015) However, the stretching conducted near the nozzle of the spinneret will not affect the mechanical properties of the fiber drastically. (Eriksson, 2015)

$$R_D = \frac{V_1}{V_0} \tag{3.3}$$

where R_D is the draw ratio, V_0 is the extrusion velocity (m/min) and V_1 is the velocity of the first godet (m/min).

More preferably stretching is done after the filament leaves the coagulation bath for example in secondary coagulation or washing bath, in which the fiber tenacity can be impacted more readily. The ratio of the velocities of the final godet and the first godet is known as the stretching ratio, which can be defined with Equation 3.4. (Vehviläinen, 2015)

$$R_S = \frac{V_2}{V_1} \tag{3.4}$$

where R_S is the stretching ratio, V_1 is the velocity of the first godet (m/min) and V_2 is the velocity of the final godet (m/min).

The total stretching ratio which is the ratio between the final godet speed and the extrusion velocity, can be calculated with Equation 3.5. The extrusion velocity can be controlled by changing the flow rate of the dope before the spinneret *e.g.*, by changing the pumping speed or by altering the spinneret hole diameters. The godets speeds can be altered by changing the godet diameter or their rotational speed, which are usually connected to electrical motor. The stretching or shrinking occurs when there is speed difference between godets. The total stretching ratio defines the linear density of the fiber. When the total stretching ratio > 1, the fiber becomes thinner, while for stretching ratios < 1, the fiber becomes thicker.

$$R_T = \frac{V_2}{V_0} \tag{3.5}$$

where R_T is the total stretching ratio, V_0 is the extrusion velocity (m/min) and V_2 is the velocity of the final godet (m/min)

The coagulation bath is followed by either secondary coagulation bath or usually consecutive washing baths. In the washing baths, the fibers are neutralized, and the residual salts or other chemicals are removed. As discussed, the stretching conducted in the washing bath can have large impact on the fiber mechanical properties. However, if the stretching is done in a secondary coagulation bath containing hot dilute acid, the fiber can be locked in a state of high orientation, as the oriented structure cannot relax as efficiently, due to faster coagulation during the stretching. This method is called the hot-stretching and is utilized for example in viscose processes. (Eriksson, 2015)

The fibers can then be cut into staple fibers of desired length or spun into continuous yarns. The after-treatment steps like oiling can then be conducted, followed by drying of the fibers. A simple wet spinning setup is presented in the Figure 13.

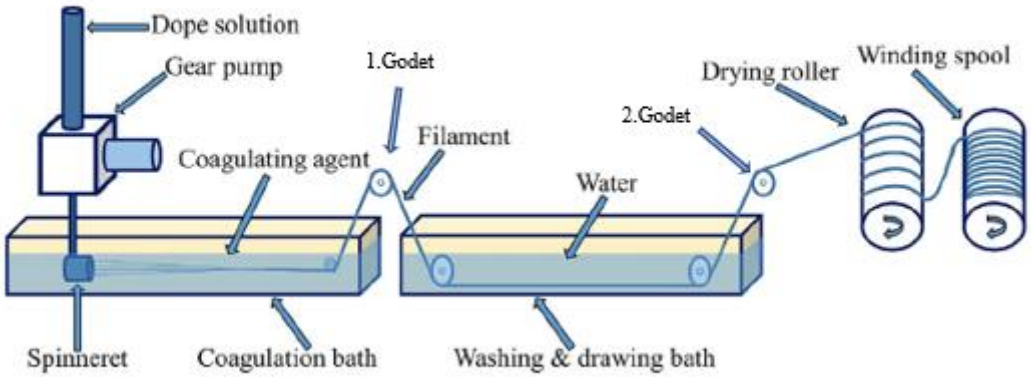

Figure 13. Diagram of a simple wet spinning process

3.3.1 Viscose processes

Viscose, also known as Rayon, is the most utilized wet spinning process in the manufacturing of regenerated cellulose fibers. The first step of this process is called steeping, in which the introduction of pulp into an NaOH solvent occurs, producing alkali cellulose. The shredding is conducted on the alkali cellulose to increase its surface area, and thus its reactivity. This is followed by the aging of the pulp to achieve desired degree of polymerization. The aged alkali cellulose is derivatized with carbon disulfide gas to form alkali-soluble cellulose xanthate. The cellulose is then dissolved in caustic solution to produce the spinning dope solution. The resulted dope is filtrated to remove impurities that might cause imperfections in the formed fiber or cause clogging or blockages of the equipment. After this, the dope is let to ripen, causing redistribution of xanthate groups that increases degree of dissolution. The ripening is followed by deaeration of the dope, to remove the air bubbles because air bubbles cause voids or imperfections in the formed fibers. The spinning dope is pumped through the spinneret, into a coagulation bath. Like in all wet spinning processes the spinneret is submerged into the regeneration bath. (Sayyed *et al.*, 2019)

Regeneration of the cellulose into thin multifilament yarn occurs, followed by its stretching. The most common coagulation bath in the viscose process comprises of sulphuric acid coupled with sodium and zinc sulphates. The formed fibers can be treated for example with

a lubrication finish to decrease friction of the yarn to prevent the fiber breakages. The fibers are dried to produce the regenerated viscose fibers in continuous or staple forms. (Sayyed *et al.,* 2019) The flowchart of the viscose process is displayed in Figure 14.

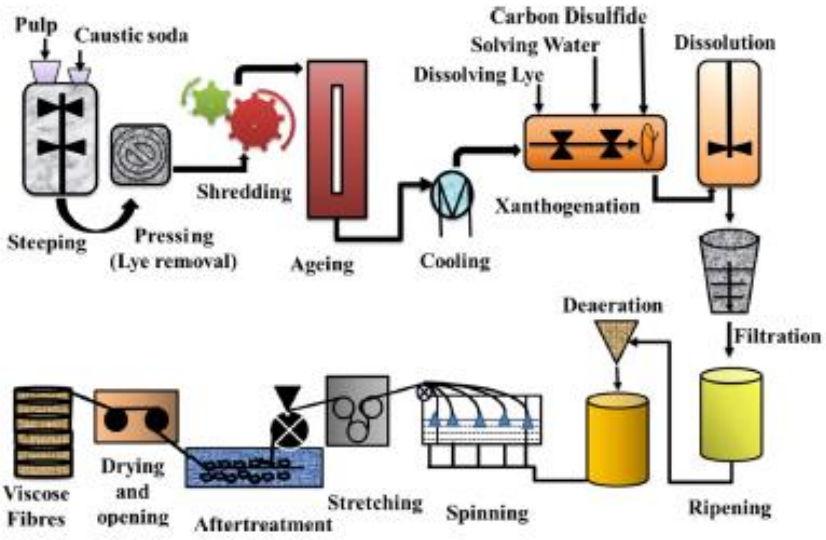

Figure 14. Flow chart of typical viscose process (Sayyed *et al.,* 2019)

The viscose process can be modified to produce fibers with higher performance also known as Modal fibers. The most utilized Modal processes include the High Wet Modulus (HWM) and Polynosic processes. These fibers can be produced by altering spinning conditions, like lowering of acid concentration and the spinning temperature. Viscose modifiers *e.g.,* polyethylene oxides, amines and quaternary bases can be added to the productions of these high performance fibers with increased tenacity. The modifiers can affect the size of the formed cellulose crystals as well as slow down the rate of the fiber regeneration, allowing more stretch to be applied during the fiber spinning. (Eriksson, 2015)

3.3.2 Lyocell

The lyocell fibers were developed to fill a need for more environmentally friendly alternative to the viscose process. The process uses a direct cellulose solvent N-methyl morpholine

oxide (NMMO) in a dry jet wet spinning method that utilizes an air gap technique to produce filament of high tenacity. (Woodings, & Woodings, 2001)

In the lyocell process, cellulose is first pre-mixed with NMMO, followed by the evaporation of water in a temperature of 90 to 120 °C coupled with vacuum, to produce clear viscous spinning dope solution. The dope is then filtered and extruded through a spinneret into an air gap, in which drawing can be conducted to produce fibers with high orientation and thus high tenacity. The air gap leads the fiber to a coagulation bath consisting of water and the used solvent. As the NMMO solvent in the lyocell process is expensive, a recovery system needs to be applied to decrease the manufacturing costs of the product. This is usually achieved with ion exchangers that remove destabilizing ions from the diluted solvent that is recycled from various baths of the spinning line. The solvent is then concentrated with evaporators to reproduce solvent capable for reuse. Similarly, to the viscose process the fiber is taken up by godets, washed and finished with chemicals like antistats and dried. The fibers can also be crimped to affect their processing performance before they are cut into desired length. (Woodings, & Woodings, 2001) An example of a lyocell process is displayed in Figure 15.

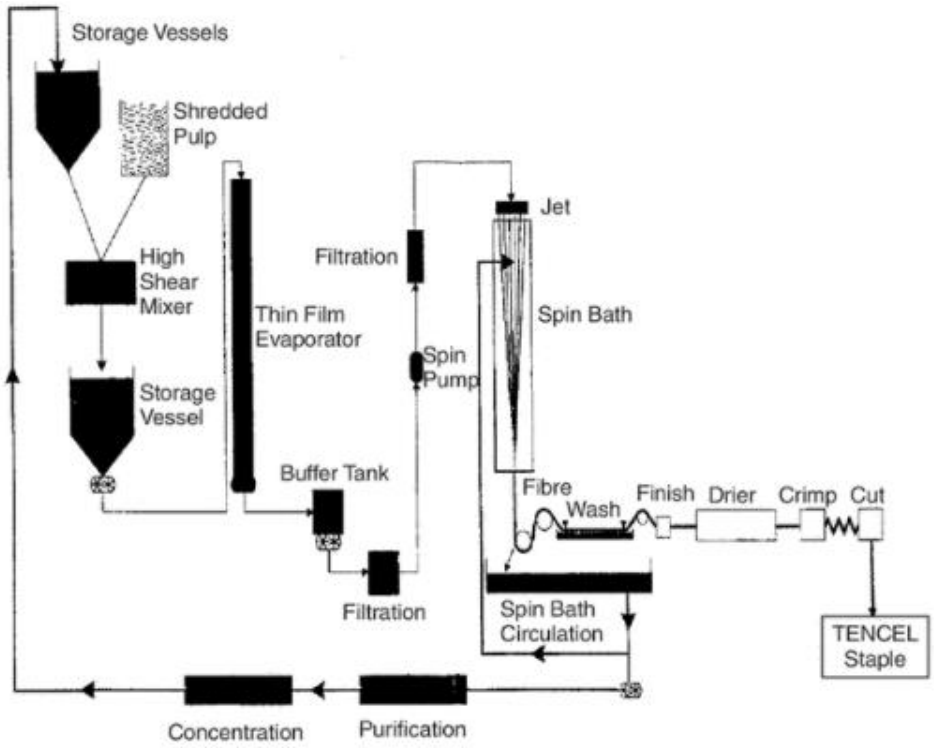

Figure 15. Lyocell process chart (Woodings, & Woodings, 2001)

3.4 Fiber structures

The regenerated cellulose fibers exhibit partial crystalline structure in which the cellulose II allomorph and the amorphous regions alter. The main difference between the native cellulose I and the regenerated cellulose II is that the regenerated cellulose chains can have anti-parallel orientation in contrast to each other, while the native cellulose chains are all parallel. (Eichhorn *et al.*, 2009) The crystallinity of regenerated cellulose is usually lower and in a range of 32-53 %. (Woodings, & Woodings, 2001)
The linear density, also known as titer, is the amount of mass per length unit, and is commonly used for definition of textile fibers. It is commonly measured in dtex units, that is equal to g/10 km. The regenerated cellulose fibers are usually in a range of 1 to 5 dtex. (Woodings, & Woodings, 2001)

The linear density of spun fibers can be estimated from the dope density, cellulose content, spinneret dimensions and the applied total stretching ratio of the fiber. Due to the shrinkage of the fiber during drying and later moisture regain, the realized fiber linear density is higher than could be expected from such estimations. This results in a need for experimental coefficient to predict the linear density of the spun fibers more accurately. The linear density of the formed fibers can be calculated with Equation 3.6. (Hummel, 2015)

$$T = \frac{10^6 * \pi * r^2 * d * c * f}{R_T} \tag{3.6}$$

where T is the linear density (dtex), r is the radius of the spinneret holes (m), d is the dope density (g/cm^3), c is the cellulose mass percentage of the dope, f is an experimental correction coefficient and R_T is the total stretching ratio.

The regenerated fibers acquired by the spinning process can exhibit heterogenous or homogenous structure, with variety of cross-sectional shapes. (Woodings, & Woodings, 2001) The heterogenous type fibers are typical for the viscose process, in which the regeneration process starts at the surface of the immersed dope solution, causing the formation of the prominent skin/ core structure. The skin area is more highly oriented and is thus more tenacious than the core. By modifying the viscose process for example with different additives, the ratio of the skin and core areas can be altered. Nowadays the viscose

process has been modified to such degree that even fibers consisting of only skin can be spun. Lyocell fibers are an example of regenerated fibers with homogenous structure. (Medronho, & Lindman, 2015, Zhang *et al.,* 2018) In the Figure 16 is presented the homo- and heterogenous fiber structures of lyocell and viscose fibers respectively.

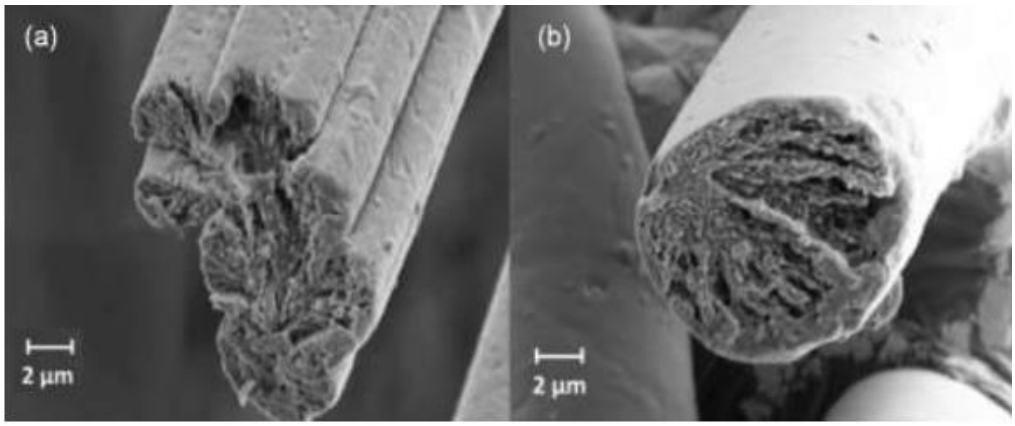

Figure 16. Cross sections of homogenous lyocell (left) and heterogenous skin-core viscose fibers (right) (Zhang et al., 2018)

The shape of the regenerated fiber's cross section can have influence on different properties of the fiber. These include dyeability, luster and moisture regain. (Zhang *et al.,* 2021) For processes like lyocell, Modal and cuprammonium the cross-sections of the spun fibers are usually of circular shape. Serrated cross-section is typical for regular viscose and acetates fibers, while the high tenacity all-skin viscose fibers are bean shaped. (Woodings, & Woodings, 2001). Other possible cross-sectional shapes include hollow, multi-lobal, triangular and square *etc*. In Figure 17 is depicted some possible cross-sectional shapes for regenerated cellulose fibers. (Gupta, 2008).

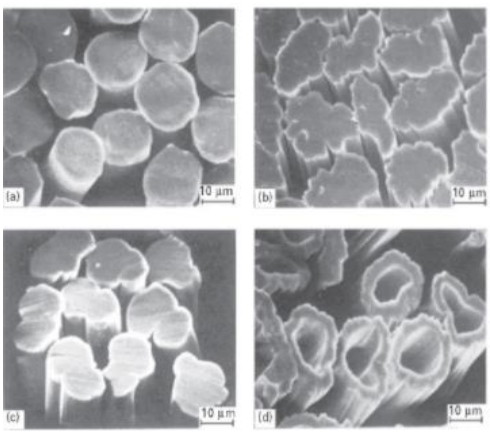

Figure 17. Different cross-sectional shapes of regenerated fibers (Gupta, 2008).

4 Novel sustainable fiber processes

The recent awakening of environmental awareness across the globe has given birth to many novel man-made cellulose fiber manufacturing processes. The main concerns about the widely used viscose process is the need for high amounts of chemicals like sulphuric acid and sodium hydroxide. Also, the derivatization stage uses toxic carbon disulphide (CS_2) to produce cellulose xanthate. (Bialik *et al.,* 2020) The emissions caused by viscose manufacturing has been reported to exceed that of cotton production. (Common Objective) The new greener methods include processes that use the direct route for the cellulose dissolution, involving the use of NaOH as well as additives like ZnO, urea and thiourea as the solubilizing agents. Few examples of these sodium hydroxide-based processes are the NeoCel, Biocelsol and Cellunova. Some methods like the Ioncell-F use ionic liquids to dissolve cellulose in the regenerated fiber production. (Bialik *et al.,* 2020). It is also possible to wet spin fibers without dissolving cellulose as is done in the production of novel Spinnova fibers. (Material district**,** 2018)

4.1 Sodium hydroxide- based processes

The sustainable fiber production methods that are based on direct dissolution in sodium hydroxide are usually coupled with additives to improve the dissolution. For example. the Biocelsol process utilizes sodium hydroxide coupled with ZnO to dissolve mechanically and enzymatically treated pulp, while in the Cellunova production NaOH is combined with urea and thiourea for the process enhancement. (NeoCel, 2020).

Another novel process that uses the caustic soda/ZnO solvent is called the NeoCel. The utilized cellulose is acquired from dissolving pulp that has been modified with enzyme-based pre-treatments for example, and then dissolved continuously in a List reactor. The fibers are spun into coagulation bath composed of H_2SO_4 and Na_2SO_4 system or either into sodium carbonate (Na_2CO_3) and NaOH coagulants. (Bialik *et al.,* 2020). Interestingly, when using sodium carbonate and sodium hydroxide as the coagulation chemicals, the recovery of the chemicals can be conducted using processes already known in the chemical pulp production. These include unit operations like causticizing, recalcination and recarbonization. (Bialik *et al.,* 2020). The life cycle assessment conducted on the NeoCel spinning indicated that the environmental effects of the process could be from 15 to 50 % lower than those of

conventional viscose. (Cordis Europa) The Diagram of the pilot-scale NeoCel process with the chemical recovery is displayed in Figure 18.

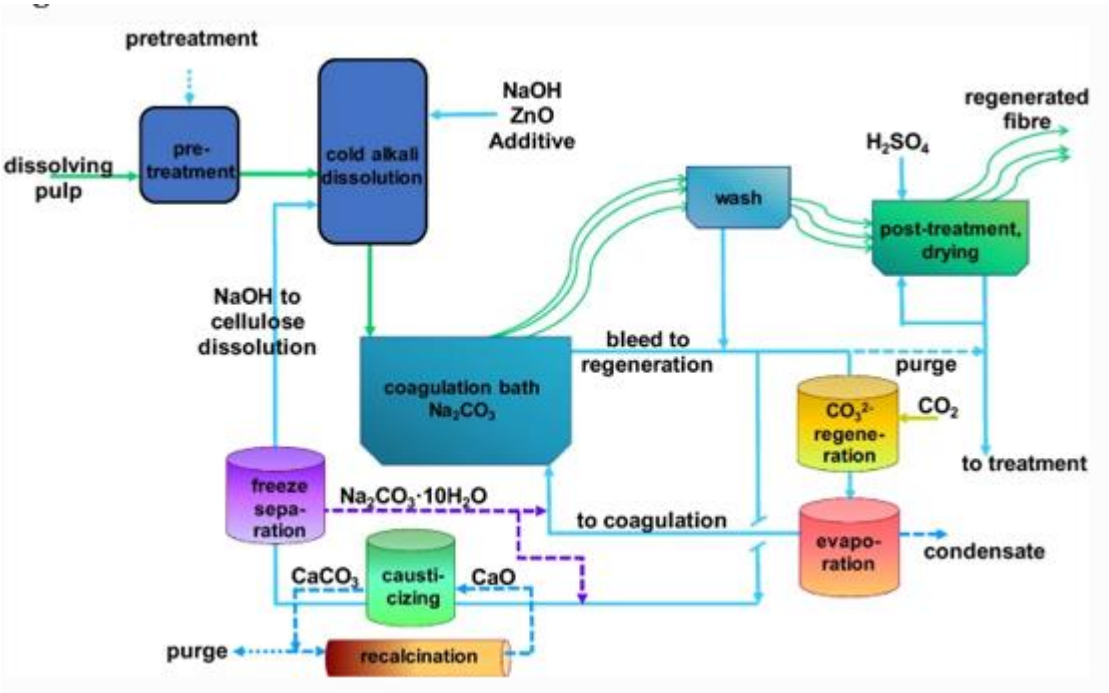

Figure 18. Process diagram for the pilot-scale NeoCel fiber spinning (Bialik et al., 2020).

4.2 Ioncell-F

The goal to replace NMMO as only commercialized direct cellulose solvent in the market lead to rediscovery of ionic liquids (IL) in the early 2000s'. Like the NMMO solvent, IL's also have high capability of cellulose dissolution and can produce fibers of at least equal tensile properties to that of the lyocell process. The ionic liquids also overcome the disadvantage of the lyocell process; the tendency of the NMMO-cellulose-water mixture to produce side reactions that may lead to a dangerous runaway, thus making it the easier and safer option. (Sixta et. al, 2015)

During the early stages of development, the ionic liquids were mostly imidazolium based. The ionic liquids based on imidazolium had one major drawback. At high operating temperatures, the cellulose chains started to degrade, causing the need for addition of stabilizers. The anionic part of the ionic liquids were usually halides, which caused corrosion in the metallic process equipment. The novel non-toxic ionic liquid spinning process developed by Aalto University and Helsinki University utilizes a superbase and acid ion pair known as the 1,5- diazacicyclo [4.3.0] non-5-enium acetate [DBNH][OAc] to produce strong

fibers with stable spinning properties. The process and the fibers produced with a dry jet wet spinning was named the Ioncell-F. (Sixta et. al, 2015)

The Ioncell-F spinning process is like that of the lyocell process. First the dissolution of recycled or new cellulosic material is conducted in temperature of ~80˚C, after which the dope is filtrated and extruded through a spinneret into an air gap. The water coagulation bath can be set at lower temperatures than in the lyocell, contributing to reduced energy consumption. The fiber can then be washed, finished, dried, and cut into desired length. The ionic liquid and water are recycled in the process. (Michud *et al.*, 2016)

The Ioncell-F is planned to be commercialized during the year of 2025. An example of the Ioncell- F production path is introduced in Figure 19. (Ioncell)

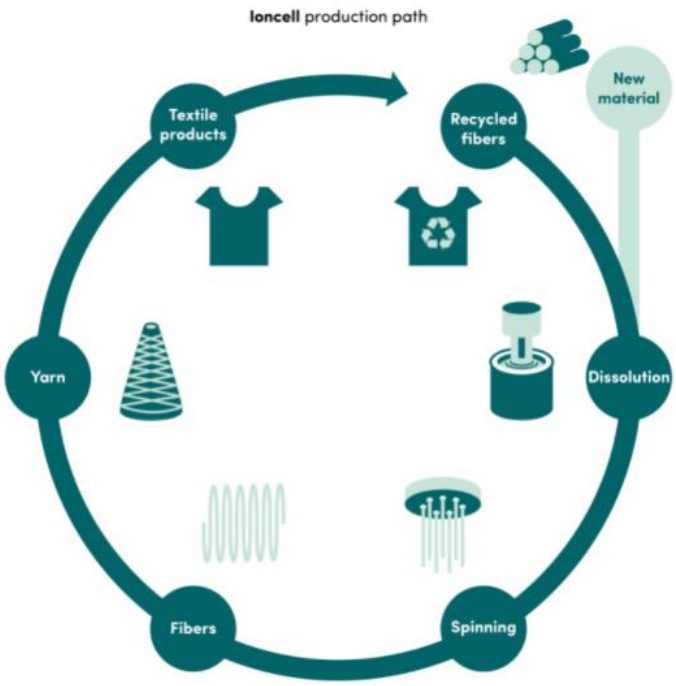

Figure 19. Ioncell-F production path (Ioncell)

4.3 Spinnova

Spinnova is a novel method developed in Finland, to produce cellulose fibers that requires no chemicals in the process. In comparison to most cellulose fiber spinning processes, it does not utilize the method of dissolution/coagulation in the fiber making. First the raw pulp material is ground into a micro fibrillated cellulose (MFC) paste. The MFC is the extruded

through a specialized nozzle that operates at high pressure. This causes rotation of the fibrils and aligning of the cellulose molecules in the flow direction, leading to increased orientation. The extruded fiber is spun through a wet-spinning device, dried and collected into a yarn. The production of Spinnova fibers uses approximately 99 percent less water than is consumed in the production of natural cotton, that is the most common natural fiber used in the textile industry. (Material district, 2018) The first industrial scale plant for the Spinnova production is planned to be opened in 2022. (Innovation in textiles, 2021)

5 Improvement of fiber tensile properties

Tensile strength, also known as, ultimate tensile strength is a measure of the maximum stress caused by stretching or pulling, that can be withstood by a material before its breakage. It is for example used as strength measure of regenerated cellulose films. The tensile strength of a material can be defined with Equation 5.1.

$$F_{TU} = \frac{F}{A} \tag{5.1}$$

where F_{TU} is the tensile strength (Pa), F is the force at break (N) and A is the cross-sectional area of a material (m^2).

In textile application the tensile properties are measured as specific strength of the fibers, due to their cross-sectional areas being hard to measure. The specific strength of textile fibers is called tenacity, which is important indicator of fiber quality. Tenacity can be calculated with Equation 5.2.

$$\sigma = \frac{F}{T} \tag{5.2}$$

where σ is the fiber tenacity (cN/dtex), F is the force at break (cN) and T is the fiber linear density (dtex).

The main parameters that affect the tenacity of a polymer fiber are the crystallite length, fiber degree of orientation in the axis direction, chain length of the polymer and the degree of crystallinity. Parameters like crystallinity index and orientation are highly dependent on spinning parameters like the coagulation bath composition and applied stretching of the filament. For example, the composition of the coagulation bath affects the rate of diffusion of the solvent and anti-solvent, thus controlling the state of the filament in the process. When diffusion rate is low, the regenerated filament is more gel-like and thus higher stretching ratio can be achieved and consequently higher degree of orientation. The rate of diffusion can also control the packing of the crystallites in the fiber. Approximate tenacity of a fiber

can be calculated when these parameters are known with the dimensional Equation 5.3. (Sixta *et al.,* 2015).

$$\sigma = \left(\frac{(Å)}{L} - \frac{1}{DP_N}\right) * C_{RI} * f_t^2\left(\frac{cN}{dtex}\right) \quad (5.3)$$

where σ is the fiber tenacity(cN/dtex), L is the crystallite size (Å), C_{RI} is the crystallinity index, DP_N is the number average degree of polymerization and f_t is the total orientation factor.

The degree of polymerization is mainly controlled by the pre-treatment of the pulp. The higher the DP, the lower the solubility, thus it should be controlled to such level that allows for high fiber tenacity, while simultaneously having sufficient solubility. The degree of orientation is mainly controlled by the applied stretching in the spinning process.

The fiber tenacity can also be influenced by spinning dope additives, which can have effect on various properties. Properties of regenerated cellulose and other cellulosic materials like paper are known to be affected by different post treatments like cross-linking reactions.

This chapter focuses on gathering ideas from the literature regarding the enhancement of the fiber tenacities, which can later be tested on fibers spun with laboratory scale wet-spinning device in the experimental section of the thesis. Different methods are divided to three categories, the first focusing on the alteration of the spinning parameters, second in the spinning dope additives and the third on the post-treatment of the filaments. As the literature regarding reinforcement of cellulose filaments is rather scarce, also the methods to improve tenacity of similar materials like regenerated cellulose or starch films are taken into consideration.

5.1 Spinning parameters

During extrusion through small holes in the spinneret, hydrodynamic shear forces are generated, that are dependent on the hole inner diameter, extrusion speed and the dope viscosity. The shear force in the spinneret can be estimated with Equation 5.4. (Hyun Chan Kim *et al.,* 2019)

$$\tau = \frac{8\eta v_0}{2r} \quad (5.4)$$

where τ is the shear force (Pa), η is the dope viscosity (Pas), v_0 is the extrusion velocity (m/s) and r is the spinneret hole radius (m).

The generated shear forces inside the spinneret can align the cellulose chains along the fiber axis causing increased orientation. In general extrusion velocity and spinneret hole diameter can influence the orientation of the spun fibers and thus the tensile properties of the filament. (Hyun Chan Kim *et al.*, 2019)

Slower coagulation rate promotes the formation of tenacious fibers by increasing the maximum allowed stretch in the spinning process as well as allowing the crystallites to pack in higher order. As the coagulation kinetics is mainly controlled by the diffusion-counter diffusion process, as discussed in earlier chapter, the concentration of the coagulant and its temperature are the two major parameters controlling this process. Of these two parameters, the coagulant concentration has been noted to affect the mechanical properties of the fiber more. Also, the coagulation rate is affected by the type of used coagulant. (Mao *et al.*, 2008)

In some spinning applications like in the viscose process, modifiers or additives are included in the coagulation bath to control the coagulation rate down even further to allow more stretch to be applied. These modifiers can also alter the size of the formed crystallites. As mentioned earlier, for viscose process some known modifiers and additives include quaternary bases, amines, polyethylene oxides and zinc sulphate. (Eriksson, 2015)

Stretching of the fiber, which is controlled by varying the speeds of the godets in the spinning line, is one of the most important parameters to affect the tensile properties of the spun filaments. Increased orientation caused by the stretching contributes to forming of tougher fibers. The maximum allowable stretch is reliant on many parameters as discussed earlier, as well the stage at which the stretching is conducted (usually more preferably after leaving the coagulation bath). The temperature at which the stretching is conducted can also affect the final tensile properties of the filament as is the case when the fiber is stretched in hot acid or water to lock its orientation in a high state. (Eriksson, 2015) The chain alignment can also be locked by minimizing the relaxation of orientation during drying, for example by drying

the fiber under tension. This has been noted to increase the fiber tenacity by 38 % compared to fibers dried in loose bundles. (Wawro *et al.,* 2009).

5.2 Spinning dope additives

Plasticizers are chemicals that can increase the volume between chains of the polymer and make them more mobile, leading to increased flexibility and softness. However, the crystallinity of the polymer decreases due to action of the plasticizer, causing the loss of tenacity in the material. The materials that have opposite effect on the polymer are called anti-plasticizers. In turn, they can decrease the free volume between chains by promoting crystallization of the polymer, causing the polymer to lose its flexibility, while improving its tenacity at ambient temperature. The anti-plasticizers can form intermolecular hydrogen bonds between polymer chains contributing to the enhanced properties. (Biswas *et al.,* 2020)

A novel anti-plasticizing material for enhancement of textile fiber tenacity has been reported in the recent literature. This substance is the called the glucaric acid. It can be derived from glucose, or for example obtained from depolymerization products of lignocellulosic material. The ammonium salts of the glucaric acid are also reported to act as an anti-plasticizer. The anti-plasticizing properties originate from the polar oxygen atoms in the glucaric acid or its salts that can form tight hydrogen bonds with the cellulose chains. The presence of these new bonds leads to the new crystal conformations of the matrix polymer. (Biswas *et al.,* 2020)

In one study, derivatized cellulose acetate was dissolved in acetic acid in the presence of the glucaric acid or its ammonium salt (ammonium glucarate). The formed spinning dope was extruded through a needle syringe and coagulated in tap water of ambient temperature. The regenerated fibers were spun on a winder, and drawn in hot air, followed by drawing in hot oil bath. The tenacity of the formed fibers improved up to 55 % upon the addition of the glucaric acid or its ammonium salt. The studies indicated higher molecular mobility at drawing temperatures above 145 °C caused by the anti-plasticizer, as the possible draw ratio increased as a result from the additive inclusion. This was accounted to glucaric acid having a melting temperature of 125 °C causing increased mobility within the cellulose acetate / additive fiber. The achieved higher drawing ratios contributed to the noted tenacity increasements. (Biswas *et al.,* 2020)

Fu et al. made a discovery that silver nitrate ($AgNO_3$) can be reduced into silver nanoparticles in the presence of sodium hydroxide based spinning dope at ambient temperature. The authors conducted a spinning experiment with a pilot scale equipment to study the effect of the silver nanoparticles on various fiber parameters like tenacity, photocatalytic properties. A cold dissolution for the cotton linter pulp was conducted with NaOH-Urea-ZnO solvent system, followed by the mixing of $AgNO_3$ into the spinning dope. The dope was wet spun into a sulphuric acid coagulation bath and the formed fibers were drawn in the coagulation bath with several draw ratios. The fibers were then washed and finished with oil before drying. After addition of the $AgNO_3$ into the spinning dope, the fiber tenacity increased by 38 %. (Fu *et al.*, 2018)

The reduction of Ag^+ and incorporation of silver nanoparticles is displayed in Figure 20.

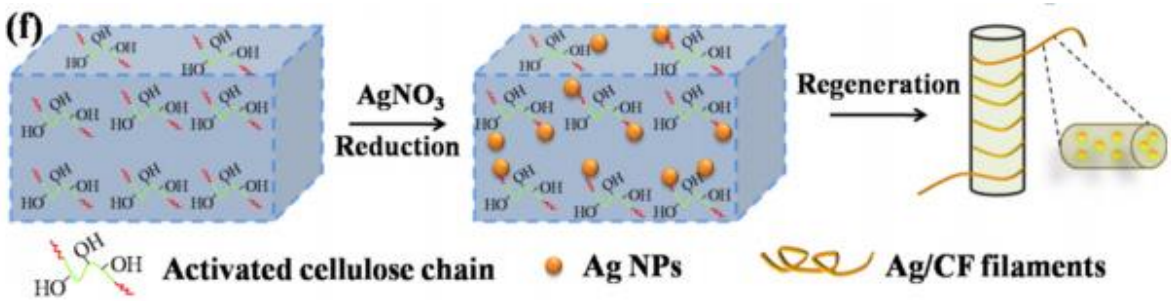

Figure 20. Silver cation reduction and forming of cellulose/silver composite fiber (Fu et al., 2018)

It was believed that the damaged hydrogen bond networks caused by the action of NaOH and urea, activated the hydroxyl groups of the cellulose, which in cooperation with the reducing ends of the cellulose caused the reduction of the Ag^+ cations into Ag nanoparticles. The nanoparticles were stuck inside and at the surface of the fiber after immersion of the dope into the coagulation bath. The uniform dispersion of the silver nanoparticles was thought to cause favorable interfacial bonding in the formed fiber/nanoparticle composite contributing to its increased tenacity. (Fu *et al.*, 2018)

Nanocellulose is a tough material that can be used as a reinforcing component in various polymer blends. For this material to be used as a spinning additive, the aspect ratio of the nanomaterial cannot be high, as the small holes of the spinnerets can get blocked due to the tendency of the high aspect ratio material to get entangled. In an article by Yao *et al.*,

microcrystalline cellulose was milled into rod-like cellulose nanocrystals (CNC), that was mixed with viscose spinning dope to produce all-cellulose composite fibers. The viscose spinning dope and CNCs at various concentrations were mixed with mechanical stirring for two hours at ambient temperature, spun with a wet-spinning device and the formed filaments tested for their tensile properties. The effect of the CNC particle size and aspect ratio on the fiber properties was also tested by centrifugation of the cellulose nanocrystals into samples of varying particle dimensions. The addition of CNCs into the viscose dope reinforced the regenerated fiber and the highest tenacities were found to be when the aspect ratio and the particle diameter were at their lowest, while the CNC concentration was at its highest. The maximum tenacity enhancement was found to be 24 % compared to a sample with no CNC addition. In Figure 21 is presented the diagram of the composite fiber spinning scheme. (Yao *et al.*, 2020)

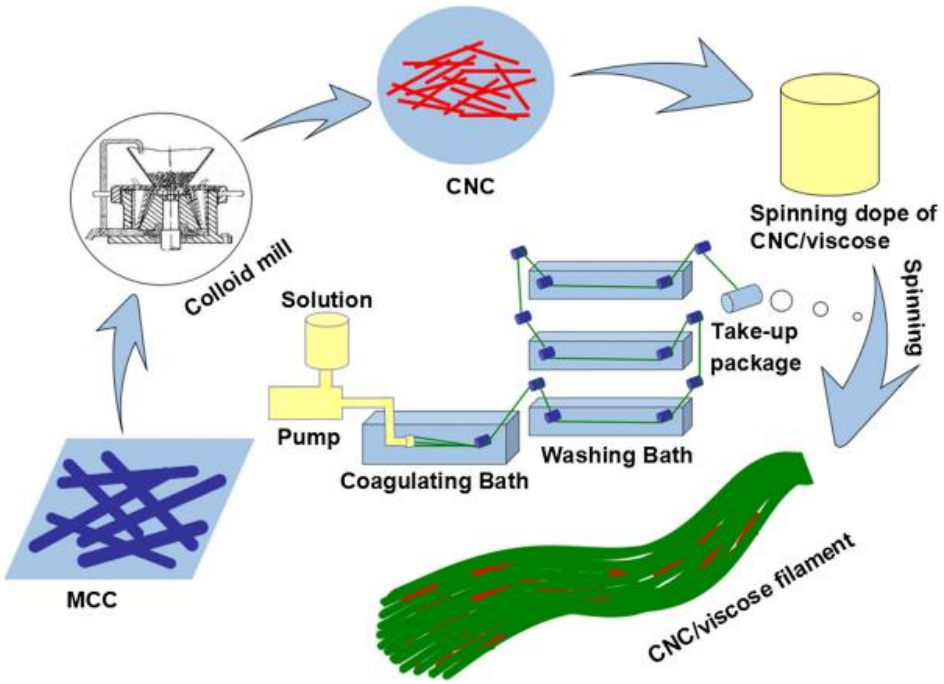

Figure 21. Diagram of the composite fiber spinning scheme (Yao et al., 2020)

In the experiments conducted by Anderson Trojer et al. cellulose was dissolved in 1-ethyl-3-methylimidazolium acetate (EMIMAc) solution, in which silica nanoparticles were mixed. Regenerated fibers were then attained by coagulating the spinning dope in a water/DMSO bath with varying DMSO concentrations. The final SiO_2 content was 10 % of the fiber dry weight. The addition of silica nanoparticles led to tensile strength improvement of up to 62

%. The reinforced fibers demonstrated increased orientation, which could be the underlying reason for the noticed improvements. (Andersson Trojer *et al.,* 2019)

One study suggested the usage of carboxymethyl cellulose in a composite film material comprised of NFC in addition. The raw material was mixed with a magnetic stirrer for 25 hours, after which they were tape casted onto polyimide supports and let to dry overnight in ambient temperature, after which they were further dried in 75 °C for 24 hours. The final films had varying CMC content, and the films containing 10 w-% of CMC had improved tensile strength of up to 42 %. This was thought to be caused by the CMC's ability to reduce the cellulose fibril to fibril interactions, allowing the film to orientate more due to action of the shear forces in the tape-casting device. The NFC/CMC composite films were also treated with glycidyl trimethylammonium chloride to increase the level of ionic cross-linking in the films to enhance their wet strength. (Pahimanolis *et al.,* 2013)

Cellulose dissolved in NaOH/urea solvent was mixed with chitin nanocrystals to produce dope, that was extruded though a needle into a sulphuric acid/sodium sulphate coagulation bath. The obtained regenerated fibers were then washed and dried. The composite fibers that contained 2 % of chitin nanocrystals from the fiber dry weight had an improved tenacity of 27 % in comparison to fibers without the additive. These effects were explained by the action of strong hydrogen bonds between the cellulose chains and the chitin nanocrystals, as well as the increased fiber alignment caused by the additive. (Chen *et al.,* 2017)

The optimum dope additive concentrations as well as realized tensile strength improvements found from the literature are gathered in Table 1.

Table 1. The effect of additives on the tensile strength of different materials

Starting material	Solvent	Coagulation bath	Product type	Additive	Additive content w-% of o.d. pulp	Tensile strength improvement (%)	Ref.
Cellulose acetate	70 % Acetic acid/	Tap water (Ambient temperature)	Filament	Glucaric acid	1,5	55	(Biswas *et al.*, 2020)
Cellulose acetate	70 % Acetic acid/	Tap water (Ambient temperature)	Filament	Ammonium glucarate	1,5	38	(Biswas *et al.*, 2020)
Cotton linter pulp	7 % NaOH/ 12 % Urea/ 0, 5% ZnO	10 % H2SO4 (20 °C)	Filament	$AgNO_3$	2,5	38	(Fu *et al.*, 2018)
Viscose dope	-	115g/L H_2SO_4/ 220g/L Na_2SO_4 12g/L $ZnSO_4$	Filament	CNC	1	24	(Yao *et al.*, 2020)
Cellulose pulp	28 % EMIMAC	Water/DMSO	Filament	SiO_2	10	62	(Andersson Trojer *et al.*, 2019)
NFC	-	-	Film	CMC	11	42	(Pahimanolis *et al.*, 2013)
Cotton linter pulp	7 % NaOH/ 12 % Urea	15 % H_2SO_4/ 10 % Na_2SO_4	Filament	Chitin nanocrystals	2	27	(Chen *et al.*, 2017)

5.3 Post-treatment

Mercerization is a process in which the transformation of cellulose I into cellulose II occurs due to action of sodium hydroxide. It is thought that the Na^+ cations can disturb the hydrogen bonding network in the cellulosic material causing rearrangement of the crystalline structure as well as the amorphous and semi-crystalline regions during the mercerization. Thus, it has

been noted that this process can improve the crystallinity of for example regenerated cellulose leading to improved tensile properties as could be expected from the Equation 5.3. (Nomura *et al.,* 2020)

In a certain article, regenerated cellulose films were mercerized with different concentrations of NaOH solution for 2 hours in various temperatures. The procedure was followed by the neutralization of the samples with 20 % solutions of H_2SO_4, CH_3COOH or H_3PO_4. Optimum conditions for the process were found to be at 80 °C and neutralization with sulphuric acid, leading to 64 % increase in crystallinity index measured with Nuclear magnetic resonance. Unfortunately, the tensile properties of the samples were not measured. (Nomura *et al.,* 2020)

TEMPO oxidation is a method that utilizes a toxic (2,2,6,6-Tetramethylpiperidin-1-yl)oxyl chemical to selectively oxidize hydroxyl groups in cellulose to carboxylate groups with sodium counter ions. It has been noted that by exchanging the Na^+ cations with higher valency ions like calcium or magnesium, the formation of cross-linkages between fibrils can occur. This has been found to increase the tensile properties of for example casted films.

One experiment utilized oxidized Na^+ form microfibrillated cellulose hydrogel obtained from various pulp types like never dried or heat-treated pulp in film casting process. The oxidized hydrogels were placed on a film mold and immersed into salt baths containing 0.3 mol/l of either $CaCl_2$ or $MgCl_2$ for three hours. The films were dried, followed by washing of the excess salts, and then dried again in ambient temperature. The ion concentrations of the samples were measured with flame atomic absorption spectroscopy. This confirmed the succeeding of the ion exchange process. When examining for example the films made from heat treated oxidized pulp samples, the tensile indexes were enhanced by 65 and 57 % when the sodium ions were exchanged with Ca^{2+} and Mg^{2+} cations, respectively.

CNF films were prepared by a solution casting method. These films were then immersed into a 50 % glutaraldehyde solution in the presence of HCl acid catalyst to promote the formation of acetal bonds between the cellulose molecules and the aldehyde. The cross-linking reaction was done in ambient temperature. The reaction time varied from 0 to 5 h. The residual cross-linker was washed from the films, and they were dried in room temperature for a day. The cross-linked films with a reaction time of one hour exhibited improved tensile strength of 180 %. The improvements were explained by the formation of

the covalent acetal bonds within the films. (Khanjani *et al.*, 2019) Another study using aldehyde cross-linker in the enhancement of cellulose tensile properties was conducted by Quero et. al. In this study bacterial cellulose was cross-linked in 5 % glyoxal solution in the presence of aluminum sulphate hexadecahydrate catalyst. The bacterial cellulose was immersed in the cross-linker solution for 5 hours, after which the reaction was completed in 150 °C for 15 minutes. Thus, obtained samples exhibited wet tensile strength increasement of up to 676 % in comparison to non- treated samples. (Quero *et al.*, 2011)

Paper product was prepared from a composite mixture of cellulose and PVA fibers. The mixture of these fibers was uniformly pressed, dried, and cut into paper strips. These strips were then impregnated in a potassium zirconium carbonate (KZC) solution of varying concentrations. After the completion of impregnation, the excess cross-linker was removed by pressing and the strips were dried at 90 °C. When cross-linking the paper composite with KZC solution of 7 w-%, the tensile strength of the paper strips increased by 153 % in comparison to non-cross-linked strips. (Lahtinen, 2009)

The optimum treatment conditions and their effects on several properties of the post-treated samples, reported in the literature can be found in the Table 2.

Table 2. The effect of post-treatment on varying properties of different materials

	Treatment						
Starting material	Type	Material	Material content	Time (min)	Temperature (°C)	Noticed improvement	Ref.
Regenerated cellulose film	Mercerization	NaOH	10 w-%	Immersion (120)	Immersion (80)	Crystallinity index 64 %	(Nomura *et al.*, 2020)
Heat treated Oxidized MFC film (Na^+ form)	Impregnation	CaCl2	0,3 mol/l	Impregnation (180)	Impregnation (Ambient)	Tensile index 65 %	(Khanjani *et al.*, 2019)
Heat treated Oxidized MFC film (Na^+ form)	Impregnation	MgCl2	0,3 mol/l	Impregnation (180)	Impregnation (Ambient)	Tensile index 57 %	(Khanjani *et al.*, 2019)
CNF film	Impregnation/ crosslinking	Glutaraldehyde/ HCl catalyst	50 w-%	Impregnation/ crosslinking (60)	Impregnation /cross-linking (Ambient)	Tensile strength 180 %	(Jeon *et al.*, 2019)
Bacterial cellulose	Impregnation/ crosslinking	Glyoxal/ Aluminum sulfate hexadecahydrate catalyst	Glyoxal (5 w-%) Aluminum sulfate hexadecahydrate (1g/L)	Impregnation (300) Crosslinking (15)	Impregnation (Ambient) Crosslinking (150)	Wet tensile strength 676 %	(Querо *et al.*, 2011)
Cellulose/ PVA fiber composite	Impregnation	KZC	7 w-%	Impregnation (Not reported)	Impregnation (Ambient) Drying (90)	Tensile strength 153 %	(Lahtinen, 2009)

6 Experimental

The experimental part of the thesis focuses on the improvement of the fiber's tensile properties by various methods, including altering of spinning parameters and different post-treatment types. To better understand the effect of the most important factors in the spinning process, a multi- variable statistical analysis tool known as the Taguchi method was utilized in the experimental section. The fiber chemical properties like the crystallinity index, crystallite size and orientation were determined for selected fibers using FTIR and WAXS.

6.1 Materials & methods

6.1.1. Pulp preparation and dissolution

The pulp samples for spinning trials were provided by UPM and was used as such. Different pulps were then dissolved in a cold alkali-based process, in which the solubility as well as the stability of the spinning dope was enhanced with the help of additives.

6.1.2 Brookfield viscosity

The Brookfield viscosities, which is an indicator of the flow resistance, of different spinning dopes were measured to assist in the prediction of spinnability and to observe the phenomena, like the gelation, that can cause increased variation in the tensile results and reduction in the fiber quality. The measurements were conducted at corresponding shear rates of spinning velocities using the rotational Brookfield DV1MRVKB0 digital viscosimeter with RV-6 spindle according to mod. SCAN-P 50:84 standard. (Ametek)

6.1.3. Dope quality microscopy

The quality of the spinning dope was assessed using a Zeiss Axio Imager 2 bright-field microscope. The method was conducted with an internal standard method in which the different undissolved fiber types were counted from a specified sample amount. These fiber types are categorized into Fiber A, Fiber B and Fiber C types. The quality of the dope background was also estimated with reference images from quality grades from 1 to 7, with the value 1 having a clear background without the presence of particles. The value 7 refers

to a dope that has undergone a gelation process, with the presence of countless small particles. (ZEISS)

6.1.4. Wet spinning of the fibers

The cellulose fibers were spun, by pumping the dope with a gear pump through a spinneret containing 250 holes with a diameter of 60 µm into a regeneration bath of varying compositions. The formed fibers were taken up by the first godet, stretched with various stretching ratios and washed in three consecutive washing baths. The collected samples were then stored in sample holders having a mixture of absolute ethanol and 0.25 ppm of Berol spin 653 surfactant to help in the separation of the fibers during drying.

6.1.5. Tensile testing

The tensile properties of the fibers were measured with Textechno Favigraph tensile tester according to ISO 5079:1995 standard from the average of 10 separate filaments. The main studied tensile parameters in this thesis are tenacity and elongation at break. (Textechno)

6.1.6 FTIR

The total crystallinity index (TCI) of selected filament samples were determined using a Fourier transform infrared spectroscopy method based on internal standard, in which the TCI is determined using the peak intensity ratio between 1 370 cm^{-1} and 2 900 cm^{-1}, that describe the CH bending and stretching respectively. The measurements were conducted with Nicolet 6700 analytical FTIR spectrometer coupled with OMNIC spectrum analysis software. (ThermoFisher)

6.1.7. WAXS

The total orientation degree, crystallinity index and crystallite sizes of filament samples were obtained from the diffractogram data provided by the XEUSS wide-angle x-ray scattering device with a 2D detector. Copper anodes were used in the process to generate Kα radiation with the wavelength of 1.54 Å. The diffraction angle $2\boldsymbol{\theta}$ was between 0.04 and 48.7 ° in the

measurements. The orientation degree was calculated using specialized software XSACT, and the crystallinity index and crystallite size were determined using separated diffractogram peaks obtained by a peak fitting software Fityk's deconvolution method. A specialized .LUA- script was constructed for the Fityk software to enable batch processing of the WAXS data and to make the crystalline property results more comparable. The crystallinity index results from the FTIR method and the WAXS method are compared to examine the validity of the method. Commercial viscose and lyocell fiber samples are used as references in the analyses. (Xenocs)

6.2 Results

6.2.1 Spinning parameters

The effect of spinning parameters on tensile properties of fibers were tested using a laboratory scale wet spinning device. S multivariable experimental method known as the Taguchi design was also utilized in the experimental section of the thesis. The main chemical properties affecting the fiber tenacity according to Equation 5.3 were measured from few different fibers. The properties of the utilized spinning dopes in the experimental part are listed in Table 3

Table 3. Dope quality properties of the spinning experiments

Sample	Brookfield		Dope quality				Results in Figures
	Viscosity (mPas)	temperature (°C)	Fiber A	Fiber B	Fiber C	Background	
	mPas	°C	1/g	1/g	1g		
1	7 240	3.4	61	91	333	2	22, 23
2	5 520	4.6	40	120	400	3	24, 25
3	6 660	6.2	0	38	462	2	26, 27, 28, 29
4	5 560	4	0	32	194	3	30, 31
5	6 380	3.8	0	39	469	3	32, 33
6	6 220	4.3	0	79	315	3	34, 35
7	4 020	6.2	151	302	528	3	36, 37, 38, 39
8	5 130	4.8	287	323	72	3	36, 37, 38, 39

6.2.1.1 Regeneration bath temperature

As discussed, temperature of the regeneration bath is an important parameter affecting fiber strength. (Mao *et al.,* 2008) A spinning dope was prepared from a cellulose pulp using cold-alkali dissolution method. It has been noted in earlier research, that a fiber with good spinnability can be produced when the Brookfield viscosity of a dope is in the range of 4 000 to 8 000 mPas. The number of undissolved fibers and background type are also counted to observe the quality of the produced dope.

Four different temperature levels of the regeneration bath (level 1 is the smallest and level 4 largest temperature) were tested with varying stretching ratios. It could be assumed that lower temperature accounts for slower diffusion rate and thus allows higher stretching ratio to be achieved in the process. Figure 22 shows that the maximum stretching ratio without fiber breakage was only 1.6 for the lowest temperature while with the higher temperature levels the maximum ratio increased to 1.7. One theory that could explain this phenomenon is that while the overall diffusion rate is lower, more salt is trapped into the forming fiber, and the trapped salt crystals act as discontinuity points. When the stretching increases, so do the stresses on these weak points, causing the fiber to break. The best fiber tenacities were obtained with temperature levels 2 and 3 that produced similar quality fibers. When the temperature was increased to level 4, a drop in the tensile properties of the fiber could be observed. This is caused by the fast solvent/anti-solvent diffusion, that leads to pre-mature locking of the fiber structure. The following stretching then leads to lower orientation degree of the fiber as the stiffer fiber structure accepts stretching less readily than a softer one. The tenacities of the filaments as a function of stretching ratio in different temperature levels are presented in Figure 22. The error bars in the Figure 22 represent the standard deviation of each trial point.

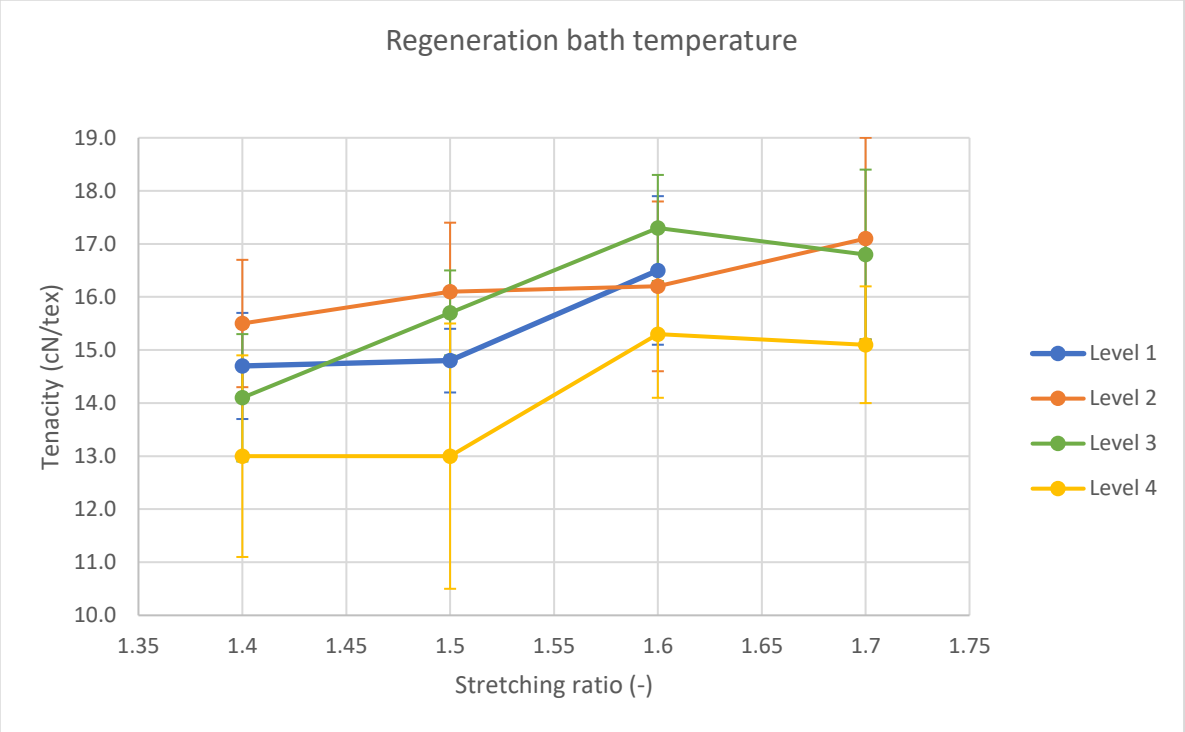

Figure 22. The tenacity of fibers as a function of stretching ratio for different temperature levels displayed as average from 10 parallel filaments ± standard deviation

The elongation at break of the filaments as a function of tenacity are presented in Figure 23. As is expected, with an increase in fiber tenacity, the elongation at break decreases. The standard deviations of the elongation results are quite high between 2 and 4 %.

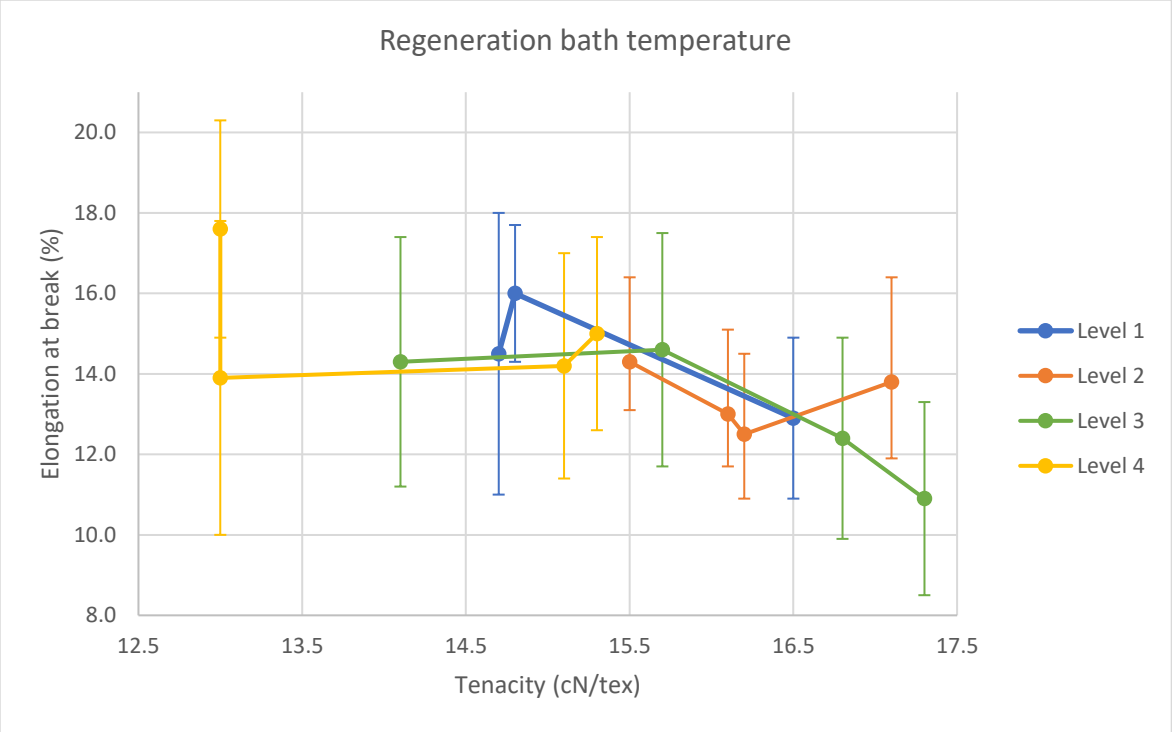

Figure 23. Elongation at break of the fibers as a function of tenacity in different temperature levels displayed as average from 10 parallel filaments ± standard deviation

6.2.1.2 Spinning dope temperature

The temperature of the spinning dope is an important factor affecting the solubility and stability of a cellulose dope. In cold alkali solvent systems, high temperatures cause the gelation of a dope, in which the reformation of hydrophobic interactions and the hydrogen bonds occurs, leading to formation of small gel particles. This is not optimal for the strength of filaments as the gel particles can disrupt the fiber structure by acting as points of weakness. To prevent the initial steps of the gelling process, a cooling loop was added before the spinneret. The loop was made of metal tube that was immersed into a salt-water bath with a slightly negative temperature, which can be observed as the level 1 spinning temperature in Figure 24. For a reference, the spinning dope was not cooled, which can be noted as the level 2 temperature in Figure 24. The tenacities of the filaments as a function of stretching ratio in different temperature levels are presented in Figure 24.

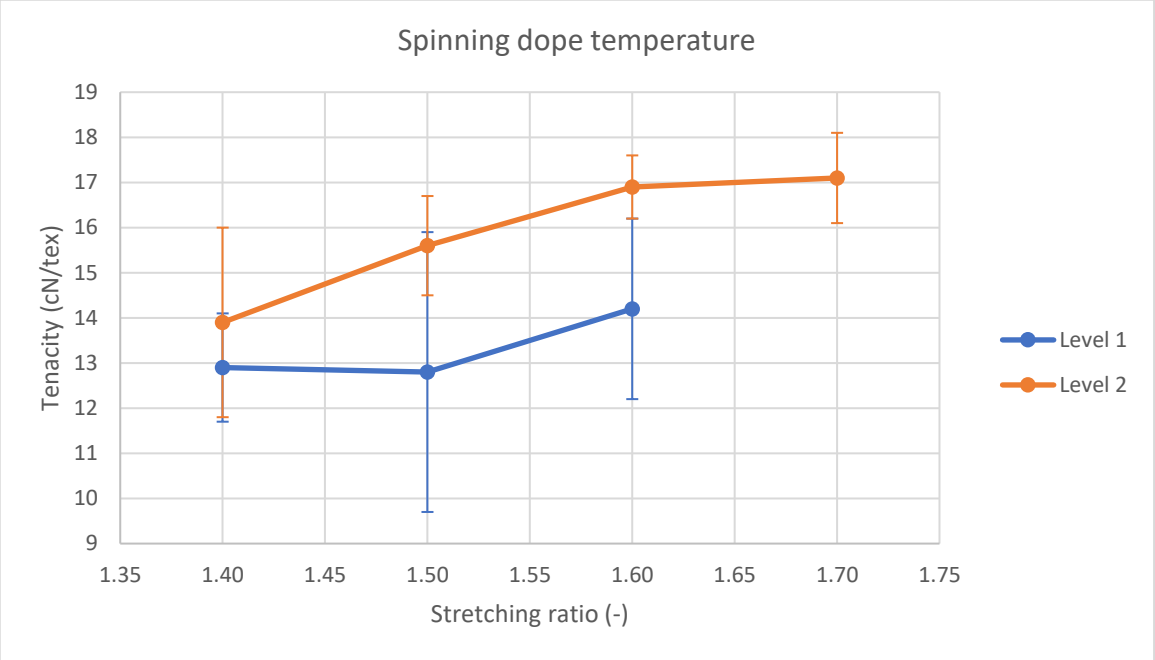

Figure 24. The tenacity of fibers as a function of stretching ratio in different dope temperature levels displayed as average from 10 parallel filaments ± standard deviation

From the Figure 24 can be seen that the lower spinning dope temperature did not increase the tenacity of the spun fibers. This is thought to be caused by a failure in the experimental set-up. At first the cooling solution was set to too low temperature, which caused the freezing of the spinning dope. The frozen dope was then melted with hot air-blower, that might have also caused the gelling of the dope to take place, as the heat transfer in the metal tubing was very efficient and the volume of the dope inside the tube was very small. The formed gel particles then weakened the regenerated fiber structure and caused the decreasing of the fiber tenacity. Due to limits in the time schedule the tests were not tried to be repeated. The elongation at break of the filaments as a function of tenacity can be observed from Figure 25.

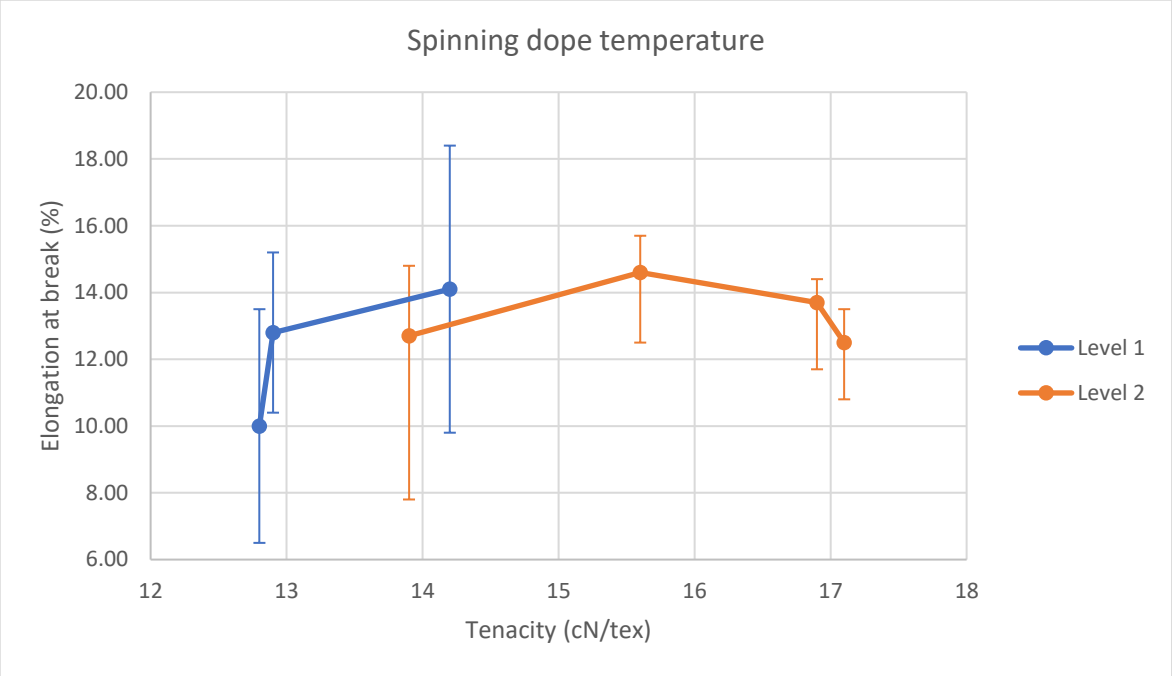

Figure 25. Elongation at break of the fibers as a function of tenacity in different dope temperature levels displayed as average from 10 parallel filaments ± standard deviation

6.2.1.3 Hot stretching

The temperature of the second washing bath in the spinning device was adjusted to near the boiling point of water to lock the orientation in the fiber structure as discussed earlier in the thesis. This should lead to increased filament orientation improving the fiber tenacity. The tenacities of the filaments as a function of stretching ratio in different temperature levels of 2nd washing bath are presented in Figure 26. The temperature level 1 indicates lower temperature, while the level 2 is the higher temperature.

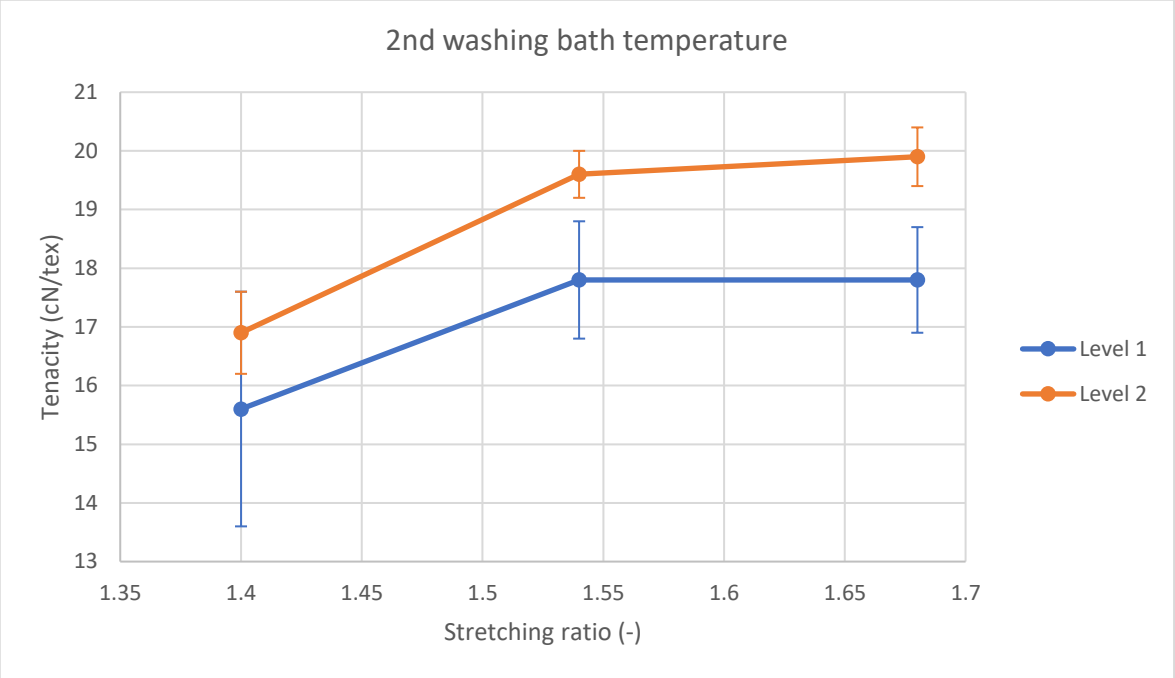

Figure 26. The tenacity of fibers as a function of stretching ratio in different 2nd washing bath temperature levels displayed as average from 10 parallel filaments ± standard deviation

As seen from Figure 26 the tenacity of filament is increased with an increasement in the 2nd washing bath temperature as expected. The most durable fibers in the experiment reached almost 20 cN/tex tenacity with the 2nd washing bath temperature level 2 and stretching ratio of 1.68. The elongation at break of the filaments as a function of tenacity is depicted in Figure 27.

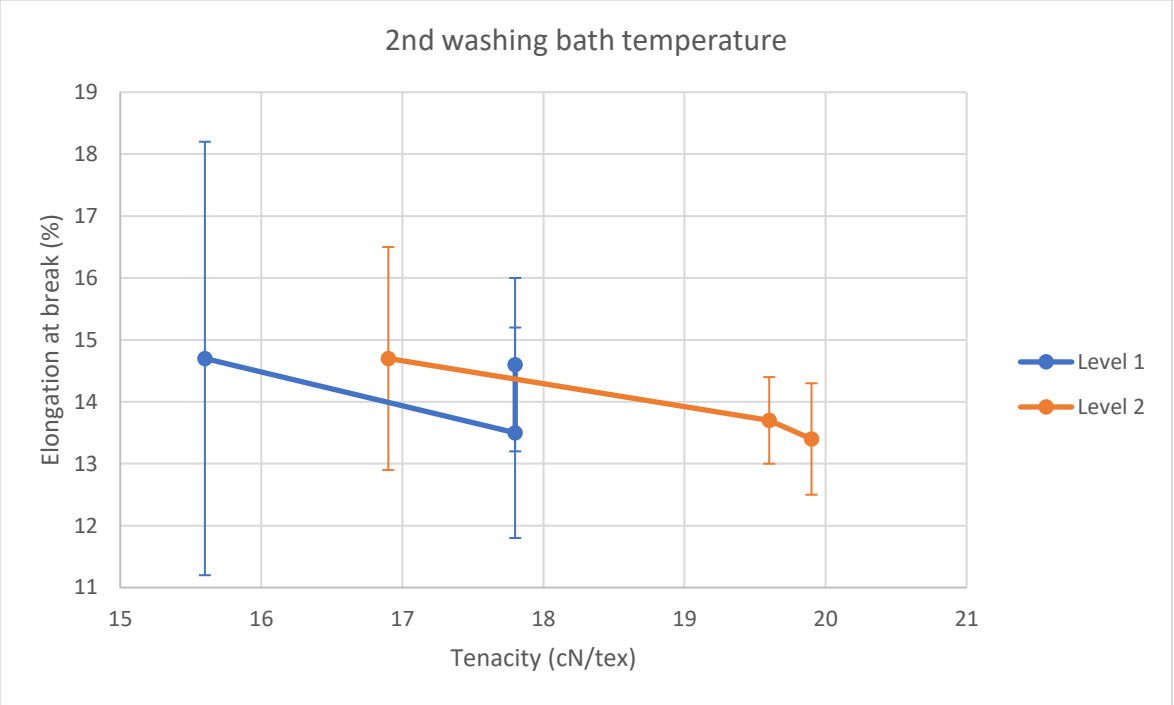

Figure 27. Elongation at break of the fibers as a function of tenacity in different 2nd washing bath temperature levels displayed as average from 10 parallel filaments ± standard deviation

6.2.1.4 Multistage stretching

Stretching of the filament is usually conducted right after the fiber leaves the regeneration bath *e.g.*, in the 1st washing bath. In this experiment it was tested if stretching the fiber in multiple stages produced different quality fibers compared to the stretching done in one stage. The samples marked as "1-stage" were done by stretching the fiber only in the 1st washing bath, while the samples marked as "2-stage" were done by first stretching the fiber in the 1st washing bath with 1.4 stretching ratio and then by increasing the stretching in the 2nd washing bath. The tenacities of the filaments as a function of stretching ratio in multiple stretching stages is presented in Figure 28.

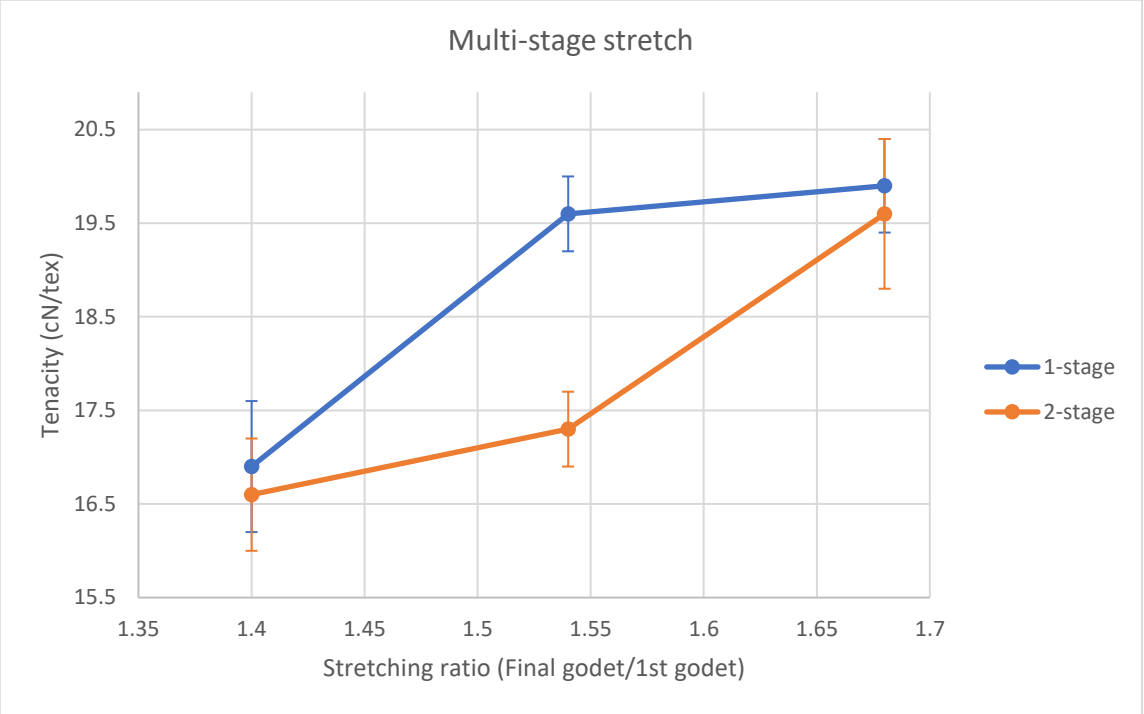

Figure 28. The tenacity of fibers as a function of stretching ratio in multiple stretching stages displayed as average from 10 parallel filaments ± standard deviation

From Figure 28 can be seen that the fiber tenacities were of similar level, when conducting the stretching process in one or two stages, with the exception of the trial point with a 1.54 stretching ratio, that displayed a tenacity of over 19.5 cN/tex with 1-stage stretching technique, while the tenacity stayed in the 17 cN/tex range for 2-stage stretch. The elongation at break of the filaments as a function of tenacity for different stretching techniques is displayed in Figure 29.

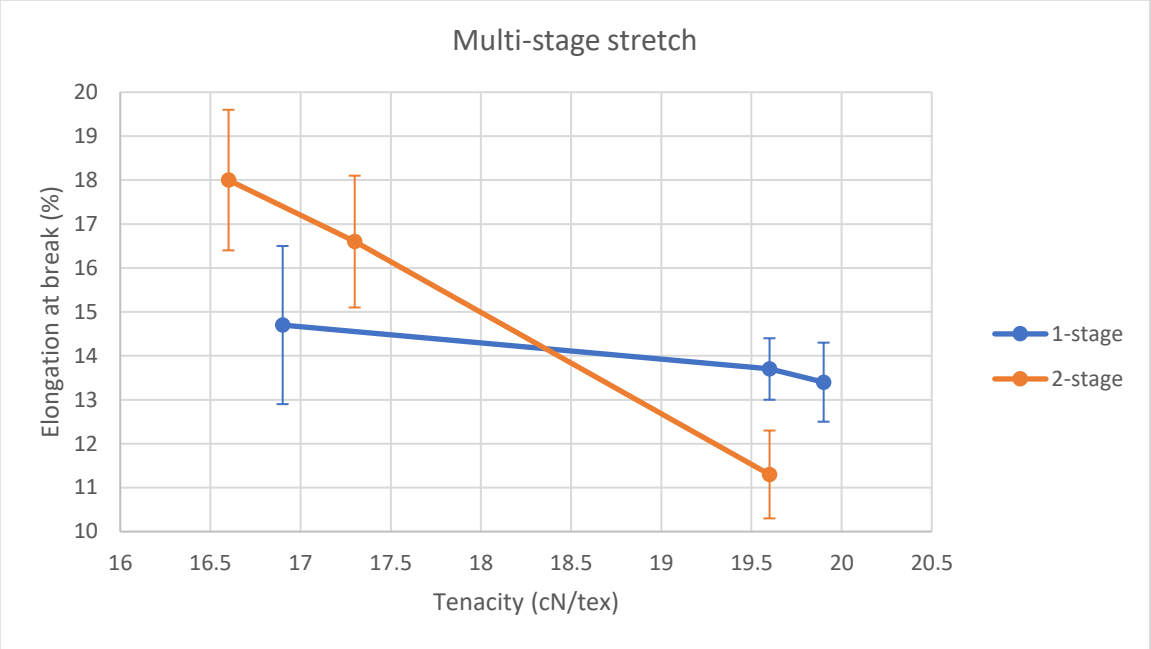

Figure 29. Elongation at break of the fibers as a function of tenacity in multiple stretching stages levels displayed as average from 10 parallel filaments ± standard deviation

6.2.1.5 Regeneration bath composition

The composition of the regeneration bath is important in determining the final properties of the spun fibers as it affects the solvent/anti-solvent exchange rate. The examined regeneration baths compositions in this experiment are weakly and strongly acidic. It was believed that when regenerating the fiber in a weak acid, the diffusion rate is lower than when using the strong acid solution. This would cause the filament to be in a more gel-like state, leading to the increasement of the possible applied stretch in the process. The fibers spun from weak acid solution would thus possess better mechanical properties than the filaments spun from the strong acid solution. The tenacities of the filaments as a function of stretching ratio with different regeneration bath compositions are presented in Figure 30.

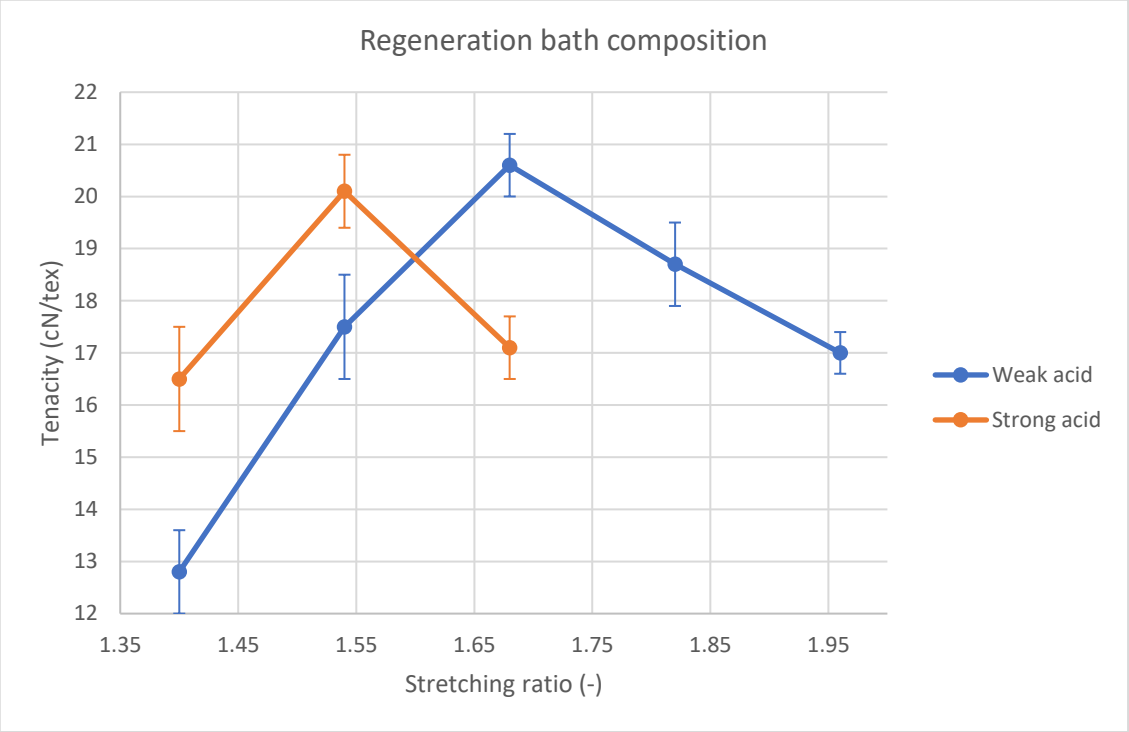

Figure 30. The tenacity of fibers as a function of stretching ratio in different regeneration bath compositions displayed as average from 10 parallel filaments ± standard deviation

The hypothesis that the weakly acidic regeneration bath produces more stretchable and tenacious fibers seemed to be correct as can be seen from Figure 30. The maximum stretching ratio increased from 1.68 to 1.96 when changing the regeneration bath from strongly to weakly acidic. The maximum fiber tenacity also increased by a small margin from 20.1 to 20.6 cN/tex. This improvement could also be originated from variation in the process. As can be seen from Figure 31 the fibers spun from weak acid solution had higher elongations at break with similar tenacity levels. The elongation at break of the filaments as a function of tenacity with different regeneration bath compositions is depicted in Figure 31.

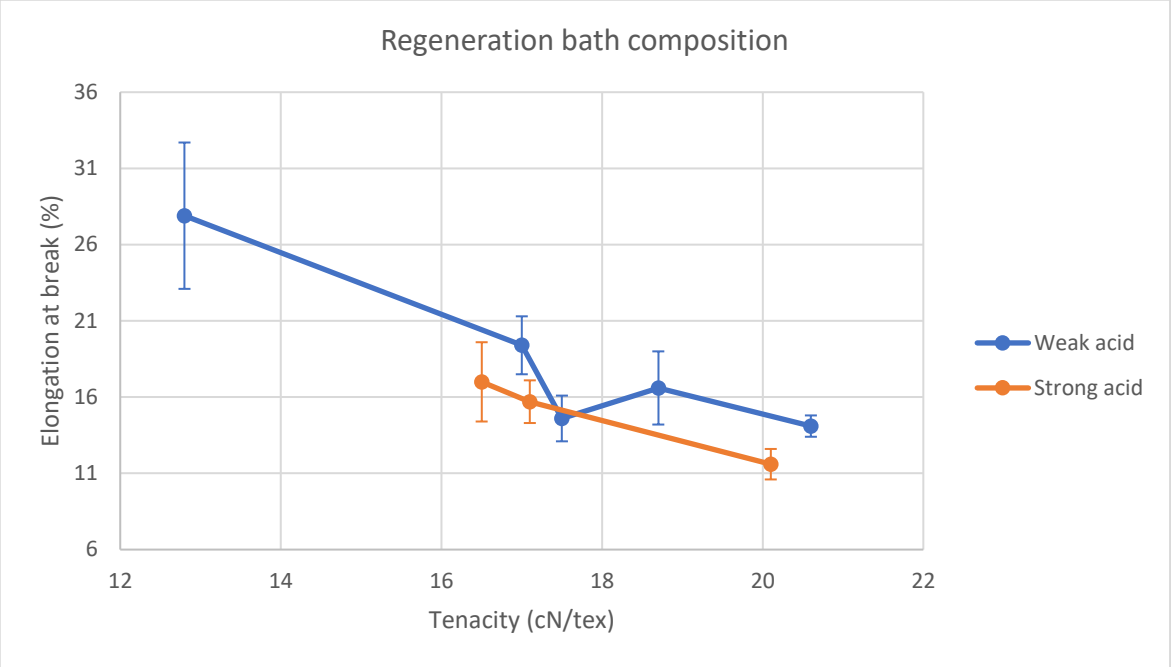

Figure 31. Elongation at break of the fibers as a function of tenacity in different regeneration bath compositions displayed as average from 10 parallel filaments ± standard deviation

Moreover, similar regeneration bath composition as is used in the NeoCel process, which utilizes sodium carbonate/sodium hydroxide in the coagulation of the filaments, was tested to see if these easily recyclable chemicals could be utilized in the production of strong filaments. A concentrated salt solution was compared against a typical strong acid bath in this experimental setup. The tenacities of the filaments as a function of stretching ratio in different regeneration bath compositions is presented in Figure 32.

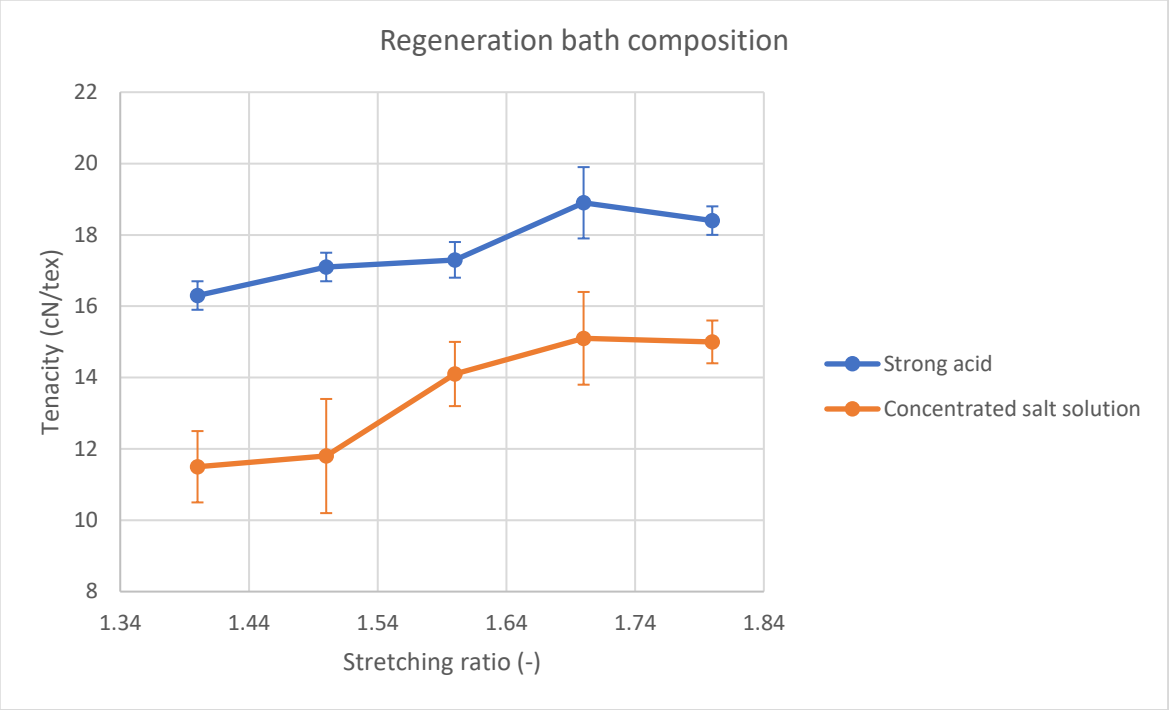

Figure 32. The tenacity of fibers as a function of stretching ratio in different regeneration bath compositions displayed as average from 10 parallel filaments ± standard deviation

Like the Figure 32 suggests the fibers spun into a regeneration bath consisting of only salt, produced fibers with poor tensile properties. This is caused by the insufficient salt removal from the fiber structure, as all the baths in the spinning device were of alkaline nature. This could also have been result of too low solvent/counter solvent diffusion rate. The filaments spun into salt regeneration bath had mat texture, due to high amounts of residual salts, which disturbed the formation of strong continuous cellulose II structure, while the fibers spun into strong acid, were shiny and smooth. The elongation at break of the filaments as a function of tenacity for different regeneration bath compositions are depicted in Figure 33.

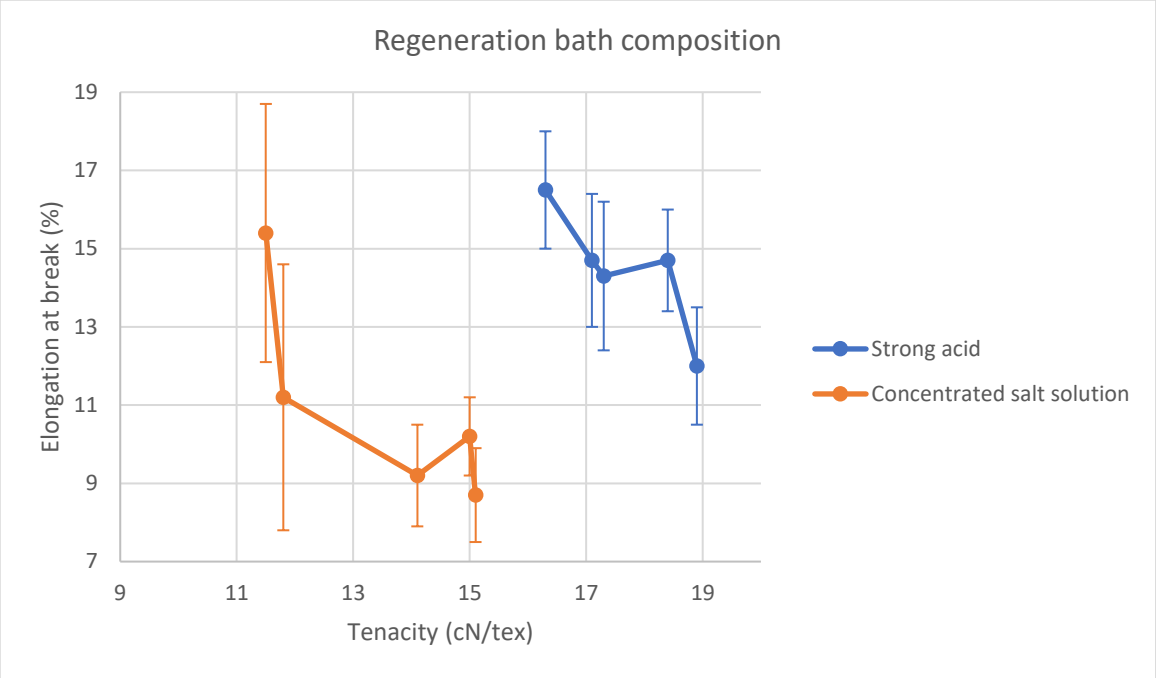

Figure 33. Elongation at break of the fibers as a function of tenacity in different regeneration bath compositions displayed as average from 10 parallel filaments ± standard deviation

6.2.1.6 Plasticization

Plasticization is a process, in which a polymer chain is made more mobile due to action of a chemicals called plasticizers. In this process the elongation at break of a material is increased, and tensile strength is decreased. However, in this experimental setup it was tested if the maximum stretching ratio of a fiber could be increased by adding a plasticizer, in this case 40 % plasticizer, into the 1st washing bath, allowing the cellulose chains to be more mobile while the stretching is conducted. A reference sample was also spun, in which no plasticizer was added to the system. The tenacities of the filaments as a function of stretching ratio are displayed in Figure 34.

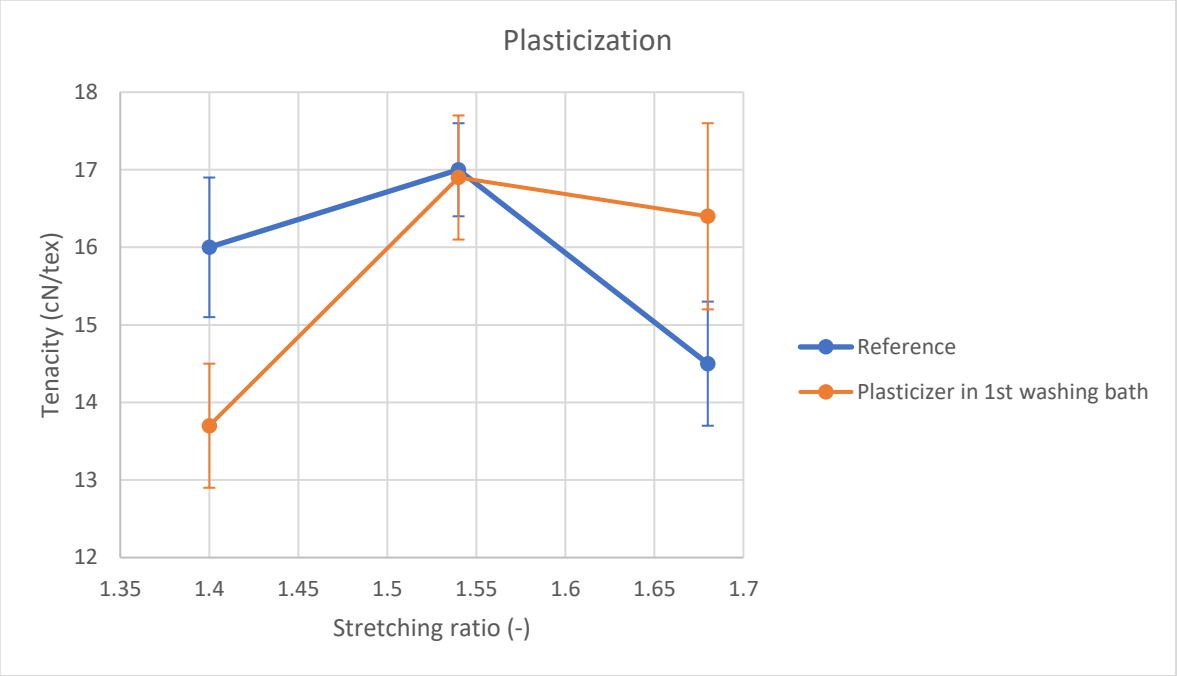

Figure 34. The tenacity of the fibers as a function of stretching ratio with added plasticizer in 1st washing bath displayed as average from 10 parallel filaments ± standard deviation

The maximum achieved fiber tenacities were in a similar range with or without the addition of plasticizer in the 1st washing bath. Also, the plasticizer did not have effect on the maximum stretching ratio during spinning. The elongations at break were also similar for both trials when the fiber tenacities were similar if the process deviation is considered. The elongation at break of the filaments as a function of tenacity for plasticized and non-plasticized samples are presented in Figure 35.

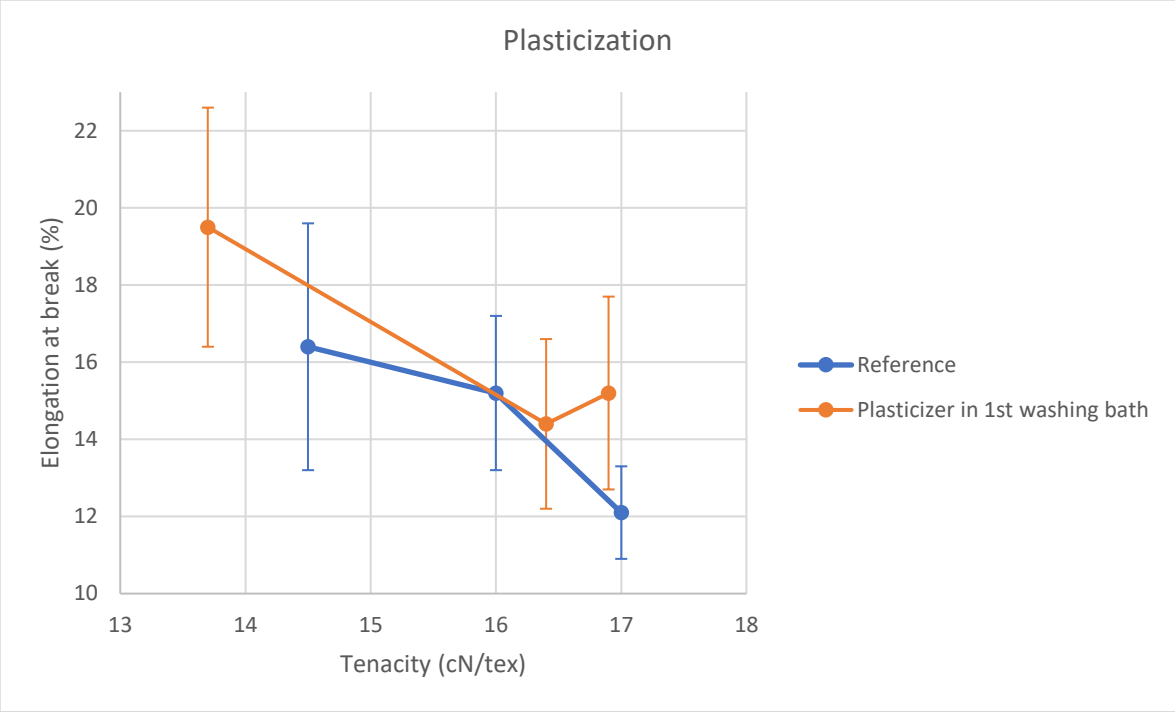

Figure 35. Elongation at break of the fibers as a function of tenacity with added plasticizer in 1st washing bath displayed as average from 10 parallel filaments ± standard deviation

6.2.1.7 Taguchi method trials

The effect of different process parameters on the fiber tenacity and elongation at break was tested in a multivariable Taguchi design experiment. L12 design matrix was constructed with 10 process variables known or believed to impact the resulting fiber properties. The L12 design matrix is displayed in Table 4.

Table 4. L12 design matrix of the Taguchi trials

	Level of parameter										
Trial number	Acid concentration	Regeneration bath temperature	Flow rate	Stretching ratio	1st washing bath temperature	Drying temperature	2nd washing bath temperature	Post stretch ratio	Cellulose concentration	Acid	L
1	1	1	1	1	1	1	1	1	1	1	1
2	1	1	1	1	1	2	2	2	2	2	2
3	1	1	2	2	2	1	1	1	2	2	2
4	1	2	1	2	2	1	1	1	2	2	2
5	1	2	2	1	2	2	1	2	1	2	1
6	1	2	2	2	1	2	2	1	2	1	1
7	2	1	2	2	1	1	2	2	1	2	1
8	2	1	2	1	2	2	2	1	1	1	2
9	2	1	1	2	2	2	1	2	2	1	1
10	2	2	2	1	1	1	1	2	2	1	2
11	2	2	1	2	1	2	1	1	1	2	2
12	2	2	1	1	2	1	2	1	2	2	1

The results are obtained by spinning three separate samples of each Taguchi trial point and obtaining average of 10 tensile measurements for each separate sample. Then from this data the averages and standard deviations are calculated and used in the data processing. The calculations are done automatically by Minitab software. (Minitab, 2019) In these experiments the studied parameters are acid concentration, regeneration bath temperature, flow rate, stretching ratio, 1st washing bath temperature, drying temperature, 2nd washing bath temperature, post stretch ratio, cellulose concentration, and acid type. One empty variable (L) was added to the design, to examine the reliability of the experimental setup. Two different level values of each parameter were used in the trials.

The higher the slope value of the mean of means line is, the bigger is the effect of that individual parameter on the observed output value. The effect of each parameter on the tenacity of fiber is depicted in Figure 36.

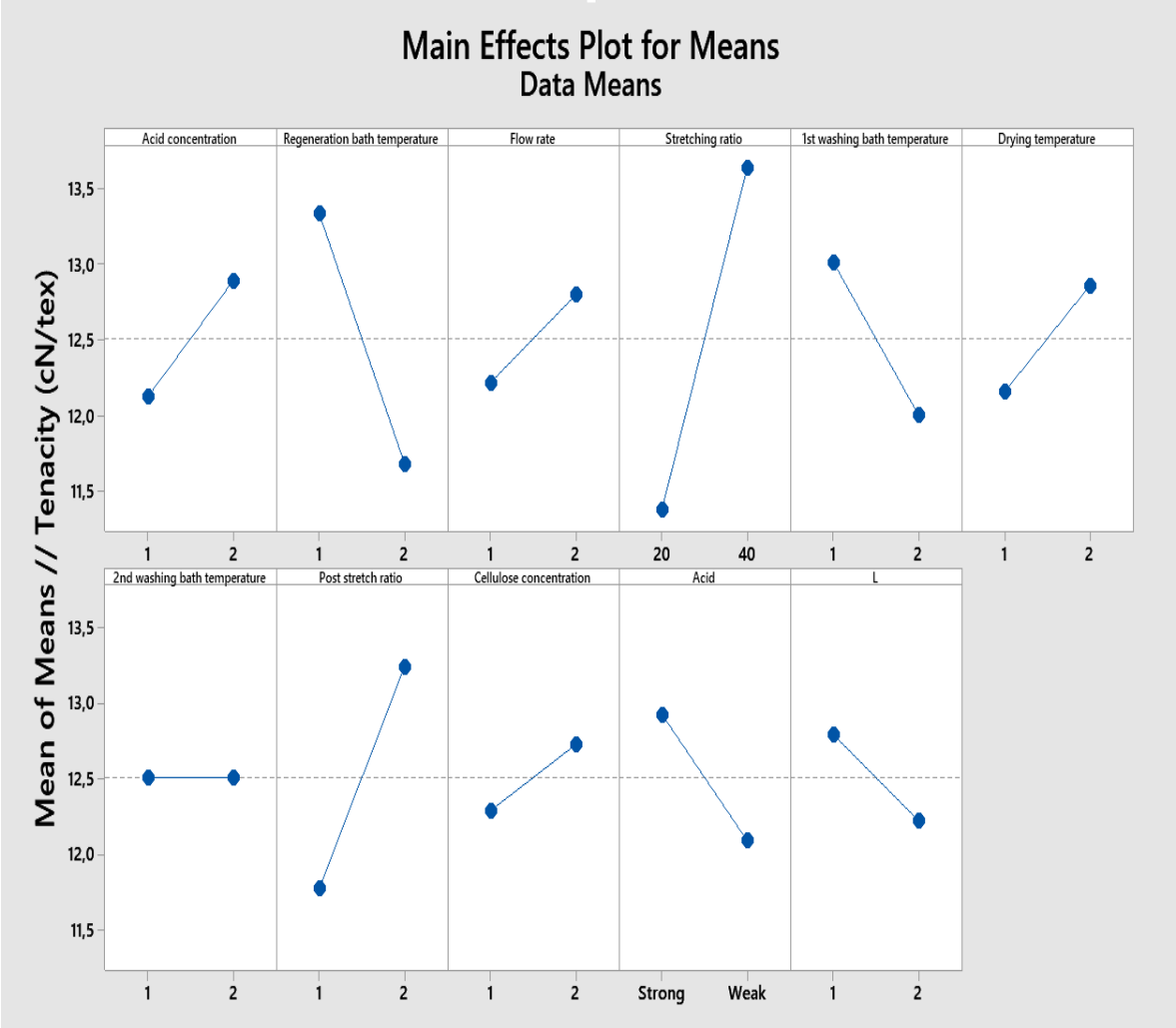

Figure 36. Effect of different parameters on mean of means for tenacity values

Figure 36 shows that the biggest factors determining the fiber tenacity are the stretching ratio, post stretch ratio and regeneration bath temperature. Stretching of the fiber induces orientation, which is the most important factor in determining the fiber tenacity according to Equation 5.3, so it is to be expected that the stretching ratio and post stretching ratio lines have the highest slope values. The lower regeneration bath temperature reduces the regeneration rate of the fiber, allowing more stretch to be applied and thus increasing tenacity. The rate of regeneration can also affect the porosity of regenerated cellulose material as was noted for cellulose films regenerated in studies conducted by Cai *et al.*, in which the higher regeneration rate caused the films to be more porous. (Cai *et al.*, 2007) In general more porous material is less tenacious.

Generally, lower acid concentration or weaker acid will produce higher tenacity fibers, this resulting from the slower solvent diffusion allowing more stretch to be applied in the system (Mao *et al.,* 2008) like it was noted for the regeneration bath temperature, but not for the acid concentration and type in the trials. In these experiments the stretching ratios were fixed into rather low levels to prevent fiber breakage to occur during the trials, so the favorable effect of lower acid concentration was not realized in the results. It can be considered that the higher acid concentration and stronger acid type increased the salt removal from the filaments leading to better tenacities with the fixed stretching ratios. The diffusion rate is also affected by the combined effect of the acid concentration, type, temperature and even dope viscosity. The solvent/anti-solvent diffusion rate needs to be sufficient to remove excess salts and impurities from the fiber but also slow enough to allow stretching to be applied. It could be that for the fixed stretching ratios in the experiment, the diffusion rates caused by the combination of above-mentioned parameters were sufficient to allow the low stretching ratios in the process, causing the higher acid concentration's ability to remove the impurities better, to show up as more beneficial for higher fiber tenacities.

The increased flow rate of the dope causes aligning of the cellulose chains in the fiber axis direction, increasing the tenacity of the fiber. This effect can also be seen from the Figure 36. When the temperature of the 1st washing bath is increased and stretching is applied to the fiber, the orientation of the regenerated filament is locked to a higher degree than with the low temperature washing bath due to higher diffusion rate preventing the relaxation of the fiber orientation. If the fiber is stretched after the locking of its structure, it can cause damage or even breakages in the fiber. Thus, the higher 1st washing bath temperature leads to decrease in fiber tenacity, like is seen from the results. Due to Taguchi design having low tolerance for synergistic parameter effects like the temperature of the 1st and 2nd washing bath the beneficial effect of the high second bath temperature was not realized in the results, unlike in the earlier results (Figure. 26)

Signal to noise ratio (SN ratio) is an indicator that depicts how significant the output signal is in comparison to the noise in the process. Thus, it is an indicator of variance. It can be calculated with Equation 6.1. (Minitab, 2019)

$$SN = 10log\frac{\bar{Y}^2}{\sigma_s^2} \quad (6.1)$$

where SN is the signal to noise ratio (-) , $\bar{Y}$ is the data mean value and σ_s is the standard deviation.

Optimally, it is important to find parameters that have desired or negligible effect on the output signal value (in this case tenacity or elongation at break), and high impact on the signal to noise ratio value. SN ratios for tenacity outputs are presented in Figure 37.

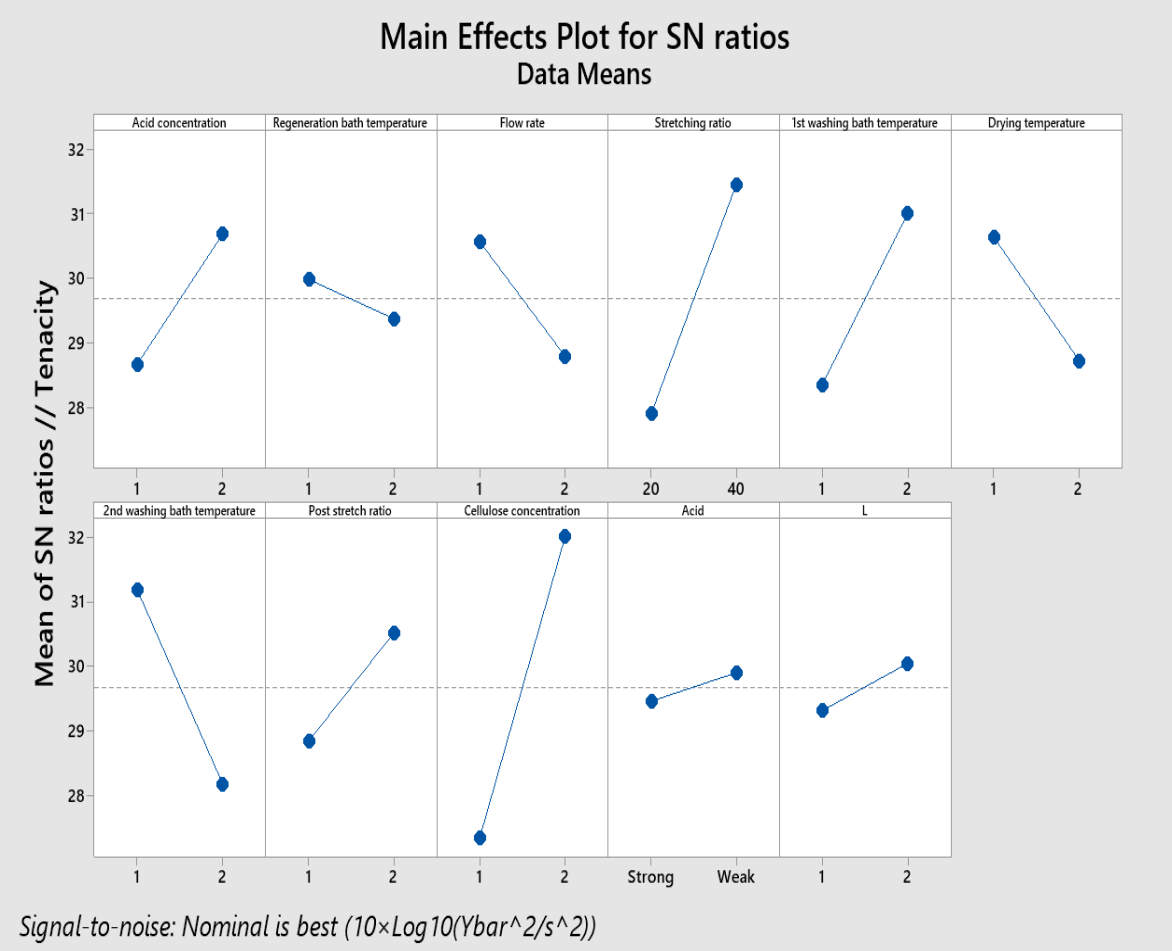

Figure 37 Mean of SN ratios for tenacity values

From Figures 36 and 37 can be seen that good parameters values for the tenacity variation control, and for preserving or increasing the tenacity level (high SN ratio and positive or negligible effect on tenacity), are the high stretching ratio, high post stretch ratio and low 2nd washing bath temperature. However, as was discussed in chapter 6.2.1.3 the higher

temperature level of the 2nd washing bath has probably larger impact on the tenacity than was realized in the experiment. As the high SN ratio is achieved with low 2nd washing bath temperature, the process variation may be reduced by setting the temperature to this level, but this might also sacrifice filament tenacity. The mean of means for elongation at break values are presented in Figure 38.

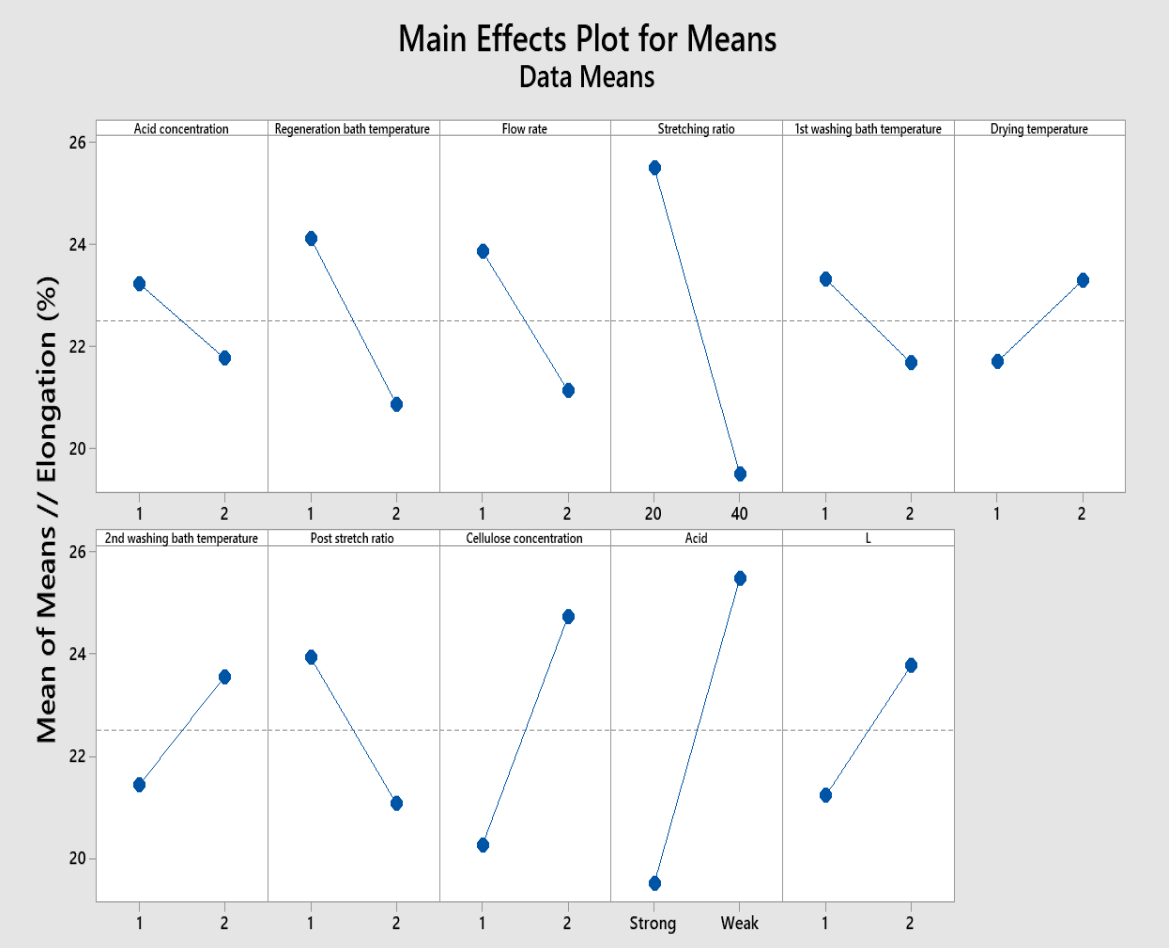

Figure 38. Effect of different parameters on mean of means for elongation at break values

The elongation at break values have usually been more subject to process variations as can be noted from the previous single variable experiments. Thus, the slope value of the empty "L" variable is also higher than it was for the tenacity output values. The biggest factors influencing the elongation at break seem to be the stretching ratio, acid type and cellulose concentration. As the stretching ratio is increased the fiber orientation increases leading to tighter bonding between the cellulose chains, which causes the fiber to lose its elasticity.

This is also the case for the post stretch ratio and for the higher dope flow rate as orientation is induced caused by the increased shear forces in the spinneret.

The weak acid, lower regeneration bath temperature and lower acid concentration inhibit the regeneration rate of the fiber in comparison to higher values of these parameters. Thus, the fiber is left in a more gel-like state, which is the reason for the better elongation at break. The same could be considered for the cellulose concentration. As cellulose concentration increases, so does the viscosity of the dope; the diffusion is slowed down as the higher viscosity resists the flow of the substance more.

By increasing the 1st washing bath temperature faster diffusion occurs which stiffens the fiber more and its elongation at break decreases like can be seen from the Figure 38. The increase in elongation at break when the 2nd washing bath temperature is higher, could be explained by the plasticizing effect of hot water, while the fiber is already in a more complete regenerated state while entering the bath. This noticed effect could also be error caused by the synergistic effects of the first and second washing bath temperatures, mentioned earlier in the chapter, as it could also be believed that high temperature completes the regeneration faster and lock the fiber orientation causing the elongation at break to decrease. SN ratios for elongation at break outputs are presented in Figure 39.

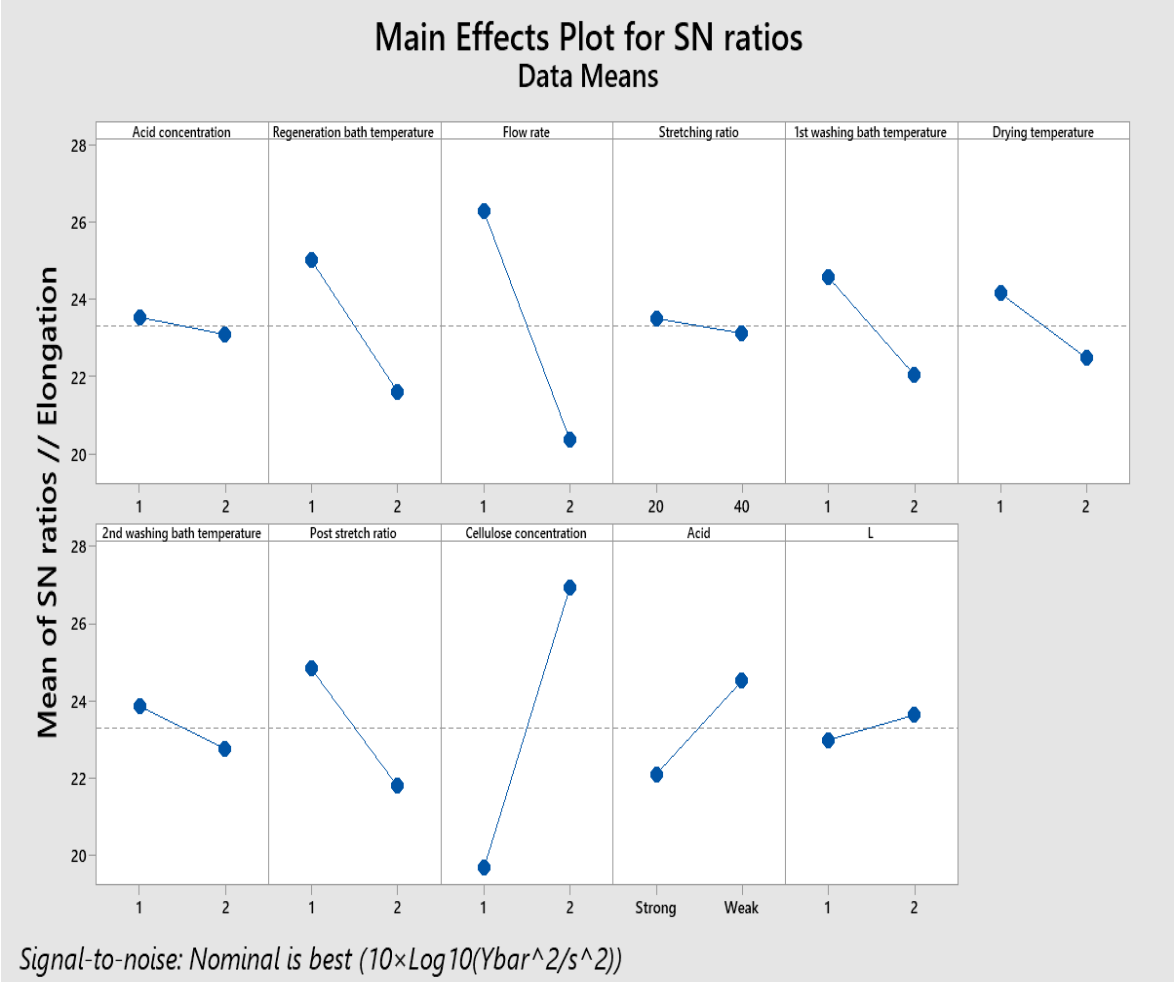

Figure 39. Mean of SN ratios for elongation at break values

The best parameters levels for controlling the elongation at break variation seem to be high cellulose concentration, low flow rate and low regeneration bath temperature, as they possess high SN ratios as well as improve the elongation mean output simultaneously.

The effects of each process parameter on the output signals' means and SN ratios are color coded in Table 5.

Table 5. Color coded effects of each parameter on the output signals' means and SN ratios

		Output	
Parameter	Mean/SN	Tenacity	Elongation at break
Acid concentration	Mean		
	SN ratio		
Regeneration bath temperature	Mean		
	SN ratio		
Flow rate	Mean		
	SN ratio		
Stretching ratio	Mean		
	SN ratio		
1st washing bath temperature	Mean		
	SN ratio		
Drying temperature	Mean		
	SN ratio		
2nd washing bath temperature	Mean		
	SN ratio		
Post stretch ratio	Mean		
	SN ratio		
Cellulose concentration	Mean		
	SN ratio		
Acid	Mean		
	SN ratio		

Effects on output value with increased parameter value
Big positive effect
Slightly bigger positive effect than with empty variable
Equal or smaller effect than with empty variable
Slightly bigger negative effect than with empty variable
Big negative effect

6.2.2 Filament post-treatment

Wet spun fibers with a tenacity of 14 cN/tex and elongation at break of 9.9 % were used in the post-treatment experiments to test the effect of various chemicals on the tensile properties of the fibers. In the first experiments the reference fibers were immersed for 2 hours into a

multi-valent salt solutions containing varying concentrations of chloride salts to study the crosslinking effect that was reported in the studies conducted by Khanjani et al. The treated fibers were then dried, and their tensile properties were measured. The fiber tenacities as a function of salt solution w-% for different salt solutions are displayed in Figure 40.

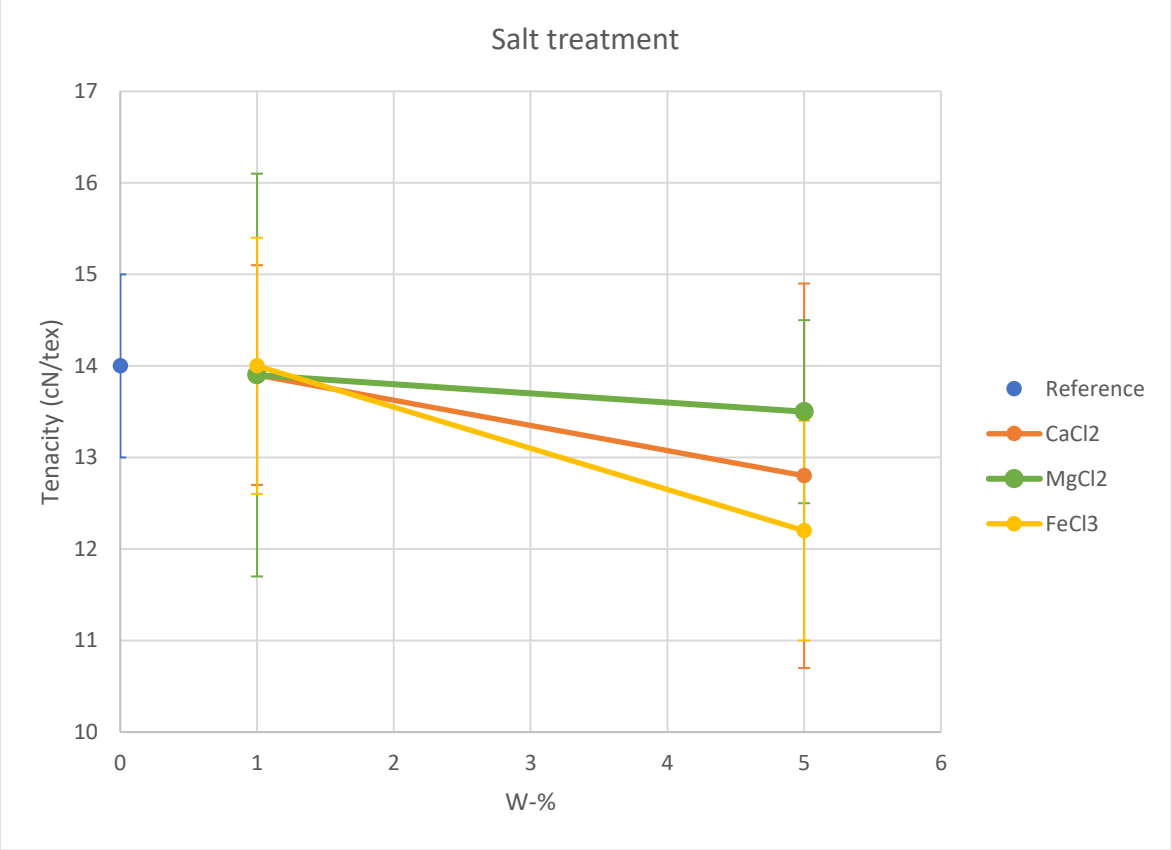

Figure 40. The tenacity of a spun fiber as a function of salt mass percentage in the solution displayed as average from 10 parallel filaments ± standard deviation

As seen from Figure 40 the fiber tenacities were not greatly affected by the immersion into the salt solution when the deviation is considered. This could be due to lack of negatively charged groups present in the initial pulp from which the filaments were spun from, as the article used TEMPO oxidized pulp while in these experiments similar effects were tried to be achieved with kraft pulp. Thus, the multivalent cations cannot attach onto the cellulose chains of the fiber and further cross-link the adjacent chains together. The elongation at break of the filaments as a function of tenacity are presented in Figure 41.

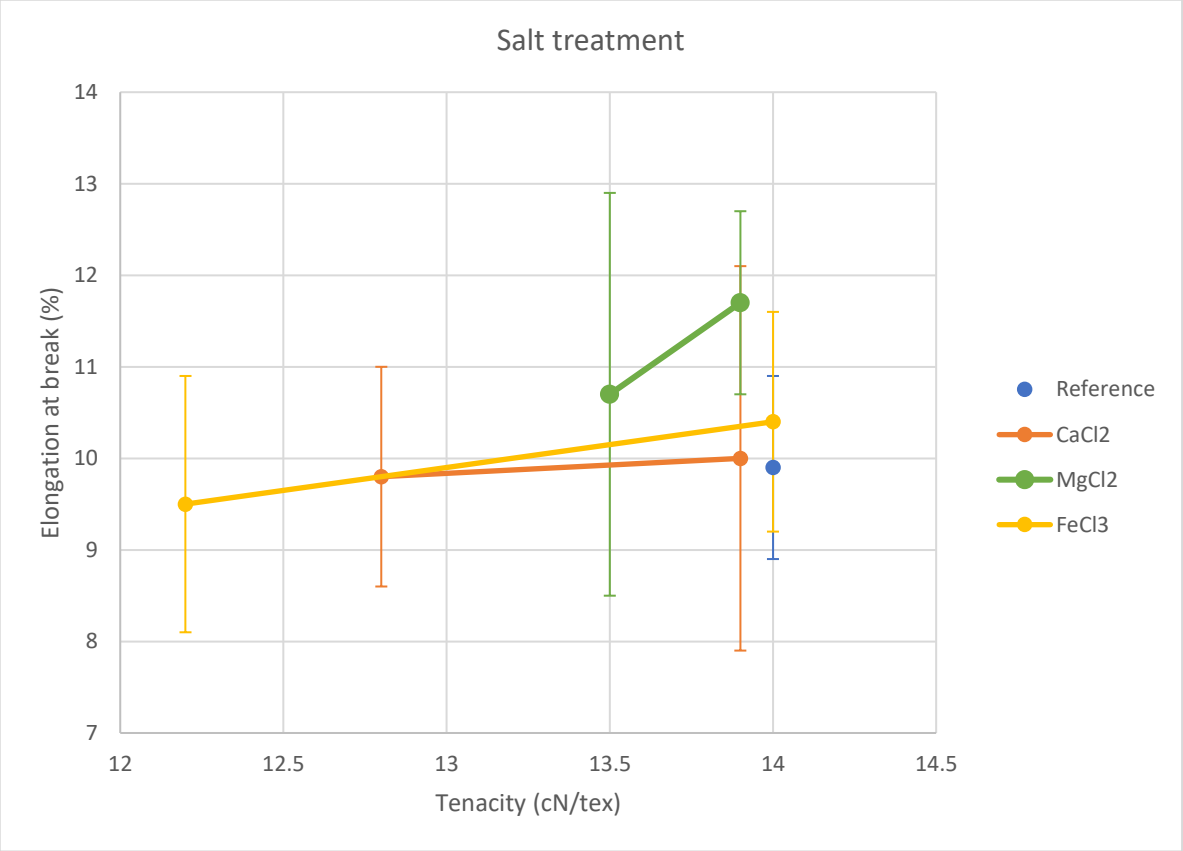

Figure 41. Elongation at break of the fibers as a function of tenacity with different salt treatment solutions displayed as average from 10 parallel filaments ± standard deviation

Further cross-linking experiments were conducted with three different chemicals: citric acid, glyoxal (without/with catalyst) and ammonium zirconium carbonate. The same reference fibers as were used in the salt treatment experiments, were immersed into solutions containing cross-linkers of varying concentrations for 2 hours. The samples immersed into glyoxal, or citric acid solutions were then dried in 100 °C for 15 minutes and then cross-linked in 150 °C for 7 minutes. The samples immersed into ammonium zirconium carbonate solution were simply dried in 60 °C as the cross-linking should occur during the removal of water from the material.

The fiber tenacities as a function of cross-linker solution w-% for different cross-linkers are presented in Figure 42.

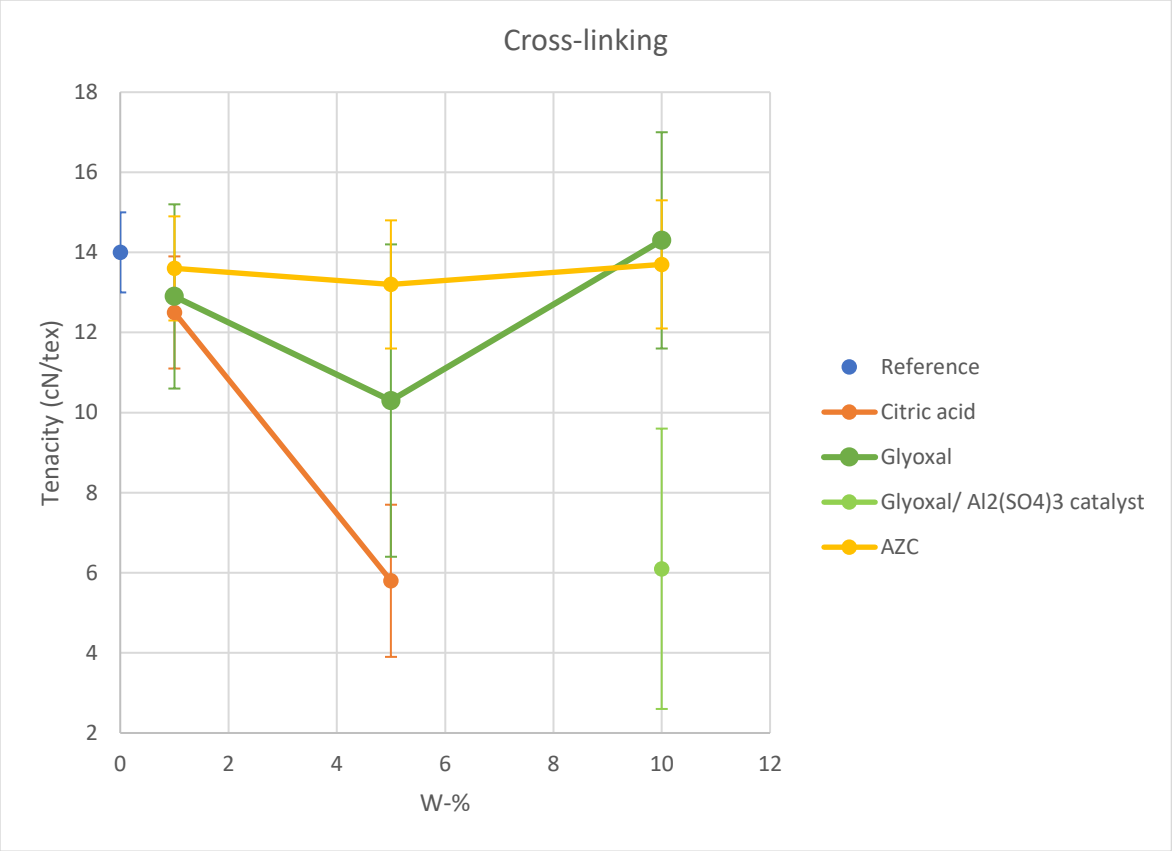

Figure 42. The tenacity of fibers as a function of cross-linker mass percentage in the solution displayed as average from 10 parallel filaments ± standard deviation

The fiber tenacities dropped drastically upon increasing the citric acid concentration. This may be caused by the hydrolysis of the filament that can take place in acidic conditions and high temperatures. The cellulose chains are cleaved from the β-1,4 glycosidic bond causing the degree of polymerization to decrease, ultimately leading to reduction in the tenacity of the fiber.

The cross-linking with glyoxal with and without the aluminium sulphate led to fiber becoming stiff and brittle as can be seen from Figures 42 and 43. The reduced elongation at break can be explained by the increasing of the number of covalent acetal linkages between cellulose chains. Surprisingly the maximum tenacity increased only by a small margin, when 10 w-% glyoxal solution was utilized without the catalyst. With the addition of aluminium sulphate catalyst, the fibers became so stiff and brittle that they were extremely difficult to measure with the tensile tester, and only one trial point was able to be tested.

No significant effects were noted on the fiber tensile properties upon the immersion in the ammonium zirconium carbonate solution.

The elongation at break as a function of tenacity for different cross-linked fibers can be examined from Figure 43.

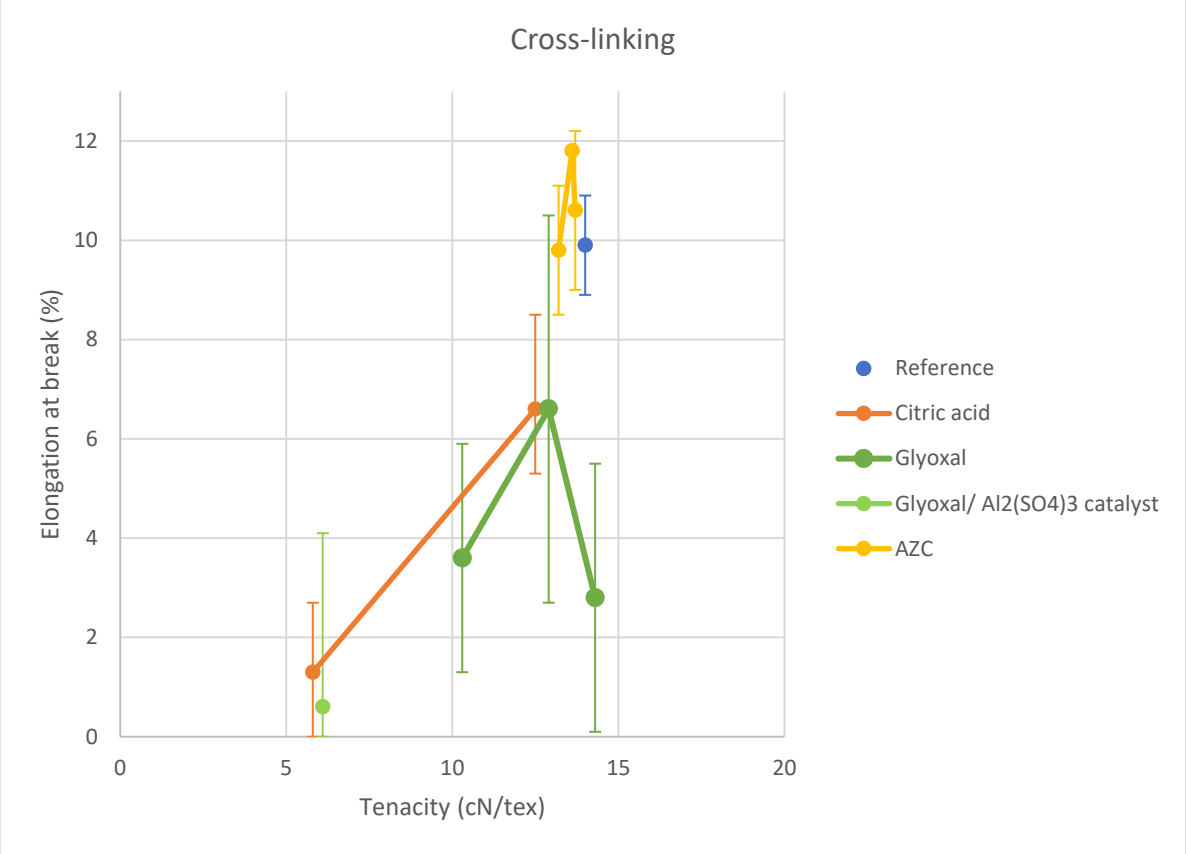

Figure 43. Elongation at break of the fibers as a function of tenacity with different cross-linker solutions displayed as average from 10 parallel filaments ± standard deviation

A specialized laboratory scale post-treatment device was used in a series of tests in which 4 levels of increasing treatment conditions were applied to the reference filaments. The treatment method was named as post-treatment A. The post-treatment tests were conducted in constant conditions. The tenacity of the fibers as a function of treatment level is depicted in Figure 44.

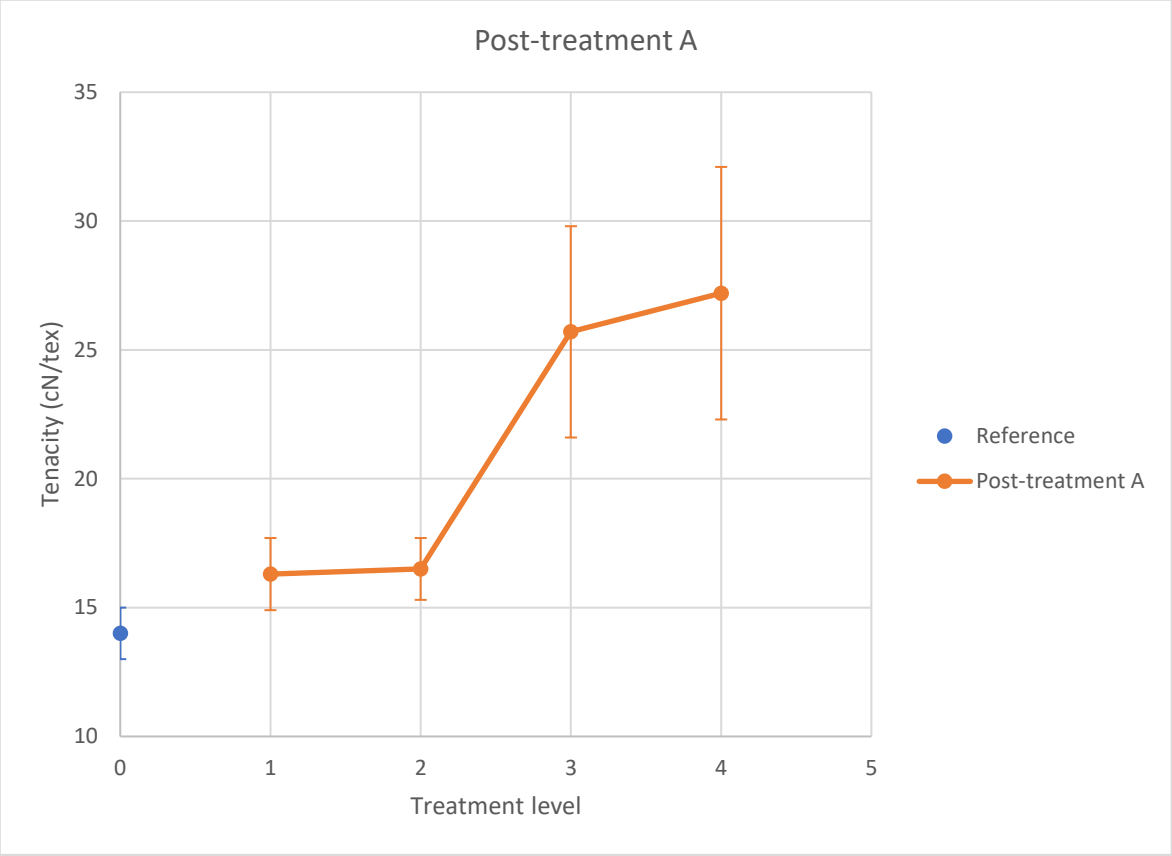

Figure 44. The tenacity of fibers as a function of treatment level with specific post-treatment type displayed as average from 10 parallel filaments ± standard deviation

The tenacity of the reference fibers increased with an increase in the level of applied treatment and reached a high of 27.2 cN/tex which is higher than regular viscose fibers and close to the properties of Modal fibers. The increasement in the tenacity could have resulted from the increase of the orientation degree caused by the applied treatment. Surprisingly, the elongation at break values also increased in the process, which could be derived from the constant conditions of the experiments, which also promote the plasticization of the fiber to take place. The fiber elongation at break as a function of tenacity is presented in Figure 45.

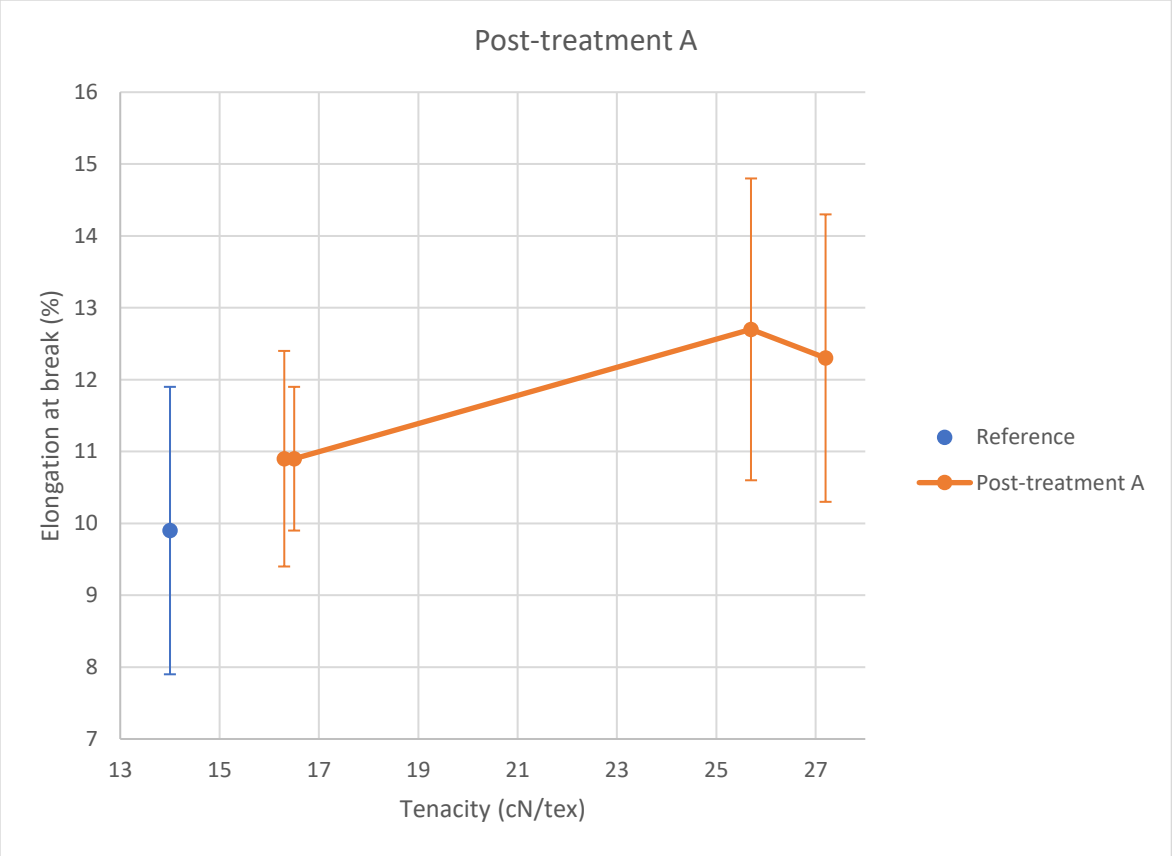

Figure 45. Elongation at break of the fibers as a function of tenacity with a specific post-treatment type displayed as average from 10 parallel filaments ± standard deviation

6.2.3. Fiber chemical properties

The crystallinity indexes of few selected samples were determined using the earlier described FTIR method as well as with WAXS. The sample coded as Viscose is commercial viscose fiber, Lyocell is commercial lyocell fiber, Reference is the reference sample used in the post treatment experiments and the Post-treated A (level 4) is the sample obtained by the post-treatment A. From the WAXS data, the crystallinity index of a sample can be determined with Equation 6.2 (Fitriana *et al.*, 2015).

$$C_{RI} = \frac{A_{Cr}}{A_{Cr}+A_{am}} * 100 \qquad (6.2)$$

where C_{RI} is the crystallinity index, A_{Cr} is the total area of the crystalline intensity peaks and A_{am} is the area of the amorphous peak.

The crystallite size of the filament can be calculated with the Scherrer Equation 6.3. (Fitriana *et al.*, 2015).

$$L = \frac{k\lambda}{\beta \cos\theta} \tag{6.3}$$

where L is the crystallite size (Å), k is the Scherrer constant (0.94), λ is the X-ray wavelength (Å), β is the full width at half maximum of the specific crystalline peak in radians and $\boldsymbol{\theta}$ is the corresponding Bragg's angle in radians.

The crystalline peaks of cellulose II that contribute to the sample total crystallinity as well as the amorphous halo are marked in the Figure 46.

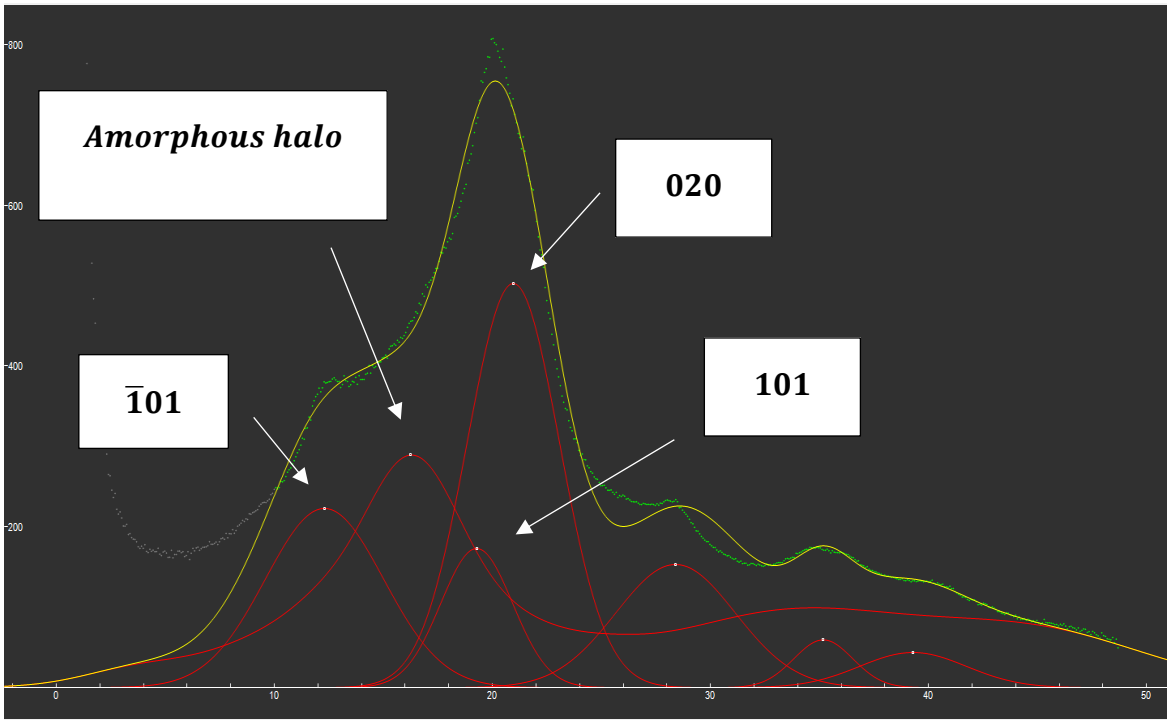

Figure 46. The crystalline peaks of cellulose II and the amorphous halo

Using the Fityk peak fitting software, deconvolution of the raw WAXS data was executed to reveal the corresponding crystallinity peaks. The amorphous halo was manually added and fitted using WAXS data obtained from reference sample containing high amounts of amorphous cellulose. An automated cellulose II batch fitting .LUA script was constructed to set the initiated peak centers and intensities in relatively same positions regardless of the

intensity levels of different datasets to produce results that are as comparable as possible. The script calculates the crystallinity index and the crystallite sizes for all the crystalline peaks using the Equations 6.2 and 6.3 and prints the results into separate files. The .LUA fitting script can be found from Appendix I.

As mentioned before, the orientation degree (f_D) of the samples was calculated using XSACT software. The crystalline properties, orientation degree and the corresponding fiber tenacity values are gathered in Table 6.

Table 6. The Crystallinity indexes, crystallite sizes, orientation degree and tenacities of selected cellulose fibers

Sample	**TCL $_{FTIR}$ (%)**	**$C_{RI,\ WAXS}$ (%)**	**L,$\bar{1}$01 (Å)**	**L,101 (Å)**	**L,020 (Å)**	**f_D (%)**	**Tenacity (cN/tex)**
Viscose	58	58.7	57.6	29.4	14.5	31.8	22.1
Lyocell	52	61.1	49.6	28.5	22.2	50	40
Reference	51	62.7	51.5	32.5	15.5	33.6	14
Post-treated A (level 4)	49	59.2	83.1	18.5	19.2	37.2	27.2

As can be seen from Table 6. no clear correlation between the crystallinity index calculated by FTIR and WAXS can be found. As the degree of polymerization data is unavailable for this thesis, fiber tenacity was plotted in Figure 47. as function of squared orientation degree times the crystallinity index estimated from the WAXS data for all samples.

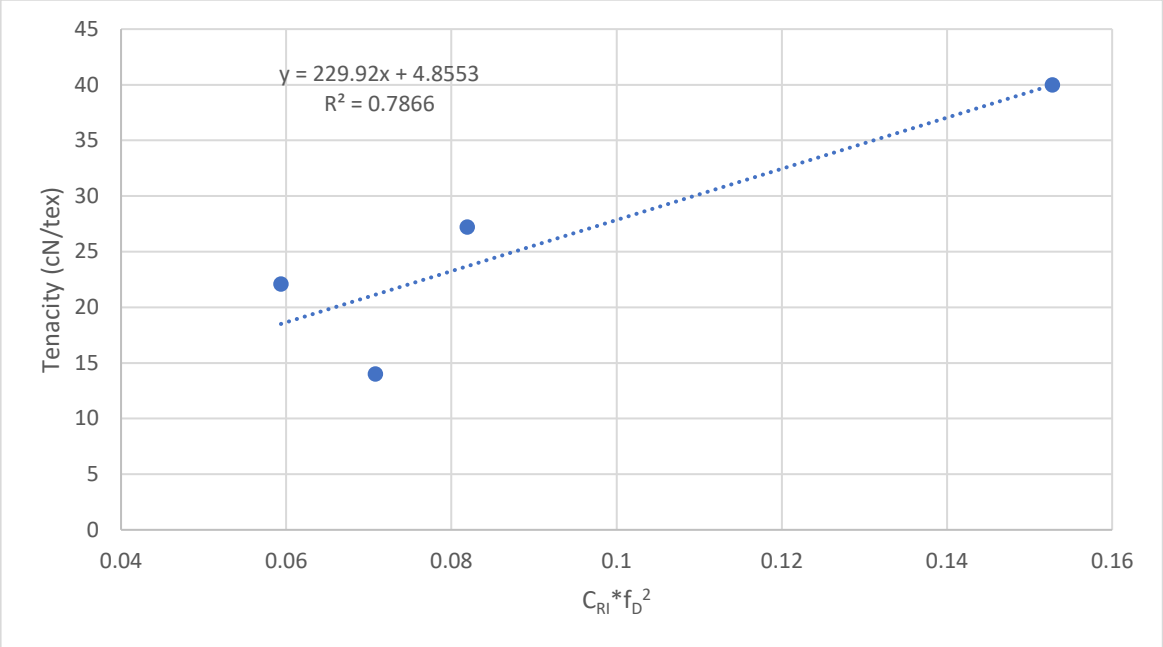

Figure 47. Tenacity as a function of crystallinity index times the squared orientation degree

The Figure 47 reveals a linear correlation between the tenacity and these above-mentioned parameters. However, as the number of samples is rather low, more measurements are needed to confirm this relation. Also, in the future, this kind of correlation should be tested with the missing term $(\frac{1}{L} - \frac{1}{DP_N})$ of the Equation 5.3 that could not be used in this thesis due to unavailability of the DP values.

7 Conclusions

Cellulose wet spinning is a complex multivariable process requiring high levels of optimization to produce fibers with sufficient tensile properties. The main parameters affecting the tenacity of the fibers were found to be the composition of the regeneration bath (temperature, acid concentration and chemical type) and the stretching conducted after the regeneration bath, according to the Taguchi design method. Due to synergistic variables being present in the design matrix (1st and 2nd washing bath temperature), the effect of some parameters like 2nd washing temperature were found to be underestimated in the results.

The post-treatment of the filaments was found to be difficult as for example the cross-linking reactions done in high temperatures seemed to make the fibers hard and brittle, decreasing the tenacity and elongation properties. With the help of tailored post-treatment device, the fiber tenacity of 27.2 cN/tex and 12.3 % elongation at break was reached, which made the fibers stronger than the regular viscose fibers. Other interesting fibers were made by the wet-spinning process with weak acid as the regeneration bath. These fibers had tenacity of 20.6 cN/tex and 14.1 % elongation at break, which are close to regular viscose fiber properties. Even though the elongation at break did not reach the desired 19 %, the fibers with these kinds of tensile properties could even be commercially significant due to greener solvent alternative used in the process.

The crystallinity index calculations done with the FTIR produced results that indicated the material to be less crystalline than with the calculations constructed from the WAXS data. These differences could originate for example from the use of amorphous reference from different pulp source than the filaments were made of. The used FITYK software coupled with automated fitting and crystallinity calculation script was found to be powerful tool in analyzing high volumes of cellulose II WAXS data. A linear correlation between the fiber tenacity and crystallinity index times the orientation squared was found for the measured samples.

The further experiments could focus on acquiring more data about the chemical properties like the crystallinity, orientation and crystallite size and their dependence on various process parameters (Taguchi design) to gain more knowledge about the fundamentals of the spinning process. Also, the WAXS method for crystallinity index and crystallite size analyzes needs to be further developed as there is still variables like the baseline correction method and

utilization of amorphous reference that need to be further refined to produce more accurate results.

One completely unexplored topic on this thesis is the effect of fiber washing efficiency on the tensile properties. The residual salts could possibly disturb the uniformity of the final fibers and so decrease the tensile properties. Thus, parameters like the number of washing baths, residence time, washing temperatures and type of washing *e.g.,* washing in stagnant or flowing water like the counter-current washing. The effect of spin bath and washing bath additives like different surfactants that can decrease the surface tension could also play an important role in improving the fiber spinnability and decreasing the breakages of the fiber during the process and possibly enabling higher stretching ratio maximums to be achieved.

The dope additives were also not tested in this thesis, so they are still open for wider experimentation. One interesting point that was realized in experiments conducted by Pahimanolis et al was that when carboxymethyl cellulose was mixed with cellulose dope, the loss and storage modulus of the solution decreased, which indicated that the fibril-to-fibril interactions had decreased in the system. When shear forces were introduced to the system, the alignment of the material was noted to have been increased in comparison to dope without added CMC. (Pahimanolis *et al.,* 2013) This would be interesting to test on a spinning device, and if these reduced inter fibril interactions would allow for increased stretching ratios to be applied in the process. Thus, the purpose of these additives that could be examined for this process would not need to have reinforcing interactions with the cellulose fiber but rather effects that disturb the interactions of cellulose chains.

References

Alexandridis, P. et al. (2018) Solvent processing of cellulose for effective bioresource utilization. Current opinion in green and sustainable chemistry. [Online] 1440–52.

Ametek. (no date) [Online]. Available: https://www.brookfieldengineering.com/

Andersson Trojer, M. et al. (2019) Directed self-assembly of silica nanoparticles in ionic liquid-spun cellulose fibers. Journal of colloid and interface science. [Online] 553167–176.

Bialik, M. et al. (2020) Design, optimization and modelling of a chemical recovery system for wet spinning of cellulose in sodium carbonate solutions. Cellulose (London). [Online] 27 (15), 8681–.

Biswas, M. C. et al. (2020) Glucaric acid additives for the antiplasticization of fibers wet spun from cellulose acetate/acetic acid/water. Carbohydrate polymers. [Online] 245116510–116510.

Cai, J. et al. (2007) Influence of coagulation temperature on pore size and properties of cellulose membranes prepared from NaOH–urea aqueous solution. Cellulose (London). [Online] 14 (3), 205–215.

Chen, J. et al. (2017) Comparison of cellulose and chitin nanocrystals for reinforcing regenerated cellulose fibers. Journal of applied polymer science. [Online] 134 (22).

Ciolacu, D. & Popa, V. I. (2010) Cellulose Allomorphs: Structure, Accessibility and Reactivity. Hauppauge: Nova Science Publishers, Incorporated.

Common Objective. (no date) Fibre Briefing: Viscose. [Online]. Available: https://www.commonobjective.co/article/fibre-briefing-viscose

Cordis Europa. (no date) NeoCel – Novel processes for sustainable cellulose-based materials. [Online]. Available: https://cordis.europa.eu/article/id/421963-fibre-benefits-more-than-your-gastrointestinal-tract

Cuissinat, C. & Navard, P. (2006) Swelling and Dissolution of Cellulose Part II: Free Floating Cotton and Wood Fibres in NaOH–Water–Additives Systems. Macromolecular symposia. [Online] 244 (1), 19–30.

Easy Biology Class. (no date) Polysaccharides. [Online].
Available: https://www.easybiologyclass.com/polysaccharides-structure-classification-and-examples-biochemistry-lecture-notes/

Eichhorn, S. et al. (2009) Handbook of Textile Fibre Structure Natural, Regenerated, inorganic and Specialist Fibres. Burlington: Elsevier Science.

Eriksson, J. (2015) Pilot spinning of viscose staple fibres. [Online] Degree Project in Engineering Chemistry

European Pulp Industry Sector. (no date) Production of pulp. [Online].
Available: https://epis.org/cellulose-products

Fitriana et al. (2015) Characterization and mechanical properties investigation of the cellulose/gypsum composite. Journal of Composite Materials. 50.

Fu, F. et al. (2018) NaOH/urea solution spinning of cellulose hybrid fibers embedded with Ag nanoparticles: influence of stretching on structure and properties. Cellulose (London). [Online] 25 (12), 7211–7224.

Gupta, B.S. (2008) Textile fiber morphology, structure and properties in relation to friction. [Online] Friction in Textile Materials. pp. 3-36

Gupta, P.K. et al. (2019) An Update on Overview of Cellulose, Its Structure and Applications.

Hagman, J. et al. (2017) On the dissolution state of cellulose in cold alkali solutions. Cellulose (London). [Online] 24 (5), 2003–2015.

Heinze, T. (2015) ‘Cellulose: Structure and Properties’, in Cellulose Chemistry and Properties: Fibers, Nanocelluloses and Advanced Materials. [Online]. Cham: Springer International Publishing. pp. 1–52.

Hummel, M. (2015) Fundamentals of cellulose regeneration. [Lecture]. Aalto University, School of Chemical Technology.

Hyun Chan Kim et al. (2019) Effect of Wet Spinning and Stretching to Enhance Mechanical Properties of Cellulose Nanofiber Filament. International Journal of Precision Engineering and Manufacturing - Green Technology. [Online] 6 (3), 567–575

Iglesias, M. C. et al. (2020) Pulping Processes and Their Effects on Cellulose Fibers and Nanofibrillated Cellulose Properties: A Review. Forest products journal. [Online] 70 (1), 10–.

Innovation in textiles. (2021) EUR 50 million factory for Spinnova sustainable fibre. [Online]. Available: https://www.innovationintextiles.com/eur-50-million-factory-for-spinnova-sustainable-fibre/

Ioncell. (no date) Commercialization. [Online].
Available: https://ioncell.fi/commercialization/

Jeon, J. G. et al. (2019) Cross-linking of cellulose nanofiber films with glutaraldehyde for improved mechanical properties. Materials letters. [Online] 25099–102.

Khanjani, P. et al. (2019) Interaction of divalent cations with carboxylate group in TEMPO-oxidized microfibrillated cellulose systems. Cellulose (London). [Online] 26 (8), 4841–4851.

Kontturi, E. (2015) Cellulose: structure, morphology, and crystalline forms. [Lecture] Aalto University, School of Chemical Technology.

Kumar, H. & Christopher, L. P. (2017) Recent trends and developments in dissolving pulp production and application. Cellulose (London). [Online] 24 (6), 2347–2365.

Lahtinen, T. (2009) Improving the strength of paper and board products. WO 2010/133762

Liu, R. & Hu, X. (2006) Precipitation Kinetics of Cellulose in the Lyocell Spinning Process. Industrial & engineering chemistry research. [Online] 45 (8), 2840–2844.

Lundahl, M. J. et al. (2017) Spinning of Cellulose Nanofibrils into Filaments: A Review. Industrial & engineering chemistry research. [Online] 56 (1), 8–19.

Mao, Y. et al. (2008) Effects of Coagulation Conditions on Properties of Multifilament Fibers Based on Dissolution of Cellulose in NaOH/Urea Aqueous Solution. Industrial & engineering chemistry research. [Online] 47 (22), 8676–8683.

Material district. (2018) THIS WOOD-BASED TEXTILE FIBRE IS MADE WITHOUT CHEMICAL SOLVENTS. [Online]. Available: https://materialdistrict.com/article/wood-based-textile-fibre/

Mathews, S. et al. (2013) Methods for Facilitating Microbial Growth on Pulp Mill Waste Streams and Characterization of the Biodegradation Potential of Cultured Microbes. Journal of visualized experiments. JoVE. 82. 10.3791/51373.

Medronho, B. & Lindman, B. (2015) Brief overview on cellulose dissolution/regeneration interactions and mechanisms. Advances in colloid and interface science. [Online] 222 (Online 28 May 2014), 502–508.

Medronho, B. et al. (2012) Rationalizing cellulose (in)solubility: Reviewing basic physicochemical aspects and role of hydrophobic interactions. Cellulose. 19. 581-587. 10.1007/s10570-011-9644-6.

Meng, X. et al. (2016) Physicochemical Structural Changes of Cellulosic Substrates during Enzymatic Saccharification. JAppl Biotechnol Bioeng 1(3)

Michud, A. et al. (2016) Ioncell-F: ionic liquid-based cellulosic textile fibers as an alternative to viscose and Lyocell. Textile research journal. [Online] 86 (5), 543–552. [Online].

Minitab. (2019) What is the signal-to-noise ratio in a Taguchi design? Available: https://support.minitab.com/en-us/minitab/18/help-and-how-to/modeling-statistics/doe/supporting-topics/taguchi-designs/what-is-the-signal-to-noise-ratio/

NeoCel. (2020) [Online]. Available: http://neocel.eu/

Niaounakis, M. (2017) The Problem of Marine Plastic Debris. [Online] Management of Marine Plastic Debris. pp. 1-55

Nomura, S. et al. (2020) 13C NMR and XRD studies on the enhancement of cellulose II crystallinity with low concentration NaOH post-treatments. Cellulose (London). [Online] 27 (7), 3553–3563.

Parry, A. (2016) Nanocellulose and its Composites for Biomedical Applications. Current medicinal chemistry. 23.

Pahimanolis, N. et al. (2013) Nanofibrillated cellulose/carboxymethyl cellulose composite with improved wet strength. Cellulose (London). [Online] 20 (3), 1459–1468.

Pinkert, A. et al. (2009) Ionic Liquids and Their Interaction with Cellulose. Chemical reviews. 109. 6712-28.

Quero, F. et al. (2011) Cross-Linked Bacterial Cellulose Networks Using Glyoxalization. ACS applied materials & interfaces. [Online] 3 (2), 490–499.

Reddy, N. & Yang, Y. (2010) Citric acid cross-linking of starch films. Food chemistry. [Online] 118 (3), 702–711.

Rodgers, B & Waddell, W. (2013) Chapter 14 - Tire Engineering. [Online] The Science and Technology of Rubber (Fourth Edition), 653-695

Sayyed, A. J. et al. (2019) A critical review of manufacturing processes used in regenerated cellulosic fibres: viscose, cellulose acetate, cuprammonium, LiCl/DMAc, ionic liquids, and NMMO based Lyocell. Cellulose (London). [Online] 26 (5), 2913–2940.

Singh, P. et al. (2015) From Cellulose Dissolution and Regeneration to Added Value Applications — Synergism Between Molecular Understanding and Material Development. [Online]

Sixta, H. et al. (2015) Ioncell-F: A High-strength regenerated cellulose fibre. Nordic Pulp and Paper Research Journal. 30. 43-57.

Sorieul, M. et al. (2016) Plant Fibre: Molecular Structure and Biomechanical Properties, of a Complex Living Material, Influencing Its Deconstruction towards a Biobased Composite. Materials. [Online] 9 (8), 618–.

Tekstil Sayfasi (2014) Man-made Fibers. [Online]. Available: https://tekstilsayfasi.blogspot.com/2014/05/man-made-fibers.html

Textechno. (no date) [Online] Available: https://www.textechno.com/product/favigraph/

ThermoFisher. (no date) [Online]
Available: https://www.thermofisher.com/us/en/home.html

Tobler-Rohr (2011) Handbook of sustainable textile production. Reference & Research Book News 26 (5).

Vehviläinen, M. (2015) Wet-spinning of Cellulosic Fibres from Water-Based Solution Prepared from Enxyme-Treated Pulp. [PhD thesis]

Wawro, D. et al. (2009) Manufacture of Cellulose Fibres from Alkaline Solutions of Hydrothermally-Treated Cellulose Pulp. Fibres and Textiles in Eastern Europe. 74. 18-22.

Woodings, C. & Woodings, Calvin (2001) *Regenerated Cellulose Fibres*. Burlington: Elsevier Science.

Xenocs. (no date) [Online]. Available: https://www.xenocs.com/knowledge-base/saxs/

Yao, A. et al. (2020) Preparation of cellulose nanocrystals and their application in reinforcing viscose filaments. Cellulose (London). [Online] 27 (17), 10553–10565.

ZEISS. (no date) [Online]. Available: https://www.zeiss.com/corporate/int/home.html?vaURL=www.zeiss.de/en

Zhang, H. et al. (2021) Influence of cross-section shape on structure and properties of Lyocell fibers. Cellulose (London). [Online] 28 (2), 1191–1201.

Zhang, S. et al. (2012) Swelling and dissolution of cellulose in NaOH aqueous solvent systems. Cellulose Chemistry and Technology. 47. 671-679.

Zhang, S. et al. (2018) Regenerated cellulose by the Lyocell process, a brief review of the process and properties. BioResources. 13. 1-16

Appendix I

-- Edit these

savedirectory = string.format("") -- save directory for results example-- savedirectory = string.format("C:\\Users\\user\\Desktop\\Conversion\\")

N=3 -- number of parallel trial points

M=18 -- number of total trial points

--Edit only if the amorphous function is wanted to be changed or the initial peak guessess need to be changed (bad fitting with current initial guesses)

psf = string.format("Gaussian")

esf = string.format("ExpAmorphous")

-- Definition of the amorphous function

F:execute("define "..esf.." (height,center) = height*820.79*exp(-0.0950819*(x-21.4263+20.5-center)^2) + height*14025.1*exp(-0.0183998*(x-49.0785+20.5-center)^2) + height*1507.09*exp(-0.304793*(x-16.2293+20.5-center)^2) + height*639.526*exp(-0.23783*(x-29.8167+20.5-center)^2) + height*2948.43*exp(-0.0930037*(x-7.68234+20.5-center)^2) + height*18570.7*exp(-0.0168208*(x-37.8278+20.5-center)^2) + height*31921*exp(-0.121094*(x-20.5685+20.5-center)^2) + height*26883.6*exp(-0.0145657*(x-20.0862+20.5-center)^2)")

```
for l=0,F:get_dataset_count()-1 do

F:execute("use @"..l.."")

--Data conversion for intensities and from scattering vector to 2theta
F:execute("Y=y*1000000")
F:execute("X=180/pi*2*asin(x*1.54189/(4*pi))")

-- Determination of the active data range, active range is now [10, 33]
F:execute("A = a and not (-10 < X and X < 10)")
F:execute("A = a and not (33 < X and X < 100)")

-- Initial guesses for peak intensities for example max(y if x > 10 and x < 33)/2.06") == intitial guess for the peak in 20.4 2theta
F:execute("$g"..l.." = max(y if x > 10 and x < 33)/2.06")  -- is acquired by taking the maximum value of the data in the range of [10, 33]
F:execute("$g"..l.."= ~{$g"..l.."}")                -- and by dividing with value 2.06 (trial and error).

F:execute("$h"..l.." = max(y if x > 10 and x < 33)/130000")-- Initial guessess are set for all the peaks.
F:execute("$h"..l.."= ~{$h"..l.."}")
```

F:execute("$j"..l.." = max(y if x > 10 and x < 33)/4.2")

F:execute("$j"..l.."= ~{$j"..l.."}")

F:execute("$q"..l.." = max(y if x > 10 and x < 33)/3.64")

F:execute("$q"..l.."= ~{$q"..l.."}")

F:execute("$w"..l.." = max(y if x > 10 and x < 33)/10.45")

F:execute("$w"..l.."= ~{$w"..l.."}")

F:execute("@"..l..": F+= "..esf.." ($h"..l..",{~17})")

F:execute("@"..l..": F+= "..psf.." ($j"..l..",{~12.3},~2)") -- Initial guessess for peak centers and hwhm's

F:execute("@"..l..": F+= "..psf.." ($q"..l..",{~20.5},~1.5)") -- {} means the peak center is locked.

F:execute("@"..l..": F+= "..psf.." ($g"..l..",~20.9,~2)") -- Sometimes the fitting yields bad results without locking of few peak centers

F:execute("@"..l..": F+= "..psf.." ($w"..l..",~28.4,~2)")

end

```
--Data fitting
F:execute("@*: fit")


--Calculations for Crystallinity indexes, crystallite sizes and their saving to earlier determined directory
for l=0,F:get_dataset_count()-1 do


F:execute("use @"..l.."")


F:execute("$CI"..l.." = (F[1].Area+F[2].Area+F[3].Area+F[4].Area)/(F[1].Area+F[2].Area+F[3].Area+F[4].Area+F[0].height*1023481.14)*100")

F:execute("$CS1"..l.." = (0.94*1.54189/(((3.14159/180)*F[1].FWHM)*cos(F[1].Center*(3.14159/180))))")
F:execute("$CS2"..l.." = (0.94*1.54189/(((3.14159/180)*F[2].FWHM)*cos(F[2].Center*(3.14159/180))))")
F:execute("$CS3"..l.." = (0.94*1.54189/(((3.14159/180)*F[3].FWHM)*cos(F[3].Center*(3.14159/180))))")
F:execute("$CS4"..l.." = (0.94*1.54189/(((3.14159/180)*F[4].FWHM)*cos(F[4].Center*(3.14159/180))))")
```

```
F:execute("print $CI"..l.." >> "'..savedirectory.."crystallinity index.dat"')

F:execute("print $CS1"..l.." >> "'..savedirectory.."crystallite size1.dat"')

F:execute("print $CS2"..l.."  >> "'..savedirectory.."crystallite size2.dat"')

F:execute("print $CS3"..l.." >> "'..savedirectory.."crystallite size3.dat"')

F:execute("print $CS4"..l.." >> "'..savedirectory.."crystallite size4.dat"')

end
```

-- Calculations for average crystallity indexes and crystallite sizes and their standard deviations. Saving the data to earlier determined directory

```
filename = string.format(""..savedirectory.."crystallinity index.dat")

F:execute("@+ < "' .. filename .. ":0:1::"')

filename = string.format(""..savedirectory.."crystallite size1.dat")

F:execute("@+ < "' .. filename .. ":0:1::"')

filename = string.format(""..savedirectory.."crystallite size2.dat")

F:execute("@+ < "' .. filename .. ":0:1::"')
```

```
filename = string.format(""..savedirectory.."crystallite size3.dat")

F:execute("@+ < '" .. filename .. ":0:1::'")


filename = string.format(""..savedirectory.."crystallite size4.dat")

F:execute("@+ < '" .. filename .. ":0:1::'")

for l=0,F:get_dataset_count()-6,N do

F:execute("use @"..M.."")

F:execute(" print avg(y if n>("..l.."-1) and n<("..l.."+"..N..")), stddev(y if n>("..l.."-1) and n<("..l.."+"..N..")) >> '"..savedirectory.."crystallinity index_average_and_STdev.dat'")


F:execute("use @"..(M+1).."")

F:execute(" print avg(y if n>("..l.."-1) and n<("..l.."+"..N..")), stddev(y if n>("..l.."-1) and n<("..l.."+"..N..")) >> '"..savedirectory.."crystallite size1_average_and_STdev.dat'")


F:execute("use @"..(M+2).."")
```

F:execute(" print avg(y if n>("..l.."-1) and n<("..l.."+"..N..")), stddev(y if n>("..l.."-1) and n<("..l.."+"..N..")) >> '"..savedirectory.."crystallite size2_average_and_STdev.dat'")

F:execute("use @"..(M+3).."")

F:execute(" print avg(y if n>("..l.."-1) and n<("..l.."+"..N..")), stddev(y if n>("..l.."-1) and n<("..l.."+"..N..")) >> '"..savedirectory.."crystallite size3_average_and_STdev.dat'")

F:execute("use @"..(M+4).."")

F:execute(" print avg(y if n>("..l.."-1) and n<("..l.."+"..N..")), stddev(y if n>("..l.."-1) and n<("..l.."+"..N..")) >> '"..savedirectory.."crystallite size4_average_and_STdev.dat'")

end

-- Saving of peak parameter data to the directory

F:execute("@*: info peaks >> '"..savedirectory.."parameters.peaks'")